

**Forschungszentrum Karlsruhe
Technik und Umwelt**

Wissenschaftliche Berichte

FZKA 5848

**Proceedings
of the Second Milestone Meeting
of European Laboratories
on
The Development of Ferritic/Martensitic Steels
for Fusion Technology**

Karlsruhe, September 9-10, 1996

Compiled by E. Daum, K. Ehrlich and M. Schirra

Institut für Materialforschung
Association FZK - Euratom

**Forschungszentrum Karlsruhe GmbH, Karlsruhe
1997**

Contents

WORKSHOP ORGANIZATION.....	V
1. INTRODUCTION.....	1
2. PRESENTATIONS AT THE MEETING.....	3
2.1 LIST OF TITLES FOR PRESENTATION.....	5
2.2 CONTRIBUTIONS AT THE MEETING.....	6
<i>Measurement of the Impurity Elements Nb and Mo in the Steel F82H-mod. by the Activation Analysis Method</i>	<i>6</i>
<i>New results of homogeneity tests on F82H-mod. material</i>	<i>7</i>
<i>Segregation phenomena in ferritic/martensitic steels</i>	<i>13</i>
<i>Comparison of heats No. 9741 and 9753 of F82H-mod. steel</i>	<i>15</i>
<i>Status of Work on Reduced Activation Martensitic Steels</i>	<i>20</i>
<i>Ferrite Formation in F82H-mod. and OPTIFER Alloys</i>	<i>24</i>
<i>Tensile- and impact bending-properties of the steels MANET II, F82H-mod. and OPTIFER-IV</i>	<i>29</i>
<i>Mechanical properties of F82H-mod.: Tensile test and low cycle fatigue</i>	<i>35</i>
<i>Structural and mechanical properties of Ti-bearing L.A. BATMAN II steels.....</i>	<i>38</i>
<i>Cyclic behavior of the martensite steel F82H-mod. compared to MANET II</i>	<i>40</i>
<i>Short summary of the ECN contribution at the AG1-MS02 discussion meeting</i>	<i>42</i>
<i>Evaluation of ferritic/martensitic steels.....</i>	<i>44</i>
<i>Pre- and post-irradiation properties of pure iron and low activation steels</i>	<i>48</i>
<i>Tensile properties of MANET and F82H-mod. after helium implantation</i>	<i>53</i>
<i>MANITU irradiation program.....</i>	<i>56</i>

3. PROPERTY COMPARISON AND EVALUATION.....	64
3.1 PHYSICAL METALLURGY	65
<i>Hardenability.....</i>	67
<i>Grain Size.....</i>	68
<i>Tempering treatment</i>	70
3.2 MECHANICAL PROPERTIES.....	71
<i>Ultimate Tensile Strength and 0,2% Yield Strength</i>	71
<i>Total and Uniform Elongation</i>	75
<i>Area Reduction.....</i>	78
<i>Creep- and creep-rupture properties</i>	80
<i>Impact properties</i>	81
4. SUMMARY AND CONCLUSIONS.....	84

Abstract

In the frame of the European Fusion Technology Program a series of ferritic/martensitic developmental alloys, the composition of which had been optimized towards low long-term activation, was investigated and compared with conventional 9-12%CrMoVNb steels.

It could be shown that by these chemical modifications neither the physical metallurgy nor the transformation behavior was changed markedly. Tensile-, creep-rupture- and fatigue properties are somewhat reduced, whereas the fracture toughness and impact data are far superior to conventional materials. This is an important advantage, especially if the expected detrimental effect of neutron irradiation on the latter properties is taken into account. First results of low-fluence irradiations indicate that the new alloys are less prone to irradiation-induced DBTT shifts.

A positive experience can also be reported about the overall performance of an alloy (F82H-mod.) which had been produced as 5 ton batch with present steelmaking technology. Homogeneity tests have provided very reproducible properties and it could also be shown that by a proper selection of the ingot material a reasonably low concentration of unwanted elements like Nb, which control the long-term activation, can be achieved.

As an overall conclusion one can say that the development of ferritic/martensitic alloys with reduced long-term activation has made progress and it is expected that at the end of the present screening phase (1998) a "Primary Candidate Alloy" for this material group can be specified.

Bericht zum „Second Milestone Meeting“ der Europäischen Laboratorien über die Entwicklung von Ferritisch/Martensitischen Stählen für die Fusionstechnologie

Zusammenfassung

Im Rahmen des Europäischen Fusionstechnologieprogramms wurde eine Reihe von ferritisch-martensitischen Entwicklungslegierungen, deren Zusammensetzung hinsichtlich niedriger Langzeitaktivierbarkeit unter Fusionsneutronenbestrahlung optimiert worden war, auf ihre Eigenschaften hin untersucht und mit konventionellen 9-12%CrMoVNb-Stählen verglichen.

Als wesentliche Ergebnisse können festgehalten werden, daß sich durch die chemischen Modifikationen Struktur und Gefüge, sowie das Umwandlungsverhalten nur geringfügig geändert haben. Hinsichtlich der mechanischen Eigenschaften wird eine leichte Verminderung von Kurzzeitfestigkeit, Zeitstandfestigkeit und Ermüdungsfestigkeit beobachtet. Hingegen ergibt sich eine deutliche Verbesserung in den Kerbschlag- und Bruchzähigkeitseigenschaften, die wegen dem zu erwartenden negativen Einfluß von Bestrahlung auf diese Eigenschaften besonders erwünscht ist.

Auch hinsichtlich der Herstellbarkeit und Qualität solcher Legierungen mit reduzierter Langzeitaktivität im industriellen Maßstab sind positive Erfahrungen gemacht worden bei der Untersuchung einer 5 Tonnen Charge. Homogenitätstests haben an dieser Legierung (F82H-mod) in den Gefüge- und mechanischen Eigenschaften reproduzierbare Ergebnisse geliefert und den Nachweis erbracht, daß nichtgewünschte Verunreinigungen wie z. B. Nb, die das radioaktive Abklingverhalten negativ beeinflussen, in befriedigend niedriger Konzentration mit der gegenwärtig verfügbaren Herstellungstechnologie eingestellt werden können.

Insgesamt ist die Entwicklung von niedrigaktivierbaren ferritisch-martensitischen Stählen auf einem guten Weg und es kann - wie geplant - am Ende der gegenwärtigen Screeningphase (1998) mit der Spezifikation einer „Primary Candidate Alloy“ gerechnet werden.

Workshop Organization

Agenda

- I.) Comparison of conventional and L.A.-ferritic/martensitic steels
 - Homogeneity tests on F82H-mod.
 - Physical metallurgy of L.A. ferritic/martensitic steels
 - (Hardenability, transformation behavior, tempering treatments, microstructural data)
 - Mechanical properties
 - (Tensile-, creep-, fatigue-, fracture toughness- and impact-properties)
 - Irradiation behavior
 - (Radiation hardening and embrittlement)

Data evaluation and conclusions
- II.) Status of R&D work and irradiation experiments
- III.) Impact of Blanket Selection Exercise on the Long-term Materials Program
- IV.) Miscellaneous

Workshop Participants

Name	Organization	Phone	Fax	E-mail
Dr. A. Alamo	CEA	+33-1-6908-6726	+33-1-6908-7130	alamo@centresaclay.cea.fr
Dr. G. Filacchioni	ENEA	+39-63048-3142	+39-63048-4864	
Dr. E. van Osch	ECN	+31-224-56-4650	+31-224-56-3442	vanosch@ecn.nl
Dr. M. del Pilar Fernandez	CIEMAT	+34-1-3466-6613	+34-1-346-6661	paredes@ciemat.dec.es
Dr. S. Tähtinen	VTT (Suomi)	+358-9-456-6859	+358-9-456-7002	seppo.tahtinen@vtt.fi
Dr. B. van der Schaaf	ECN	+31-22456-4665	+31-22456-3490	vanderschaaf@ecn.nl
Dr. B. Singh	Riso	+45-4677-5709	+45-4635-1173	
Dr. M. Victoria	CRPP-FTM	+41-56-310-2111	+41-56-310-2199	max.victoria@psi.ch
Dr. M. de Vries	ECN	+31-224-56-4637	+31-224-56-3490	devries@ecn.nl
Dr. N. Wanderka	HMI	+49-30-8062-2079	+49-30-8062-3059	wanderka@hmi.de
W. Dietz	EC Brüssel	+49-2207-2679	+49-2207-2679	dietz@mcs.de
E. Materna-Morris	FZK	+49-7247-82-2162	+49-7247-82-4567	materna-morris@imf.fzk.de
Dr. A. Möslang	FZK	+49-7247-82-4029	+49-7247-82-4567	anton.moeslang@imf.fzk.de
M. Schirra	FZK	+49-7247-82-2909	+49-7247-82-4567	
Dr. J. Aktaa	FZK	+49-7247-82-4946	+49-7247-82-	jarir.aktaa@imf.fzk.de
C. Petersen	FZK	+49-7247-82-3267	+49-7247-82-	claus.petersen@imf.fzk.de
M. Rieth	FZK	+49-7247-82-4568	+49-7247-82-	michael.rieth@imf.fzk.de
L. Schäfer	FZK	+49-7247-82-3577	+49-7247-82-	
Dr. E. Daum	FZK	+49-7247-82-4243	+49-7247-82-4567	eric.daum@imf.fzk.de
Prof. Dr. K. Ehrlich	FZK	+49-7247-82-2338	+49-7247-82-4567	karl.ehrlich@imf.fzk.de

1. Introduction

In the current 1995-98 Fusion Technology Program of the European Community four milestone meetings had been foreseen at which the status and progress of the development of low-activation ferritic/martensitic steels should be reviewed. Scope of Milestone 2, which had been scheduled for autumn 1996 was to present the data on the commonly investigated IEA alloy F82H-mod. (Homogeneity Tests), to report on the progress of LA-alloy development in the different European laboratories and to compare the properties of the conventional 9-12%CrMoVNb steels with the new 7-10% CrWVTa alloys. Also first results of low-dose irradiation experiments in the HFR-reactor Petten, the Dual-Beam Facility/Karlsruhe and PIREX-experiments/Villigen were expected in order to understand the effect of irradiation on the low-temperature hardening and embrittlement and the shift in ductile-to -brittle transition temperature in these materials. The presentation of the data, their discussion and evaluation was expected to lead to recommendations for future work.

In mid 1996 the planning for the Second Milestone Meeting was started and it was held on September 9 and 10, 1996 at Karlsruhe. It was attended by 20 participants from 9 different European laboratories ; their names, addresses and the agenda are attached to this report. A total of 15 papers was presented and compacts of these contributions are collected in Chapter 2. A comparison of data on physical metallurgy and mechanical properties was prepared in advance for the meeting by FZK based on informations released by the different laboratories which made it easier to evaluate the data and come to common conclusions. This data collection and evaluation is found in Chapter 3 of this report. The conclusions of this meeting are finally summarized in Chapter 4.

This work is based on the data provided by the following associations : CEA (F); CIEMAT (Sp); CRPP (CH); ECN (NL); ENEA (I); HMI (D); Risø (DK); VTT(SF) and FZK (D).

Chapter 2

Presentations at the Meeting

2.1 *List of titles for presentation*

E. Daum	Measurement of the impurity elements Nb and Mo in F82H-mod. by the activation analysis method
R. Lindau	New results of homogeneity tests on F82H-mod. material
M. Victoria	Segregation phenomena in ferritic/martensitic steels
S. Tähtinen	Comparison of heat 9741 and 9753 of F82H-mod. steel
A. Alamo	Status of work on reduced activation martensitic steels
E. Materna-Morris	Ferrite formation in F82H-mod. and OPTIFER alloys
L. Schäfer	Tensile- and impact bending-properties of the steels MANET-II, F82H-mod. and OPTIFER-IV
M. Fernandez Paredes	Mechanical properties of F82H-mod. : Tensile test and low cycle fatigue
G. Filacchioni	Structural and mechanical properties of Ti-bearing L.A. Batman II steels
C. Petersen / R. Schmitt	Cycling behaviour of the martensitic steels F82H-mod. compared to MANET II
E.V. van Osch	Mechanical properties of F82H-mod.
N. Wanderka	Evaluation of ferritic/martensitic steels
B. Singh / P. Toft	Pre- and post-irradiation properties of pure iron and low activation steels
R. Lindau / A. Möslang	Tensile properties of MANET and F82H-mod. after helium implantation
M. Rieth	MANITU irradiation program

2.2 *Contributions at the meeting*

Measurement of the Impurity Elements Nb and Mo in the Steel F82H-mod. by the Activation Analysis Method

E. Daum

Forschungszentrum Karlsruhe

Within the fusion technology program the development of low activation steels for First Wall components has become a major activity. A joint effort in fusion neutron activation calculations and material development has led to a number of candidate low activation steels. One of this steels is the Japanese reference alloy F82H-mod. This material has been manufactured from pure ingot materials and is characterized by its very low Nb content of nominally 1 ppm.

Since first analytical results of a European round robin test indicated differences in the measured Nb-content of more than one order of magnitude, an activation experiment was made with a 19 MeV α -particle beam at the Isochron Cyclotron of the Forschungszentrum Karlsruhe and followed by γ -spectroscopy. The sample used for irradiation was a 47 μm thick rolled F82H-mod. foil. Under α -irradiation the radionuclide ^{96}Tc with $T_{1/2} = 4.35$ d is produced from the element Nb via the reaction $^{93}\text{Nb}(\alpha, n)^{96}\text{Tc}$. Unfortunately, the element Mo leads also to the nuclide ^{96}Tc . In order to exclude any interference the ^{96}Tc production by Mo had to be quantified. This was done by an independent measurement of the concentration of Mo in F82H-mod. via another activation product, ^{97}Ru . Because the excitation functions of Nb \rightarrow ^{96}Tc , Mo \rightarrow ^{96}Tc and Mo \rightarrow ^{97}Ru are not well known or even missing, α -irradiations of high purity Nb- and Mo-foils were carried out at the same setup as for F82H-mod. The analysis of these high purity foils led to mean excitation functions of $\sigma(\text{Nb} \rightarrow \text{Tc}) = 46.4$ mbarn ($\pm 8\%$), $\sigma(\text{Mo} \rightarrow \text{Tc}) = 5.7$ mbarn ($\pm 9\%$) and $\sigma(\text{Mo} \rightarrow \text{Ru}) = 110.3$ mbarn ($\pm 8\%$).

In spite of an extremely high background caused by many other activation reactions from the major constituents of the alloy it was possible to undertake an evaluation of the γ -spectrum of the F82H-mod. and to derive after correction of the Mo-contributions to the ^{96}Tc -peak mass concentrations of (2.5 ± 1) ppm Nb and (46 ± 17) ppm Mo, respectively.

Comparing these values with the data (1 ppm Nb and 30 ppm Mo) given by the manufacturer and the results of a chemical analysis at the Forschungszentrum Karlsruhe (< 8 ppm Nb and (18 ± 1) ppm Mo) one can state a quite good agreement. Thus, the very low

content of the highly undesired element Nb as claimed by the manufacturer, can be confirmed. Also the specified Mo-concentration is in a reasonably good agreement with our measurements.

New results of homogeneity tests on F82H-mod. material

R. Lindau

Forschungszentrum Karlsruhe

Plates of the reduced activation ferritic/martensitic steel F82H-mod. provided by JAERI and produced by the Japanese steel manufacturer NKK were distributed to different European Laboratories: CEA-Saclay, CIEMAT-Madrid, ECN-Petten, ENEA-Casaccia, EPFL-Villigen, FZK-Karlsruhe, NFR-Nyköping, VTT-Espoo.

In order to check the homogeneity of different properties of the semifinished products (rolled plates of 7.5 and 15 mm thickness) a quality assurance and homogeneity test program had been arranged. The test program given in Table 1 included the analysis of the chemical composition, hardness measurements and metallographic examinations. Preliminary results of the homogeneity tests have been reported earlier [1] and a complete summary of results is given in [2].

Table 1: Test program to check the homogeneity of F82H-mod. plates

Property	characteristic value	sampling
chemical composition		each plate
hardness	HV 30	3 directions
metallography:		
delta-ferrite	amount	3 directions
grain size	ASTM or μm	3 directions
non metallic inclusions/precipitates	size/kind/distribution	3 directions
primary carbides	size/kind/distribution	3 directions

Although for the main alloying elements Cr, W, Mn, V and C a good agreement of the measured chemical composition could be established, there were some deviations concerning Nb and Mo contents. New analyses performed at FZK by different methods exhibited lower contents in Nb and Mo than measured in the early analyses. Table 2 gives a comparison of the chemical composition of F82H-mod. (Heat 9741) as determined by JAERI/NKK and the different EU-Laboratories.

Table 2: Chemical composition of F82H-mod. (Heat 9741) [wt-%]

	C	Mn	Cr	V	W	Nb	Mo
JAERI	0.09	0.16	7.64 - 7.71	0.16	1.94 - 1.97	0.0001	0.003
EU	0.086 - 0.107	0.16 - 0.21	7.40 - 8.36	0.14 - 0.17	1.88 - 2.10	< 0.001 - 0.010	< 0.002 - < 0.01

	Ni	Cu	Al	Zr	Si	Ti	Co
JAERI	0.02	0.01	0.003		0.11	0.006 - 0.008	0.005
EU	0.002 - 0.022	0.003 - 0.006	< 0.001 - 0.004	0.01	0.10 - 0.23	< 0.001 - 0.007	0.0037 - 0.009

Table 3: Comparison of Nb and Mo-content

	JAERI	FZK (Adelhelm)	FZK (Daum)
Nb (wt-ppm)	1	< 8	2.5 ± 1
Mo (wt-ppm)	30	18 ± 1	46 ± 17

The new results on Nb and Mo-content elaborated at FZK, especially those of E. Daum [3], who utilized nuclear activation analysis and who was able to give error bands although the absolute contents were very low, give rise to the assumption that the manufacturer's analysis is reliable.

The results of the tensile tests (according to DIN EN 10 002) in the temperature range between RT and 750 °C are shown in Fig. 1 to 5.

The results can be summarized as follows:

- there are no differences in tensile properties within one plate
- there is no texture in tensile properties visible
- 15 mm plates are slightly higher in strength and slightly lower in ductility than 7.5 mm plates
- the tensile results of the different laboratories show quite good agreement
- the strength is below 500 °C lower, above 500 °C equal MANET II
- the ductility is comparable to MANET II
- the deviation in total elongation is due to the different ratio of diameter to gaugelength ($d_0:L_0$), i.e. smaller part of the necking elongation at the total elongation of specimens with a higher gaugelength ratio (e.g. 1:5 or 1:12).

CEA, ECN, ENEA FZK and VTT performed round robin impact bending tests on KLST-specimen. The results are given in Fig. 6 and reveal the following:

- the scatter in the upper shelf energy (USE: 9.3-10.4) is relatively small
- but large scatter can be found in the ductile to brittle transition temperature DBTT, (-45 °C to 80 °C).

The homogeneity tests have shown, that there is good agreement concerning microstructural and mechanical properties for F82H-mod. (Heat 9741) independent of product form.

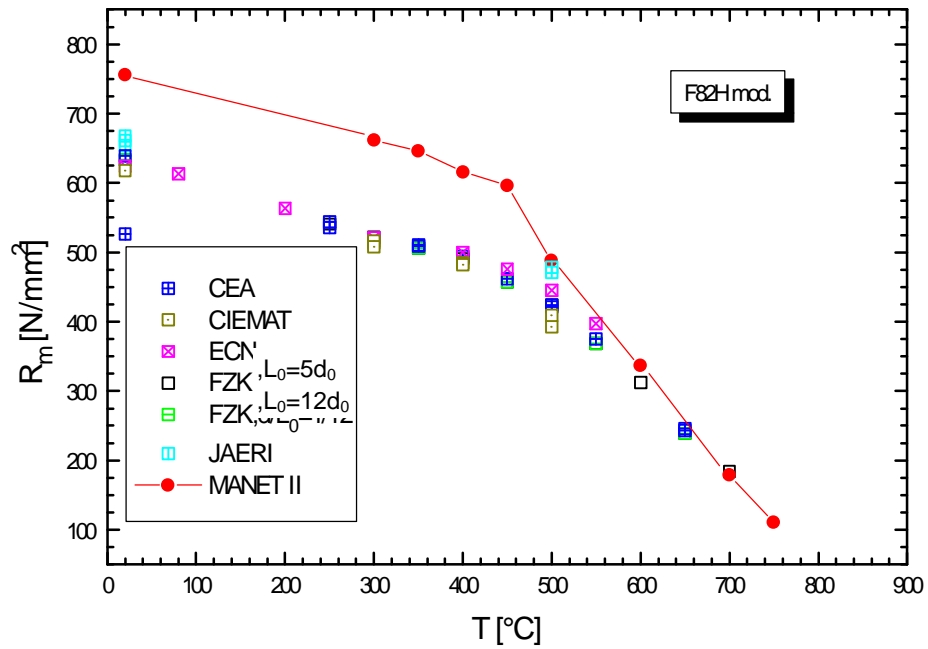


Fig. 1: Comparison of Ultimate Tensile Strength R_m

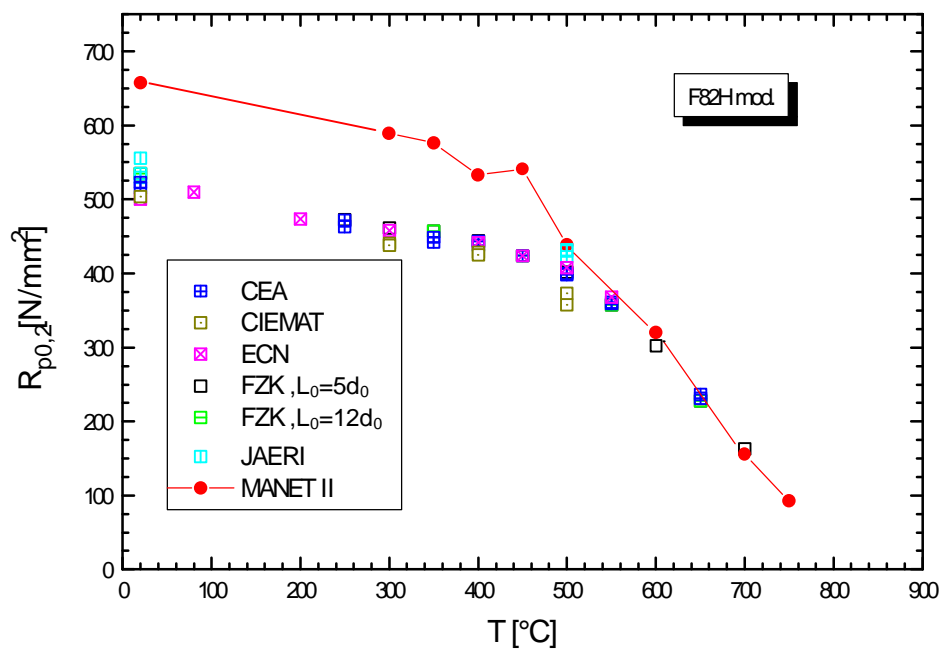


Fig. 2: Comparison of Yield Strength $R_{p0.2}$

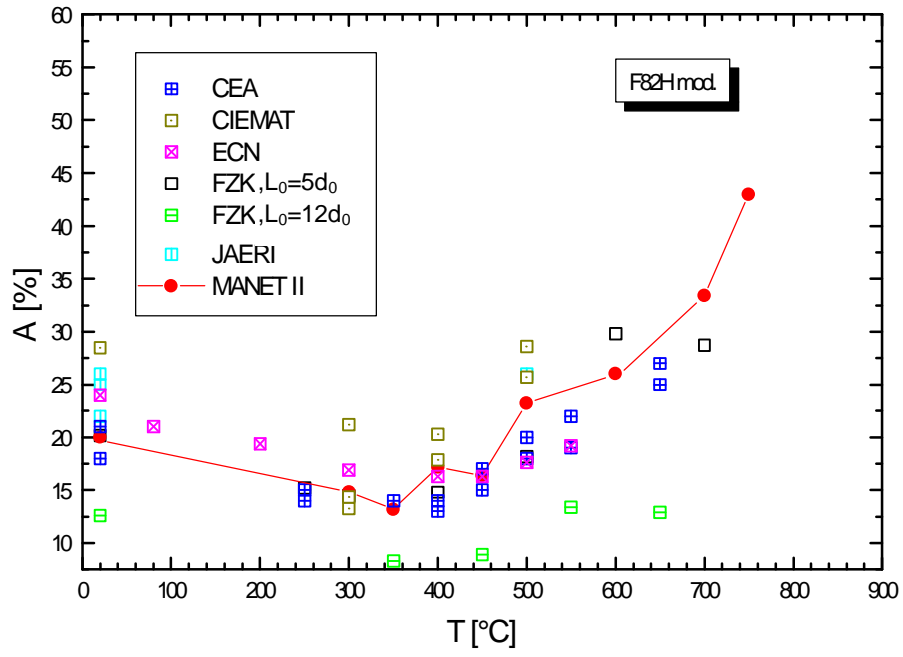


Fig. 3: Comparison of Total Elongation A

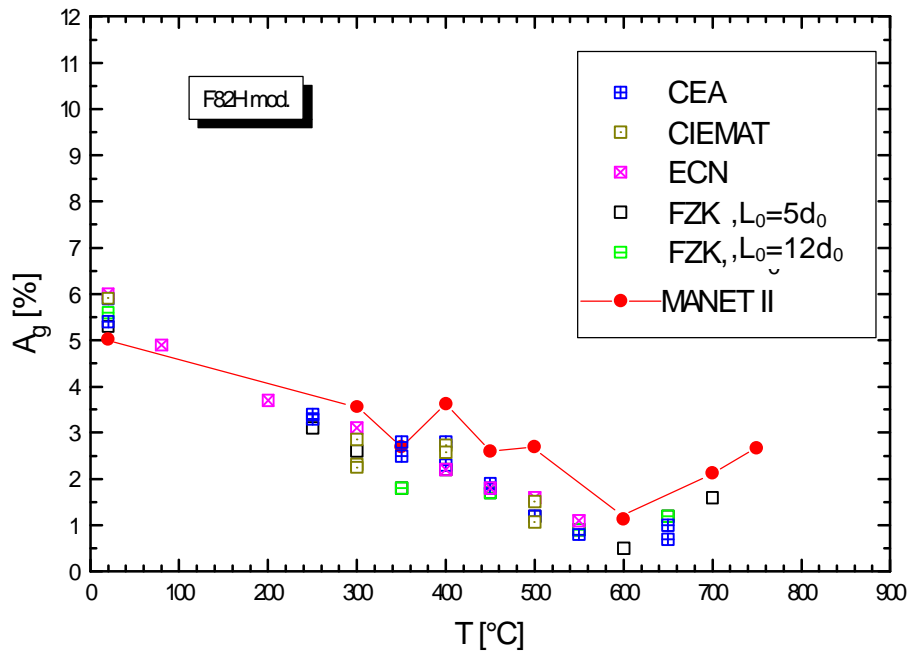


Fig. 4: Comparison of Uniform Elongation A_g

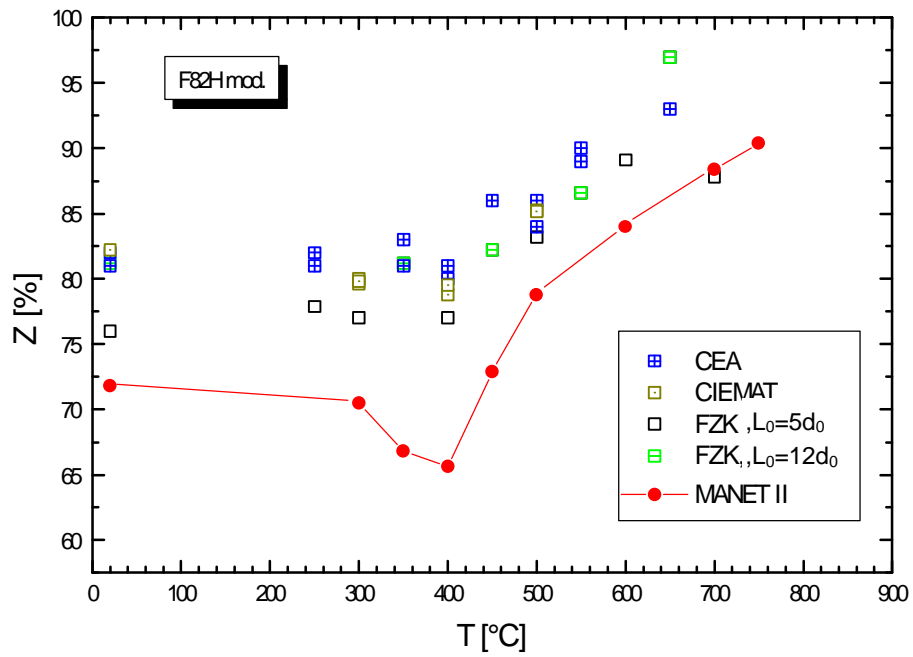


Fig. 5: Comparison of Reduction of Area Z

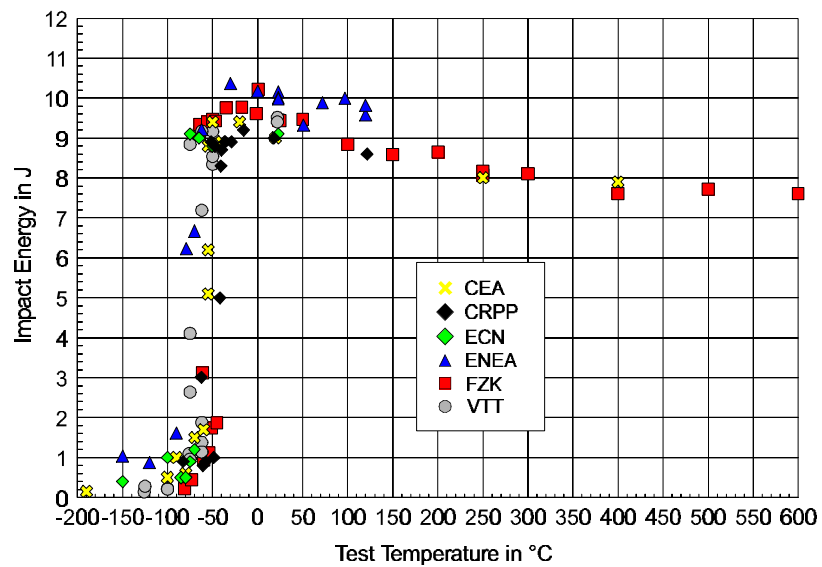


Fig. 6: Comparison of Impact Bending Tests between -200 and 600 °C

Literature:

- [1] K. Ehrlich, Minutes of the AG1/AG2-Meeting at Karlsruhe 11th. July 1995
- [2] R. Lindau (Ed.), Homogeneity Tests of European Laboratories on Alloy F82H-mod. FZKA-Report 5814, 1997 in press.
- [3] E. Daum, Measurement of the impurity elements Nb and Mo in the steel F82H-mod. by the activation analysis method, this report p. 3
- [4] M. Rieth, MANITU Irradiation Program, this report p. 76

Segregation phenomena in ferritic/martensitic steels

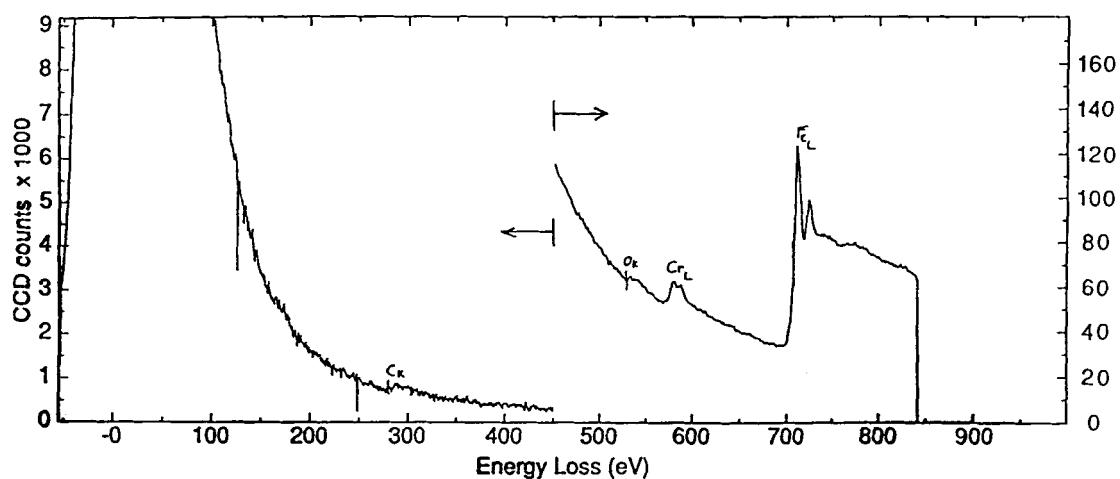
M. Victoria

CRPP-FTM

EFTEM technique

The three windows method

The EFTEM technique consists in acquiring three images at three different energy losses; two are taken before the EELS edge of the selected element (pre-edge images) and one is taken on the edge (post-edge image). The subtraction of the latter with an extrapolated image from the two first images will result in an image which contrast is proportional to the chemical content.



EELS of F82H-mod.

Summary

In this preliminary work, it appeared that in all of the as received specimens of martensitic steels segregation is present. This is indicated by the fact that there is a depletion in Fe at both PAG and martensite lath boundaries. All three specimens show Cr segregation.

In MANET II there is strong indications for Si segregation at the PAG boundary. In F82H-mod. and OPTIMAX B, Si segregation is not clearly determined.

Further work is continued in order to quantify the segregation with the help of a FEG-STEM, and to investigate irradiated specimens.

Acknowledgements

Prof. C.J. Humphreys is acknowledged for providing us access to the EFTEM of the Dpt. of Materials Science and Metallurgy, University of Cambridge, UK

Drs. C.B. Boothroyd and R. Dunin-Borkowski are thanked for their valuable help during the measurements on the EFTEM.

The EURATOM association is acknowledged for financial support.

Long Term Fusion Materials Program 1995-1998

Association EURATOM-TEKES

Comparison of heats No. 9741 and 9753 of F82H-mod. steel

S. Tähtinen

VTT Manufacturing Technology

VTT Manufacturing Technology have received two F82H-mod. steel plates identified as 15 mm plate RB802-1-3 from the heat No. 9741 and 25 mm plate 31W-18 from the heat No. 9753. Metallurgical characterization as grain size, chemical composition, inclusion analysis and hardness were measured the from both steel plates. VTT Manufacturing Technology also participated Round Robin on miniaturized impact test using KLST specimens. Additionally impact tests using both KLST and ISO-V Charpy specimens were also performed on plate from the heat No. 9753.

Metallurgical characterization showed no orientation dependency in chemical composition, inclusion analyses, grain size or hardness in the studied F82H-mod. steel plates RB802-1-3 from heat No. 9741 and 31W-18 from heat No. 9753. The average hardness value of plate RB802-1-3 was 211 HV₃₀ and the average hardness value of plate was 205 HV₃₀. The average grain size was 84 µm and 90 µm for plates 31W-18 and 31W-18, respectively. Two types of inclusion were found in both steel plates. The larger inclusions, non spherical more than 5 µm in diameter, were mainly Ta, Ti, and Al rich mixed oxides and smaller, almost spherical less than 1 µm in diameter, could not be analyzed due to small size of the inclusions. Chemical composition showed small variations between the two heats. The first heat No. 9741 showed somewhat lower content of Cr, W, V and Ta and somewhat higher content of Mn and S when compared with chemical composition of heat No. 9753. It was also noted that the Nb content varied between 2.2 and 3.0 ppm. Results of grain size, hardness and chemical compositions are summarized in Tables 1 - 3.

Impact test results from Round Robin on miniaturized impact test using KLST specimens from heat No. 9741 and impact test results using KLST and ISO-V specimens from heat No. 9753 showed a small difference between the two heats. Characteristic transition temperature T_{50%} using KLST miniaturized impact specimens was -65 °C and -75°C for

heats No. 9741 and No. 9753, respectively. Impact test results using KLST specimens are shown in Figure 1 and summarized in Table 4.

These preliminary results showed that there is a small difference in chemical composition and impact properties between the two heats of F82H-mod. steel.

Table 1: Grain size determined as average intercept distance (μm) in three orientation for plates 1-3 and 31W-18.

	Average intercept distance(μm)					
Plate	Orientation					
	YZ	XZ	XY- bottom	XY- middle	XY- top	Average
1-3	85	74	88	100	76	84
31W-18	88	98	87	90	88	90

XY rolling plane (Y rolling direction); XZ long transverse plane;
YZ short transverse plane.

Table 2: Hardness of plates 1-3 and 31W-18

	Plate	YZ	XZ	XY- bottom	XY- middle	XY- top	Average
HV10	1-3	212	209	213	213	206	211
HV30	1-3	213	208	213	209	213	211
HV10	31W-18	212	214	207	215	206	211
HV30	31W-18	209	208	200	205	202	205

XY rolling plane (Y rolling direction); XZ long transverse plane;
YZ short transverse plane.

Table 3: Chemical Composition of F82H-mod. steel plates 1-3 and 31W-18. (Induction Coupled Plasma Massspectrometry (ICP-MS), * Emission Spectrometry Spectra lab5 model (OES),** Shield gas method Leco model TC-136).

Element	plate 1-3		plate 31W-18		NKK-JAERI, Ch 9741
	top	bottom	top	bottom	
Group A (wt%)					
Fe	bal	bal	bal	bal	bal
C*	0.07	0.09	0.07	0.10	0.09
Cr*	7.8	7.9	8.1	8.1	7.64-7.61
W	2.2	2.3	2.3	2.5	1.94-1.97
Mn	0.18	0.2	0.1	0.12	0.16
V	0.18	0.21	0.21	0.24	0.16
Ta	0.026	0.025	0.029	0.036	0.02
B*	0.002	0.002	0.002	0.002	0.0002
N**	0.006	-	0.008	-	0.006-0.008
P*	0.005	0.005	0.005	0.005	0.002
S*	0.006	0.006	0.005	0.005	0.001-0.002
Group C (ppm)					
Nb	3.0	2.6	2.2	2.4	1
Mo	22	26	41	50	30
Ni	217	220	154	167	200
Cu	66	68	63	72	100
Al	<100		<100		30
Si	-		-		1100
Ti	29	32	20	22	100
Co	32		30	33	50
Zr	0.9	2.4	1.2	2.0	-
Zn	26	20	15	20	
As	8	15	10	17	
Se	<60		<60		
Ru	1.5	1.4	<1	2.8	
Rh	<0.1		<0.1		
Pd	<0.1		<0.1		
Ag	0.2		0.23	0.2	

Element	plate 1-3		plate 31W-18		NKK-JAERI, Ch 9741
	top	bottom	top	bottom	
Sb	3.0	2.9	2.9	3.2	
Te	<0.1		<0.1		
La	<0.02		<0.02		
Ce	0.01		<0.02		
Sm	<0.02		<0.02		
Eu	<0.02		<0.02		
Gd	<0.02		<0.02		
Tb	<0.09		<0.02		
Dy	<0.02		<0.02		
Ho	<0.02		<0.02		
Er	<0.02		<0.02		
Tm	<0.02		<0.02		
Yb	<0.02		<0.02		
Lu	<0.02		<0.02		
Hf	<0.2		<0.1		
Ir	<0.1		<0.1		
Pt	<0.5		<0.4		
Au	10	1	10		
Pb	<4		1.4	2	
Th	<0.1		<0.3		
U	<0.02		<0.02		

Table 4: Coefficients and characteristic transition temperatures for F82H-mod. steel from heats No. 9741 and No. 9753. (* Round robin on KLST).

Heat No.	Type	T _{50%}	C	USE (J)	T _{3.15 J} (°C)	T _{3.1 J} (°C)	T _{1.9J} (°C)	T _{28 J} (°C)	T _{41 J} (°C)	T _{68 J} (°C)
9753	ISO-V	-42	-6.0	232				-54	-51	-47
9753	KLS T	-75	-3.3	8.65	-77	-77	-79			
9741*	KLS T	-65	-3.6	9.27	-67	-67	-70			

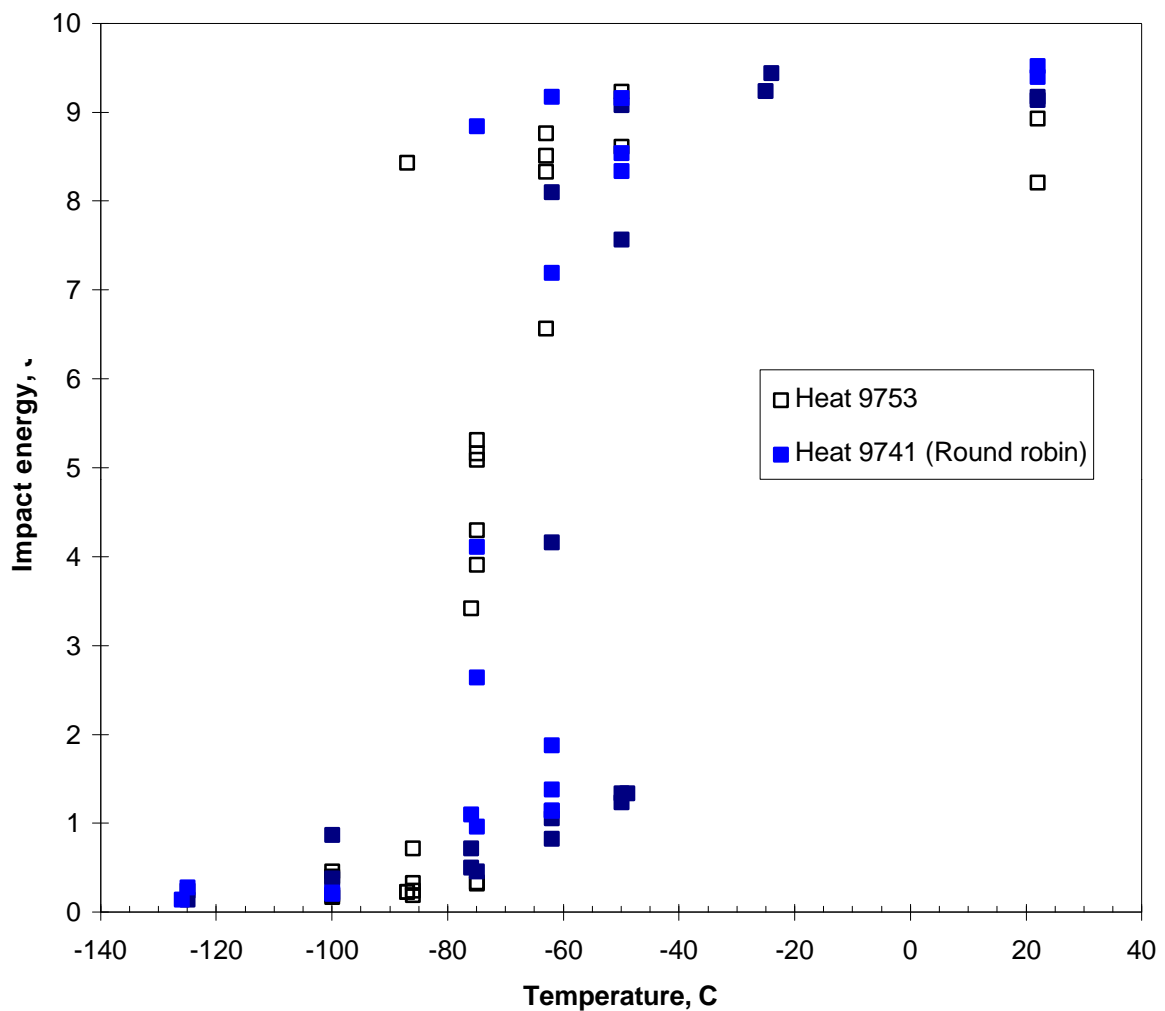


Figure 1: KLST impact test results of F82H-mod. steel from heats No. 9741 and 9753.

Status of Work on Reduced Activation Martensitic Steels

A. Alamo

CEA CONTRIBUTION

Investigations performed at CEA concern the physical metallurgy and mechanical characterization of low activation (L.A.) martensitic steels. Two experimental alloys, named LA12LC and LA12TaLC, and large-scale heats produced in Japan, that is F82H and JLF-1 steels, have been examined. Their chemical compositions, summarized as follow, essentially differ in Cr, W and Ta contents.

LA12LC: Fe-9Cr-0.7W-0.01 Ta-0.1C

LA12TaLC: Fe-9Cr-0.7W-0.10Ta-0.1C

F82H: Fe-7.5Cr-2W-0.02Ta-0.1C

JLF-1: Fe-9Cr-2W-0.08Ta-0.1C

Physical metallurgy

Temperatures of phase transformations martensite/ferrite \rightleftharpoons austenite were determined during heating and cooling by dilatometric techniques. Thus, non-equilibrium phase diagrams were established under anisothermal conditions (using different heating/cooling rates, CCT diagrams) and under isothermal conditions (TTT diagrams). Table I summarizes main characteristics of transformation behavior corresponding to L.A. martensitic steels examined.

During heating, the martensite to austenite transformation starts at about 850°C in the case of F82H and JLF-1 steels, at 805-820°C for LA12LC and LA12TaLC alloys, temperatures which have been measured for a heating rate of 0.01°C/s.

Phase transformations during cooling have been studied after austenitisation treatment at 1050°C for 30 minutes. The critical cooling rate, that is the minimal rate to obtain a fully martensitic product, are much higher for alloys containing higher content on Ta, JLF-1 (160°C/h) and LA12TaLC (90°C/h), compared to steels presenting lower Ta concentration, F82H (60°C/h) and LA12LC (45°C/h). This fact is certainly related to fine prior austenite

grain sizes of materials with a higher Ta content. A finer structure implies a higher density of grain boundaries, which constitute the nucleation sites for the phase transformation.

TTT diagrams describing the austenite to ferrite transformation in isothermal conditions, presented in all the cases the typical « C » Temperature-Time curves. Materials containing 9Cr exhibited the same microstructural evolution, precipitated carbide morphology and kinetic behavior, the faster transformation kinetic occurring at 725-750°C. TTT diagram corresponding to F82H alloy with 7.5Cr is displaced to the higher temperatures and short times regions compared to 9Cr steels, the faster kinetic for transformation occurs at 775-800°C. In particular, mechanisms of carbide precipitation in F82H seem to be rather different.

Table 1: Transformation behavior of L.A. martensitic steels.

Steel	On-heating		On-cooling		
	A _s (°C)	A _f (°C)	R _m (°C/h)	M _s (°C)	M _f (°C)
F82H	850	910	60	430	205
JLF-1	842	895	160	380	200
LA12LC	807	875	45	375	200
LA12TaLC	820	940	90	402	200

A_s, A_f: start and finish temperatures of martensite to austenite transformation measured during heating with a rate of 0.01°C/s.

M_s, M_f: start and finish temperatures of austenite to martensite transformation measured during cooling with a rate cooling ³ R_m.

R_m: minimal cooling rate to obtain a fully martensitic product.

Effects of austenitization and tempering treatments on hardness and TEP values have been investigated. Austenitization treatments have been performed in the range 850 - 1150°C for 30 minutes. The recovery of the as-quenched martensite have been examined for isochronal tempering of 1h from 20°C to 800°C. Equivalent hardness levels were obtained for all materials. Reduced activation alloys exhibited a lower sensitivity to secondary hardening, in the range 450-550°C, compared to conventional martensitic steels.

Mechanical characterization of as-received materials

Tensile and impact properties have been performed on as-received plates of F82H (first heat n° 9741), JLF-1 and experimental heats LA12TaLC and LA12LC.

F82H and JLF-1 specimens have been obtained from as-received plates of 7.5 mm and 15 mm thick in the normalized and tempered (N&T) condition. LA12TaLC and LA12LC specimens were obtained from 3.5 mm thick plates in the normalized + tempered + 10% cold-worked (N&T-CW) condition. Tensile and impact properties of F82H and JLF-1 have been determined in the longitudinal and transverse directions of plates. Charpy tests have been conducted with three types of specimens: subsize (3 x 4 x 27 mm³) used in HFR irradiation, quasi-standard (2.5 x 10 x 55 mm³) used in Phenix irradiation and standard ones (10 x 10 x 55 mm³) to study the effects of small samples on the DBTT and USE parameters.

Mechanical properties of RA martensitic materials present adequate strength and ductility levels, comparable to conventional 9Cr-1Mo martensitic. No significant differences were obtained between specimens tested in the longitudinal and transverse direction of plates.

Tensile properties are sensitive to the metallurgical condition. Up to 500°C, cold-worked (N&T-CW) materials exhibited higher tensile strength than N&T specimens, that is 0.2%P.S. of about 660 MPa for N&T-CW and 520 MPa for N&T measured at 20°C.

In contrast to tensile behavior, all L.A. alloys presented quite similar impact properties for both metallurgical conditions. Table II displays results obtained from Charpy V tests performed on subsize specimens.

Table 2: Tensile characteristics measured at 20°C and impact properties of L.A. martensitic steels.

Steel	Tensile properties at 20°C		Impact properties	
	0.2% P.S. (MPa)	Reduction in Area (%)	DBTT (°C)	U.S.E. (J)
F82H	520	81	-75	9.4
JLF-1	504	79	-90	9.9
LA12LC	655	80	-75	8.6
LA12TaLC	661	77	-70	9.3

Ageing treatments

Different kind of specimens have been machined (tensile, Charpy V, samples for hardness and TEP measurements) to characterize the evolution after thermal ageing of initial metallurgical structure and mechanical properties.

In the case of F82H and JLF-1 materials, samples have been obtained from as-received plates of 7.5 mm thick in the normalized and tempered condition. LA12TaLC and LA12LC specimens were obtained from 3.5 mm thick plates in the normalized + tempered + 10% cold-worked condition.

Ageing treatments, performed at 250, 350, 400, 450 and 550°C for 2000h and 10000h, started on beginning 96. Treatments for 2000h ageing time have been finished on July 96. In the next time, mechanical properties of aged specimens will be determined and compared to the initial condition.

Ferrite Formation in F82H-mod. and OPTIFER alloys

E. Materna-Morris

Forschungszentrum Karlsruhe

The martensitic structure of F82H-mod. was tested with regard to thermal stability. As found in former investigations, the martensitic structure can transform partly into ferrite at the temperature range of α - γ transformation e.g. at 875 °C for 0.5 h or 2 h. This ferrite transformation was found for the as-received condition of 1040 °C 38 min + 750 °C or after a second austenitization of 1040 °C and higher annealing temperatures. Small samples of the steel F82H-mod. and several OPTIFER alloys were tempered in the furnace to determine systematically the temperature range of start and end of the ferrite formation. The heat treatments were performed in 20°-paces between 800 and 920 °C. The chemical composition of these alloys are collected in Table 1.

The material was studied in etched metallographic cuts by light microscopical and scanning electron microscopical methods. The chemical compositions were determined by EDX. The ferrite components were quantitatively measured by image analysis. First transmission electron microscopical images were made.

The temperatures of the analyzed samples are marked in the phase diagram of 0.1 % C steels (Fig.1-3). The black area of the spots indicates the relative content of the ferrite formations. Ferrite was found between the temperatures of A_{C1b} and A_{C1f} . The maximum ferrite contents were found in:

Alloy	Ferrite %	Temp. °C
F82H-mod.	17	880
736	12	840
735	5	860
734	3	840

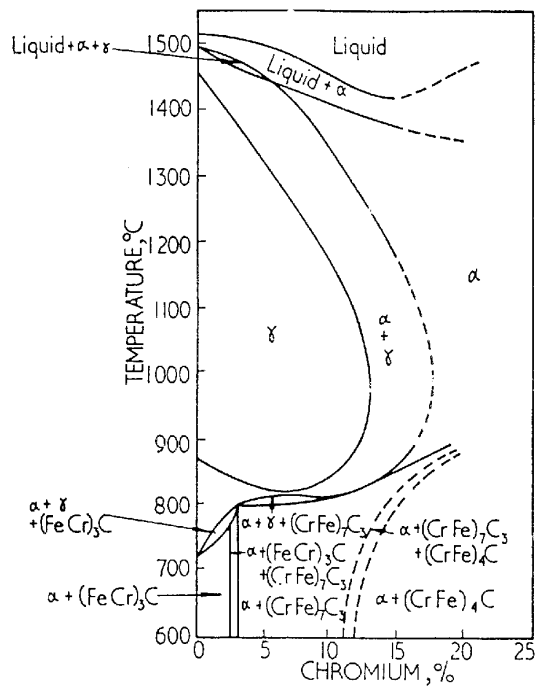


Figure 1: Effect of chromium content on equilibrium relationships in 0.1% C steels.

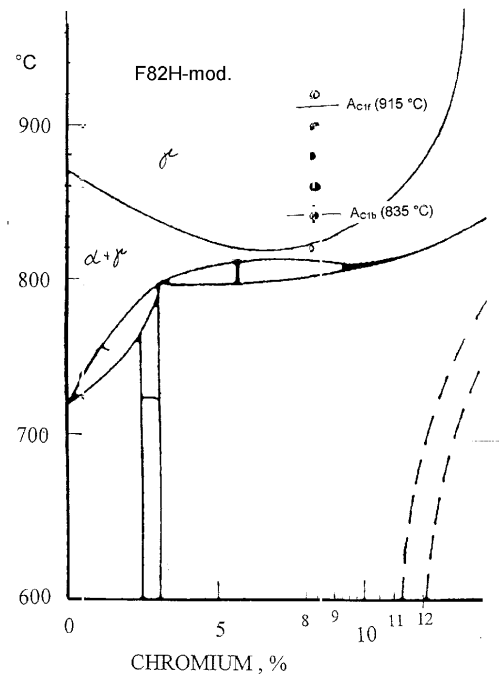


Figure 2: Phase diagram of F82H-mod.

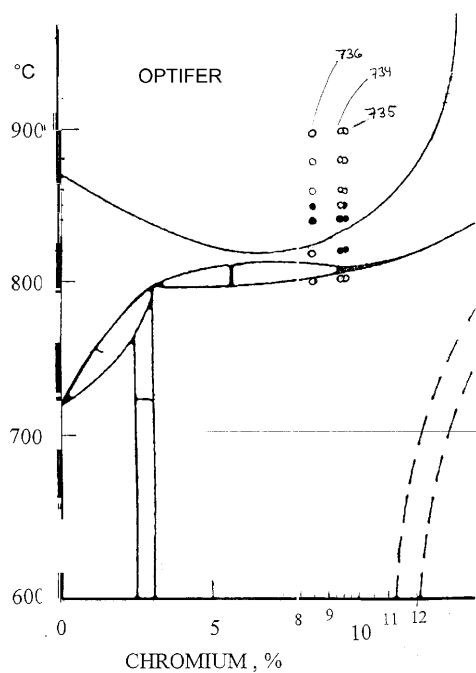


Figure 3: Phase diagram of OPTIFER 734, 735 and 736.

The Vickers hardness was measured in the F82H-mod., too. The ferrite was very soft with 200 HV_{0.1}. The martensite was relatively hard and the hardness of 450 HV_{0.1} is the value of quenched martensite. The EDX analysis of the Cr contents showed a small increase of about 0.5 - 1.0 wt.% in the martensite. In transmission electron microscopy the structureless ferrite and the quenched martensite with the M₂X phase could be observed (Figs.4a and 4b).

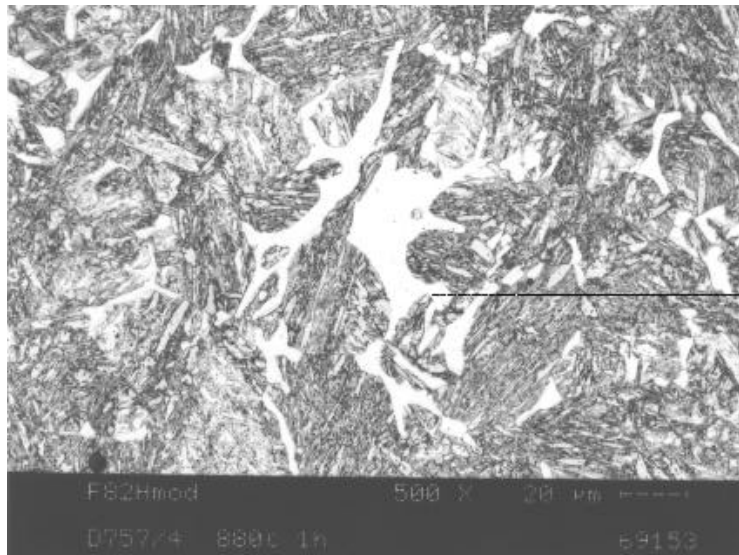


Figure 4a: F82H-mod., metallographic cut
(880 °C, 1h)

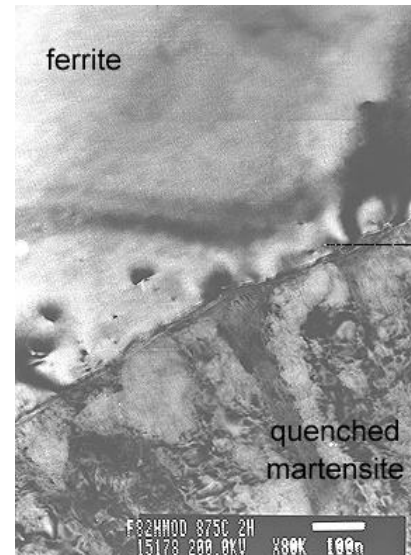


Figure 4b: F82H-mod., TEM,
(875°C, 2h)

The investigations show that in the region of a α - γ -transformation not only austenite is formed, but also ferrite. A possible explanation for this behavior is the following: Some grains which start transformation into austenite can solve a high concentration of carbon. Carbon is partially provided by the dissolution of carbides like M₂₃C₆ and partially dragged by diffusion from neighbor grains which thus loose carbon and then transform into ferrite. During the follow-on cooling process to RT ferrite is retained whereas the austenite phase is retransformed to martensite. Fig. 5 shows such a „duplex“ structure in TEM observation. Partly, the materials had the appearance of bainitic structure, too, but this phase could not be proved by dilatometric measurements.

In F82H-mod. a part of the carbon was not bound by strong carbide forming elements like Ta or Ti, because these elements often formed large inclusions with the following composition of Al-Ta-Ti-V-O. Probably, the elements were added too early to the melt and oxidized.

The mechanical behavior of the irradiated material is finally important. Probably, the soft ferrite phase can influence positively the impact properties during or after irradiation.

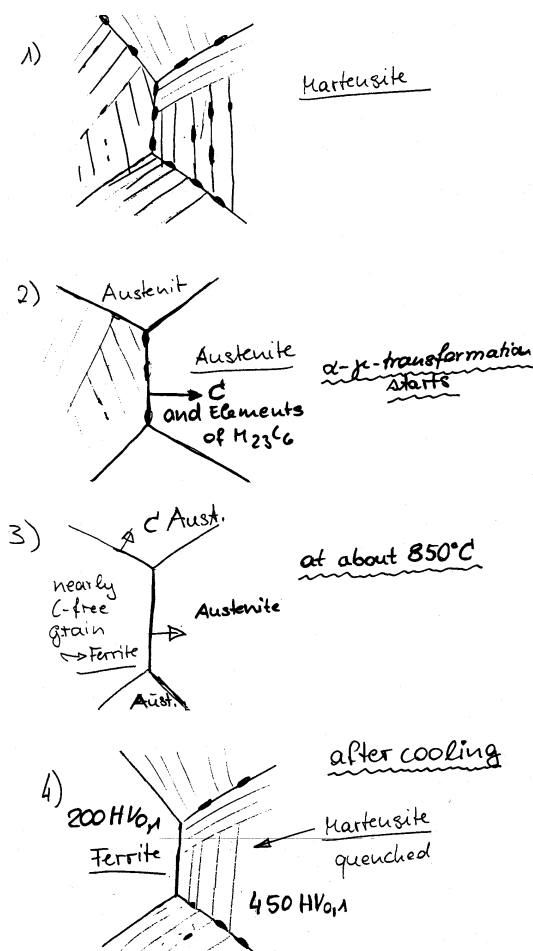


Figure 5: Schematic formation of Ferrite.

Tab.1: Chemical composition of the investigated alloys.

	F82H-mod.	OPTIFER 736	OPTIFER 734	OPTIFER 735
Fe	Basis	Basis	Basis	Basis
Cr	7.68	8.46	9.41	9.48
C	0.088	0.095	0.13	0.125
Mn	0.156	0.38	0.61	0.55
P	-	0.004	0.002	0.0015
S	-	0.0025	0.004	0.003
V	0.162	0.21	0.277	0.245
B	-	-	-	-
N	-	0.0263	0.0222	0.044
W	-	1.04	-	0.985
Ta	0.009	0.076	0.095	0.065
Ge	-	-	0.37	-
Ce	-	-	<0.01	-
Nb	0.01	-	-	-
Mo	<0.003	-	-	-
Ni	0.021	-	-	-
Cu	0.0063	-	-	-
Al	0.0016	-	-	-

Si	-	-	-	-
Ti	<0.003	-	-	-
Co	0.0037	-	-	-

Tensile- and impact bending-properties of the steels MANET F82H-mod. and OPTIFER-IV

L. Schäfer

Forschungszentrum Karlsruhe

Figs. 1, 2 and 3 show the impact energy of the steels MANET-II, F82H-mod. and OPTIFER-IV in dependence of the test temperature. The ductile-to-brittle transition temperature, DBTT, increases with increasing austenitization temperature T_{AV} and decreases with increasing annealing (tempering) temperature T_{AN} . The best values are: DBTT = -50°C for MANET II; DBTT = -55°C for F82H-mod., and DBTT = -118°C for OPTIFER-IV. The upper shelf energy, USE, is sufficient for all alloys.

Figs. 4, 5 and 6 show the 0.2% yield strength at 500°C of the mentioned steels in dependence of the austenitization temperature. The strength increases with decreasing annealing temperature T_{AN} . Below an exhaustion temperature the strength increases with increasing austenitization temperature T_{AV} . The strength fulfills the requirements. The ductility at 300°C is limited below $A = 15\%$.

Figs. 7, 8 and 9 show the 0.2% yield strength at 500°C and the DBTT of the mentioned steels in dependence of the austenitization temperature and the annealing temperature. With decreasing austenitization temperature DBTT decreases and with decreasing annealing temperature the strength increases, as mentioned above. It is possible to obtain any combination of strength and toughness in the tested region by varying T_{AV} and T_{AN} . Fig. 10 shows a comparison of the mentioned steels. The OPTIFER-steels are much more tough than MANET II and F82H-mod.

Comparison of the steels OPTIFER Ia, Ib, II, III and IV

Fig. 11 shows the hardness and grain size of OPTIFER-steels in dependence of the austenitization temperature T_{AV} . Between 900 and 1050°C the values are generally sufficient.

Fig. 12 shows the hardness of OPTIFER-steels in dependence of the annealing temperature. The behavior of all steels is very similar (with exception of OPTIFER-III).

Fig. 13 shows the impact energy of OPTIFER-steels in dependence of the test temperature. The succession beginning with the test steel (lowest DBTT) is: OPTIFER-IV, -Ia+b, -II and -III.

Fig. 14 shows the tensile properties of OPTIFER-steels in dependence of the test temperature. The properties of all steels are very similar (with exception of OPTIFER-III). The demands are fulfilled with exception of total elongation at $\sim 300^{\circ}\text{C}$.

Fig. 15 shows the creep rupture strength of OPTIFER-steels in dependence of the Larson-Miller-parameter $P = T_K (25 + \log t_m) \cdot 10^{-3}$. There are no important differences between the steels (with exception of OPTIFER-III).

Table 1 contains some properties from tensile and impact bending tests in order to compare the steels OPTIFER-Ia, OPTIFER-IV, F82H-mod. and MANET-II. These values complete the data in Fig.10.

Table 1: Comparison of some tensile and impact bending properties of the steels OPTIFER-Ia, OPTIFER-IV, F82H-mod., and MANET II

T _{AU} in °C	T _{AN} in °C	Steel	DBTT in °C	USE in J	T = 500°C		
					R _{p0.2}	R _m in Mpa	A in %
900	700	OPT.-Ia	-	-	489	513	15,1
"	"	OPT.-IV	-102	260	458	482	18,3
"	"	F82Hm.	-	-	507	523	15,8
"	"	MAN.-II	-34	-	518	546	18,2
"	730	OPT.-Ia	-91	260	435	463	16,0
"	"	OPT.-IV	-110	260	408	442	21,8
"	"	F82Hm.	-49	-	457	475	16,6
"	"	MAN.-II	-39	-	463	495	18,6
"	750	OPT.-Ia	-	-	-	-	-
"	"	OPT.-IV	-118	260	392	430	18
"	"	F82Hm.	-55	-	406	428	17,0
"	"	MAN.-II	-50	160	419	457	20,4
950	700	OPT.-Ia	-	-	516	539	14,6
"	"	OPT.-IV	-	-	514	538	16,6
"	"	F82Hm.	-34	260	506	524	15,4
"	"	MAN.-II	-16	-	527	558	23,0
"	730	OPT.-Ia	-	-	444	472	16,2
"	"	OPT.-IV	-105	260	410	445	20,5
"	"	F82Hm.	-40	260	468	486	16,5
"	"	MAN.-II	-30	160	487	519	20,5
"	750	OPT.-Ia	-	-	-	-	-
"	"	OPT.-IV	-111	260	390	425	20,0
"	"	F82Hm.	-44	270	410	432	16,9
"	"	MAN.-II	-38	-	427	469	21,4

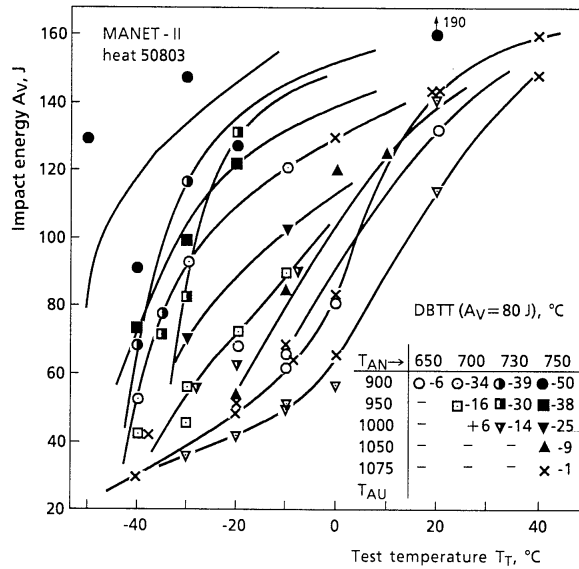


Figure 1: Impact energy of the steel MANET-II with different thermal treatment in dependence of the test temperature. The best DBTT is -50°C

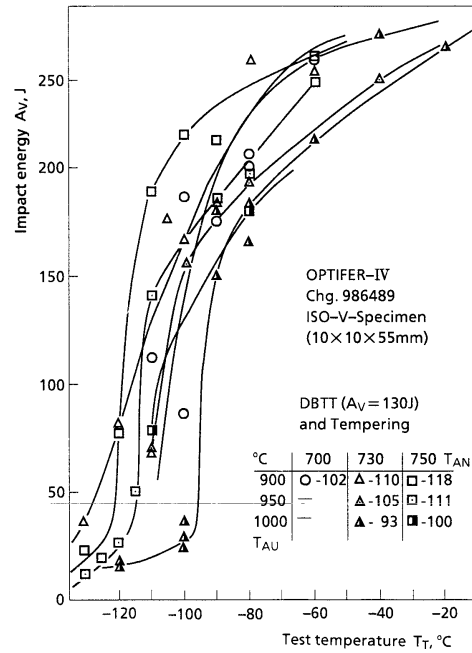


Figure 3: Impact energy of the steel OPTIFER-IV with different thermal treatments in dependence of the test temperature. The best DBTT is -118°C

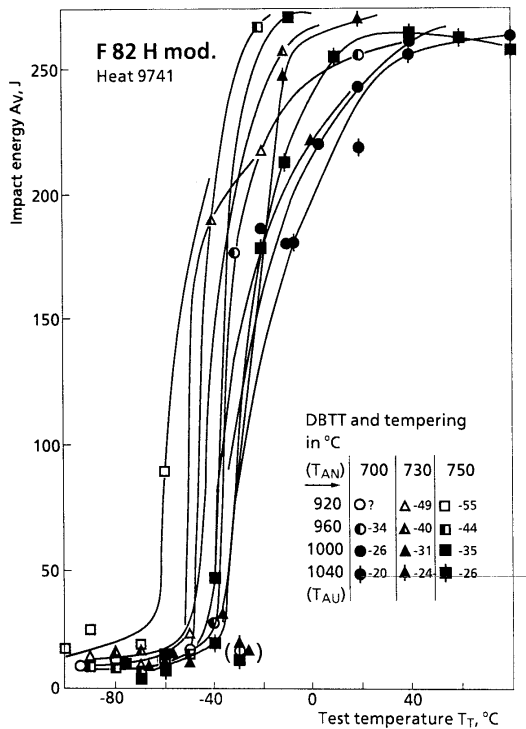


Figure 2: Impact energy of the steel F82H-mod. with different thermal treatment in dependence of the test temperature

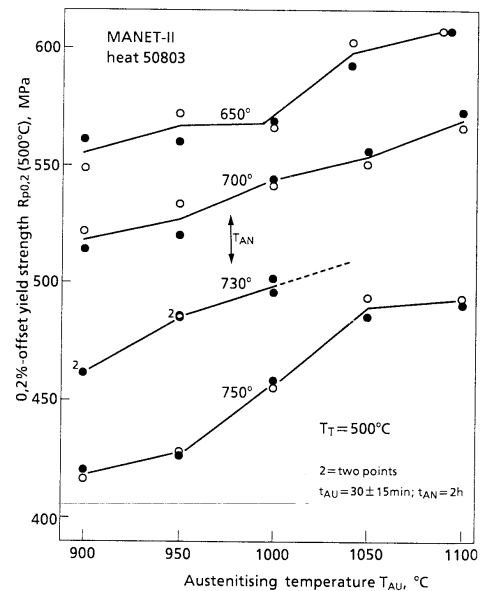


Figure 4: 0,2%-yield strength at 500°C of the steel MANET-II in dependence of the austenitization temperature and the annealing temperature

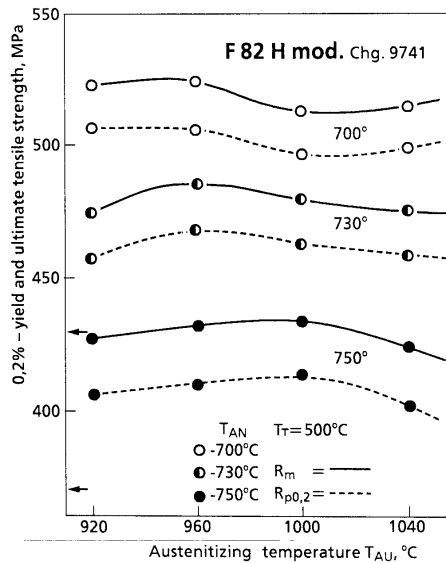


Figure 5: 0,2%-yield strength and ultimate tensile strength at 500°C of the steel F82H-mod. in dependence of the austenitization temperature and the annealing temperature

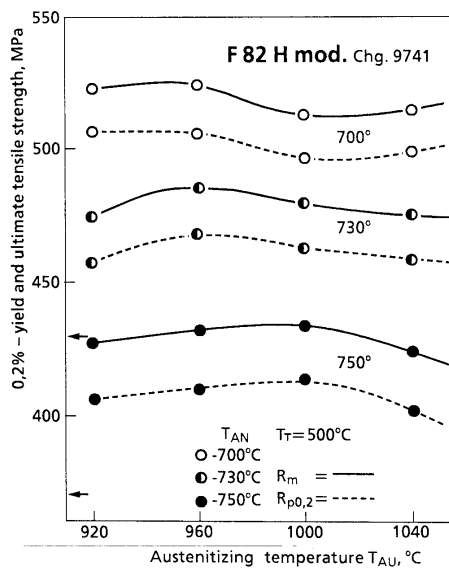


Figure 6: 0,2%-yield strength and ultimate tensile strength at 500°C of the steel OPTIFER-IV in dependence of the austenitization temperature and the annealing temperature

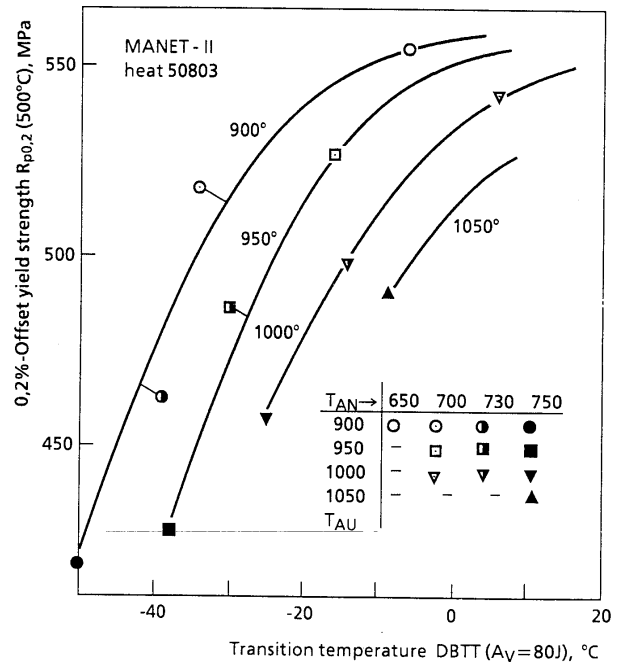


Figure 7: 0,2%-yield strength at 500°C and DBTT of the steel MANET-II in dependence of the austenitization temperature and the annealing temperature

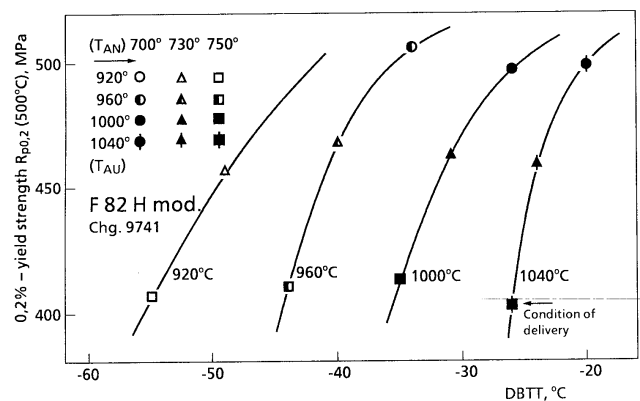


Figure 8: 0,2%-yield strength at 500°C and DBTT of the steel F82H-mod. in dependence of the austenitization temperature and the annealing temperature

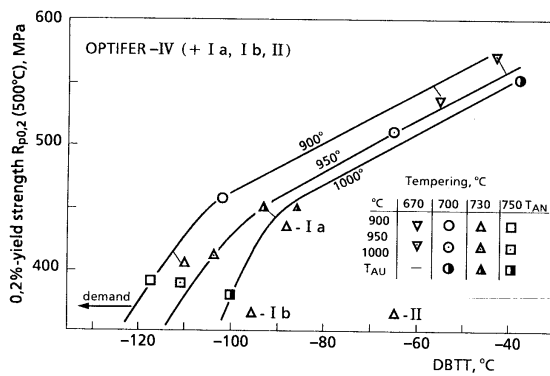


Figure 9: 0,2%-yield strength at 500°C and DBTT of the steel OPTIFER-IV in dependence of the austenitization temperature and the annealing temperature

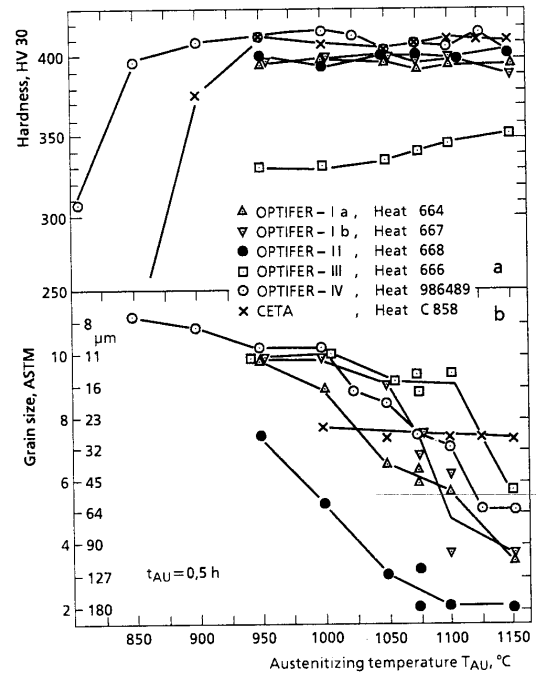


Figure 11: Hardness and grain size of OPTIFER-steels in dependence of the austenitization temperature, $900^{\circ}\text{C} \leq T_{\text{AU}} \leq 1050^{\circ}\text{C}$ is sufficient

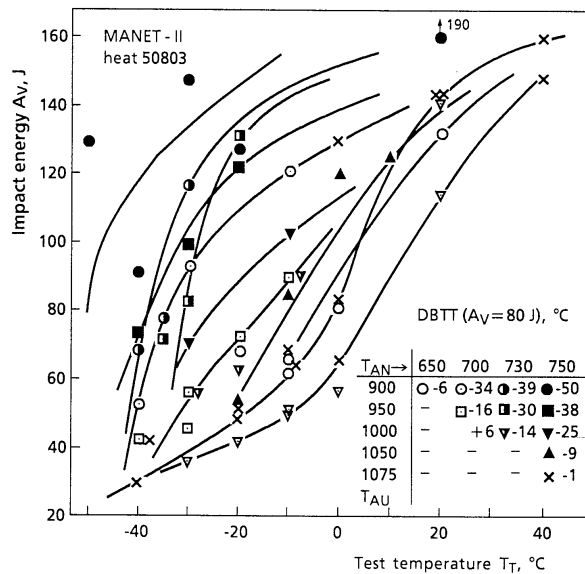


Figure 10: Comparison of the steels MANET-II, F82H-mod. and OPTIFER-IV concerning the 0,2%-yield strength and the DBTT, OPTIFER-IV is tougher than MANET-II and F82H-mod.

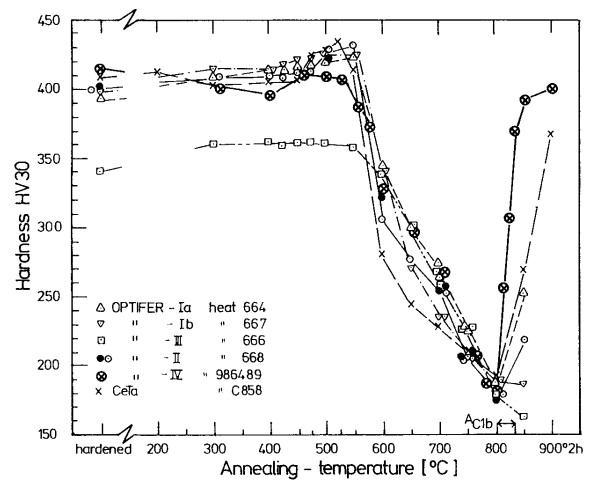


Figure 12: Hardness of OPTIFER-steels in dependence of the annealing temperature

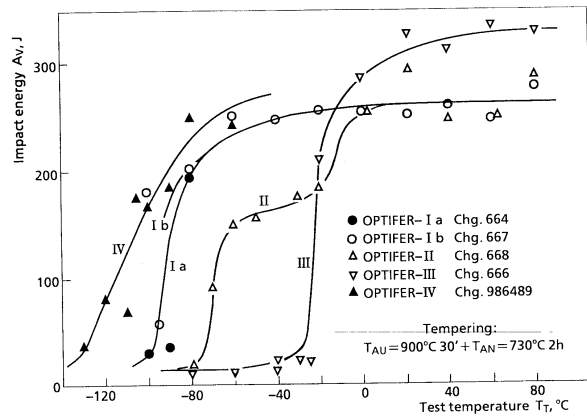


Figure 13: Impact energy of OPTIFER-steels in dependence of the test temperature. The lowest DBTT shows OPTIFER-IV

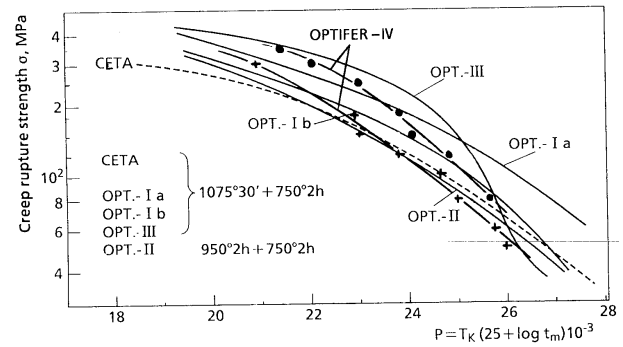


Figure 15: Creep rupture strength of OPTIFER-steels in dependence of the Larson-Miller-parameter

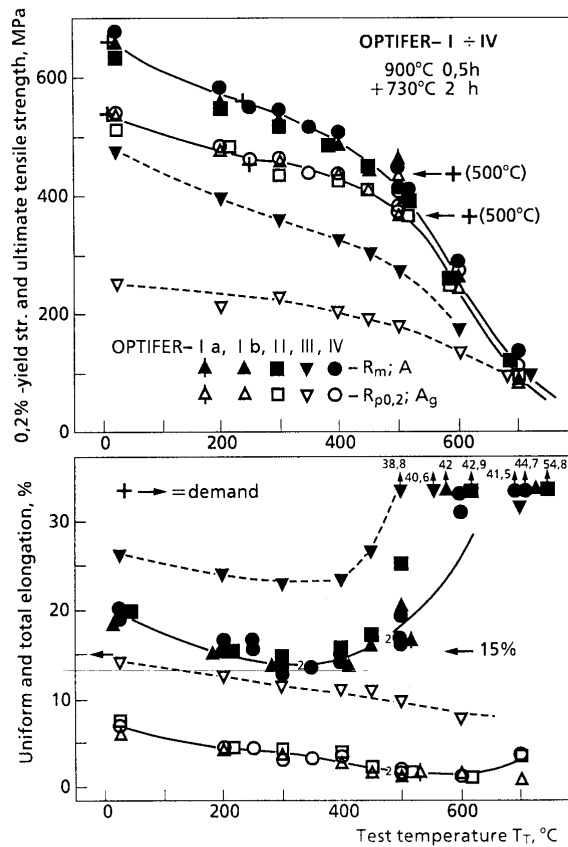


Figure 14: Tensile properties ($R_{p0.2}$, R_m , A and A_g) of OPTIFER-steels in dependence of the test temperature

Mechanical properties of F82H-mod.: Tensile test and low cycle fatigue

M. del Pilar Fernandez Paredes

CIEMAT

With the objective to study the mechanical behavior of this low activation steel (F82H-mod.), CIEMAT have performed tensile tests and low cycle fatigue tests for the as-received material and aged material in the range of 300 - 500 °C during 500, 1000 and 5000 hours. The selection of these treatments have been chosen in function of the temperature gradient (300 - 500 °C) in which the first wall materials in fusion reactors will operate.

In a primary phase of mechanical characterization we have studied the tensile behavior of the steel F82H-mod. as-received in function of the temperature (ambient, 300, 400 and 500 °C), comparing the results of this alloy with others steel with similar characteristics such as OPTIFER alloys (Fig 1).

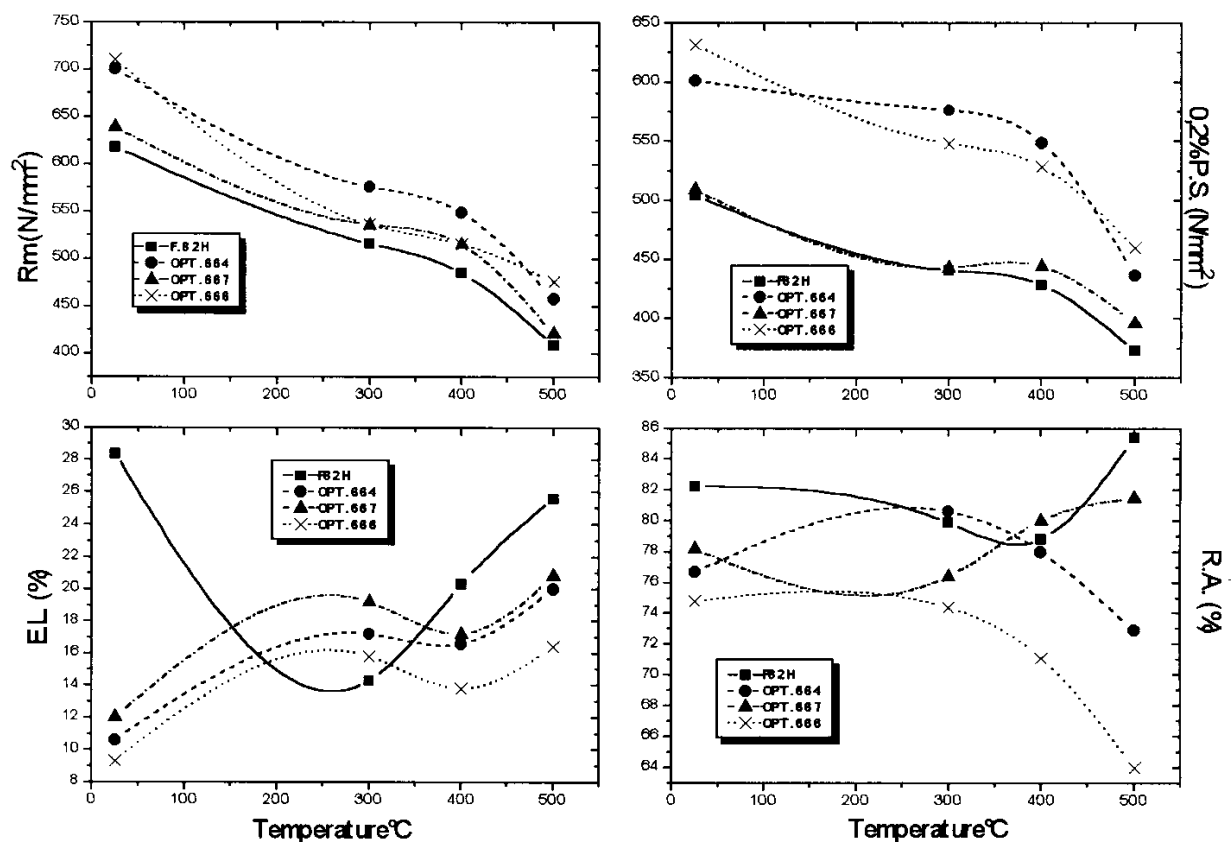


Figure 1: Tensile test results on as-received materials.

Both steels show a behavior characteristic of ductile materials, having a decrease of ultimate stress and 0,2 % proof stress with increasing test temperature. As can be seen in the figure, F82H-mod. alloy shows similar properties in tensile test with respect to 667 OPTIFER alloy. Not only do both materials show similar values in the tensile test but also have similar hardness values of about 210 HV30 for the as-received material.

In a second step, tensile tests on aged material also have been performed. F82H-mod. was aged at 300, 400 and 500 °C during 500, 1000 and 5000 hours. The test temperature was the same as that for the ageing treatment. The results are plotted in figure 2. As can be seen in this graph the time of ageing has not influenced the ultimate tensile test and yield stress. This fact is in concordance with the hardness values, which for all ageing treatments are similar, approximately 210 HV30. The hardness measurements on as-received and aged material is the same. This is in agreement with the higher stability of microstructure observed on aged material by optical and scanning microscopes.

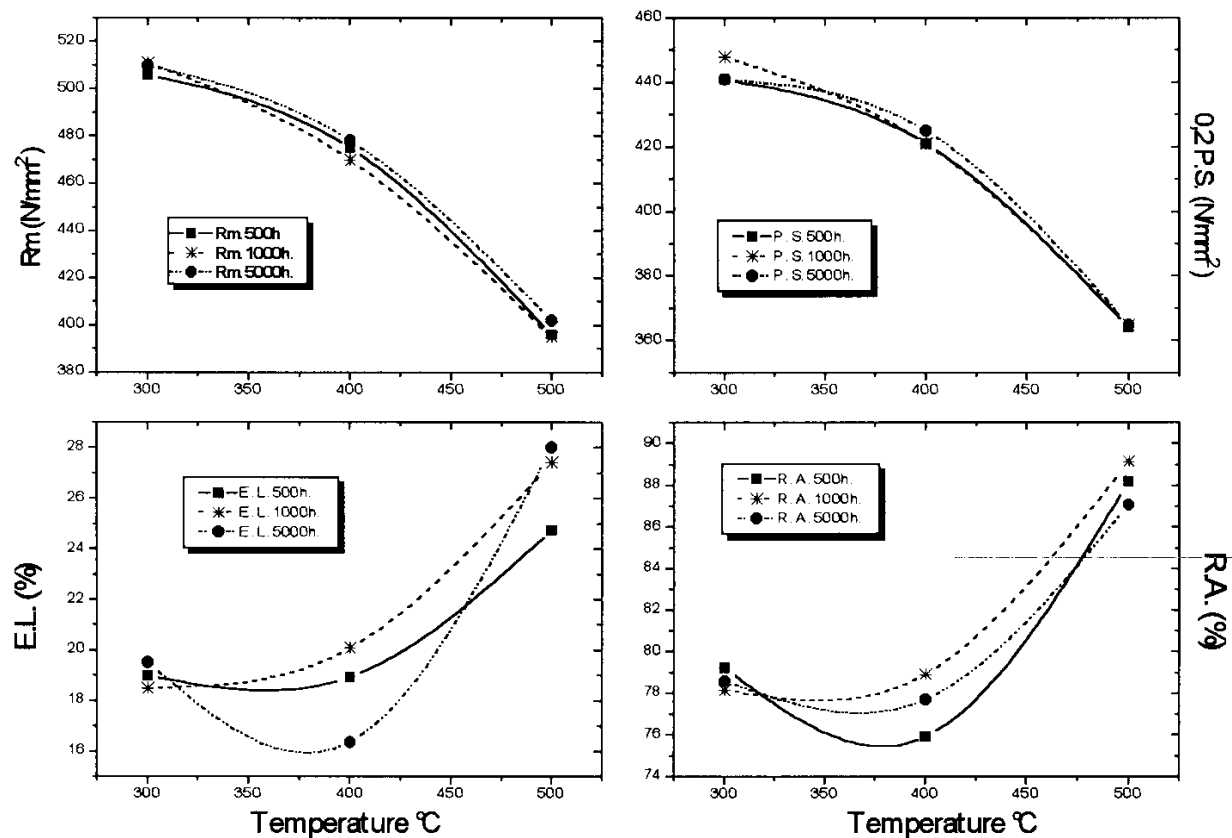


Figure 2: Tensile Test results on aged material.

If one compares Figure 2 and 3, it can be observed that the results for the ultimate tensile stress and 0,2 % proof stress are the same as for the as-received and aged material. For example at 300 °C, the ultimate tensile stress is about 512 MPa and for aged material is approximately 5 MPa.

The fracture surface was entirely ductile for all specimens tested. Examination of ductile fracture surface by SEM revealed equiaxed dimples formed during microvoid coalescence under conditions of uniaxial tensile load.

Another type of mechanical characterization test that CIEMAT has performed to date is Low Cycle Fatigue on as-received material (test temperature 400 °C and strain rate $5 \cdot 10^{-3} \text{ s}^{-1}$), because fusion reactor systems will operate under pulsed power condition, leading to cycles stressing and fatigue of the first wall structural materials. The first results are shown in Figure 3. In this figure total deformation against cycles to failure are plotted.

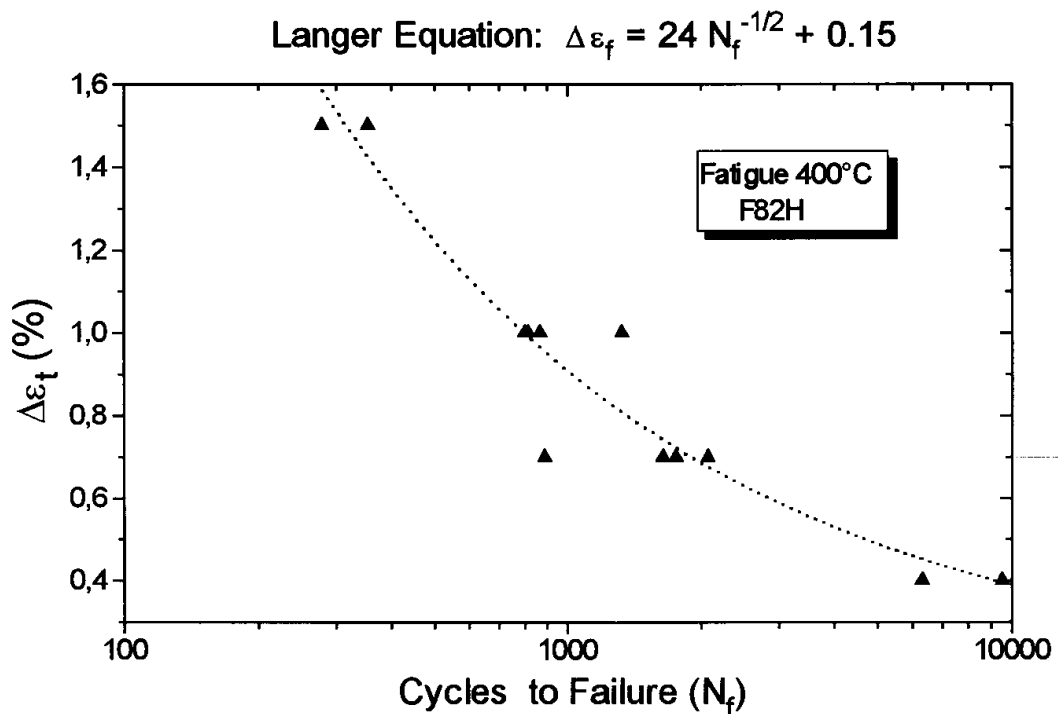


Figure 3: *Low cycle Fatigue Test on as-received material.*

The study of the fracture surfaces of samples tested showed that the fracture occurred transgranularly with various cracks initiation. The propagation took place via plateaus presenting fatigue surface with high density of striations characteristic of stage II crack growth. Another important factor is the existence of microcracks in all crack growth surface, which in some cases are associated with Ta and Al inclusions characteristic of this type of steels.

Structural and mechanical properties of Ti-bearing L.A. BATMAN steels

G. Filacchioni, F. Attura, E. Casagrande, U. de Angelis, G. de Santis,
D. Ferrara, M. di Martino, L. Pilloni, and M. Traficante

ENEA

O. Background

Activities carried out in the past years and those presently running, are essentially devoted to study the validity of the use of titanium as an alternative choice to the „universal“ utilization of tantalum from the standpoint of Prior Austenite Grain Size's control and precipitation strengthening (via Carbides) element.

The primitive chemical composition (BATMAN 91X) was responsible of some drawbacks like undesirable coarse „blocky“ and preferentially oriented primary carbide-nitride precipitation. Moreover, transformation temperature (A_{c1}) was found to be too low (high Mn amount) so limiting the useful tempering temperature's domain.

As a consequence a second generation of BATMAN (7 nuances) steels was realized: most relevant differences in elemental compositions were a reduced Ti and N amount, a drastic reduction on Mn content and a Cr wt.% between 7.5 to 8.5. Tungsten was maintained in the order of $\approx 1.5\%$ so to have sufficient creep strength.

Then, the new heats of L.A. Ti-bearing steels have been tested either from the standpoint of structural or mechanical behavior.

1. Experimental activities

Physical metallurgy knowledge of BATMAN alloys was improved and completed by drawing CCT diagrams and determining transformation temperatures for each nuance.

The investigation on thermal-mechanical treatment's effects on mechanical properties, essentially impact toughness, of BATMAN IIC and IID (the nuances chosen for irradiation Phase Ia) was done by performing different thermal treatments on as hot rolled 25 mm thick plates.

tempering of „as received“ product at $730^{\circ}\text{C} \times 1 \text{ h}$ (plates have been realized with initial and final rolling temperature of 1200 and 1050°C respectively) so to study the solubility level and topography of TiC precipitation in a coarse grain structure

austenitization at 1100°C (1 h) followed either by air cooling or water quenching. Each one of the so obtained structures, have been subsequently tempered at 730°C (1 h) and cooled by the same cooling media used for austenization.

the same above reported procedure of austenitization + tempering with different cooling rates but austenitization temperature decreased to 970°C

austenitization at 1100°C + 24 hours exposition at 630°C + tempering at 730°C (1 h), air cooling.

Finally we dispose of nominally very different metallurgical states (a, b and c procedures) plus an interesting structure due to the d) treatment: a secondary induced precipitation preceding the tempering treatment (precipitates likely decorating the partially recovered dislocation network without coarsening or ripening effects on particles).

Finally, BATMAN's tensile behavior and impact properties have been compared to those of European L.A. candidates as well as to the ones of „reference“ F82H-mod. steel.

2. Discussion of results

The work performed on the first and second generation of Ti-bearing martensitic steels and the results we obtained have shown and confirmed the effectiveness of an alternative carbide forming element, titanium instead of tantalum. Titanium could represent a reduced activation substitute for Nb as far as the grain control is a capital feature to get ductility and toughness.

Ti alloying allows higher normalization temperature and a fully martensitic structure is still obtained up to cooling rates of 70°C/h. A double normalization treatment has proven to be an effective tool to get a fine and homogeneous grain's morphology.

Tempering temperature field has been largely increased (A_{c1} critical temperature has been raised up to $\approx 840^\circ\text{C}$) and coarse, blocky appearance and preferentially oriented presence of Ti(C, N) avoided. Round-shaped Ti carbo-sulphides provide no difference between longitudinal or transverse mechanical properties.

Tensile properties are adequate and the impact resistance improved. Mechanical resistance is comparable to that of the strongest EU candidate, while tensile ductility is inferior only to that of the weakest L.A. martensitic steel. Upper Shelf Energies are even better than those of other candidate L.A. alloys.

Cyclic behavior of the martensite steel F82H-mod. compared to MANET II

C. Petersen and R. Schmitt

Forschungszentrum Karlsruhe

1. Isothermal fatigue results

A comparison of isothermal fatigue behavior between F82H-mod. and MANET II shows at temperatures of 450°C and 550°C with a total strain range of 1 % only a small reduction in number of cycles to failure, but with decreasing total strain range (0.6 %) the reduction in number of cycles to failure decreases of about 40 to 50 percent.

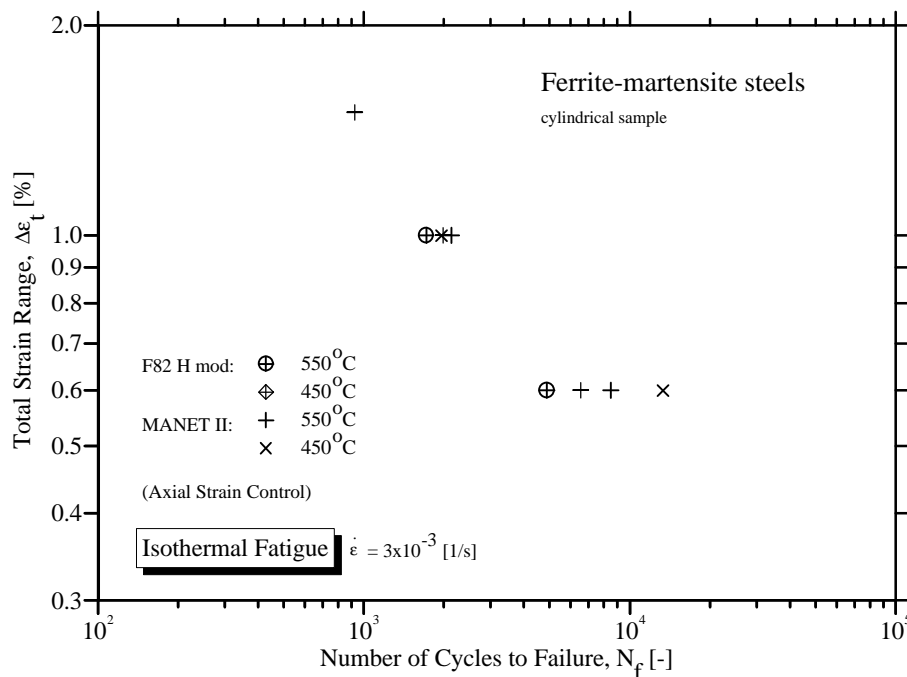


Fig 1: Comparison of isothermal fatigue behavior between F82H-mod. and MANET II (First results)

2. Thermal fatigue results.

The comparison of thermal fatigue behavior between F82H-mod. and MANET II shows at temperature changes of 200 - 600°C and 200 - 650°C at increased total mechanical strain ranges a drastic reduction in number of cycles to failure of about one order of magnitude.

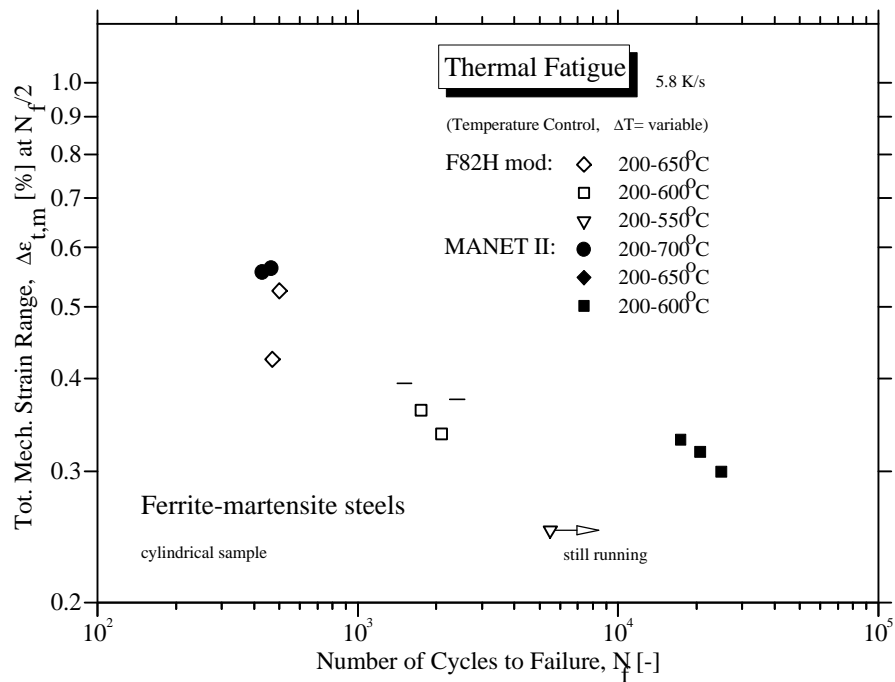


Fig. 2: Comparison of thermal fatigue behavior between F82H-mod. and MANET II. (First results)

3. Parameter definition for thermal fatigue round robin (TFRR).

Thermal fatigue and thermomechanical fatigue tests will be performed in air atmosphere.

- Heating and cooling rate is 5 K/s.
- Temperature range is defined to 200°C - 600°C, to reach total mechanical strains of about 0.4 % in case of thermal fatigue and convenient testing times.
- Mechanical clamping of the sample in case of thermal fatigue should be performed at the low temperature (200°C) of the cycle.
- Total mechanical strain value in out of phase thermomechanical fatigue experiments should also be chosen to 0.4%.

4. Sample manufacturing for participants of TFRR.

Sample manufacturing for the four participants of TFRR, which are ENEA, EPFL, JRC and FZK, each with their specific shape, from F82H-mod. (28mm plate), perpendicular to the rolling direction, will be finished in Dec. 1996.

SHORT SUMMARY OF THE ECN CONTRIBUTION AT THE AG1-MS02 DISCUSSION MEETING KARLSRUHE, SEPTEMBER 1996

E.V. van Osch

ECN Petten

Recent results on F82H-mod. in the non-irradiated state (reference testing) and on irradiated conventional 9Cr-steel T91, have been presented as contribution to the characterization of F82H-mod. steel.

In addition to the characterization testing of the various plates of the first heat, ECN has also characterized the 25 mm plate of the second heat. Results from metallography, hardness and tensile testing, fracture resistance and impact testing have shown a fully martensitic, homogeneous and equiaxed microstructure without texture in properties. Both heats are almost identical, with minor variations in tensile properties. At 500 C a severe strain rate dependency of tensile properties has been demonstrated. The uniform elongation values are rather low, although this is common to all FM steels (AG 5% strain). Conventional tensile tests at 500 C, with strain rates ranging from $5 \cdot 10^{-6} \text{ s}^{-1}$ to $1 \cdot 10^{-4} \text{ s}^{-1}$, have shown even lower uniform elongation with minor strain hardening capacity. Fracture resistance (J-a) tests at various temperatures, ranging from 300 K to 600 K, provided highly reproducible R-curves for thickness (B) of 10 and 12 mm. The ECN tests with RR-KLST specimens provided a small transition range with fully brittle or fully ductile fractures (overlap of LSE and USE temperature regions). A similar test series with ECN-KLST specimens provided oscillations around the transition curve, similar to the FZK compilation of all RR-KLST results. Ranking of F82H-mod. in terms of fracture toughness, places this

material in the second position between T91 (first) and MANET (third). The results on thermal expansion and thermal conductivity differ from literature data for MANET steel. This will be verified experimentally.

Post-irradiation testing of F82H-mod. with 2.5 dpa will start, according to the original time schedule, during the final quarter of 1996. The delayed delivery of welded materials will effect the irradiation planning.

Results on irradiated T91 were presented for comparison with F82H-mod. and other steels (e.g. MANET). Tensile properties of tested (40 mm thick) T91 steels are in accordance with RCC-MR17S average and minimum curves. Irradiation at 80 C and 300 C provide almost identical tensile properties for a temperature range of 150 C (75 C-225 C). At higher temperatures up to 400 C, the 80 C irradiated specimens show annealing of the irradiation hardening whereas the 300 C irradiated specimens do not show this recovery effect. Irradiation does not significantly affect the fatigue life for applied strain ranges between 0.6 and 1.4% strain, whereas cyclic stress-strain curves are strongly changed (irradiation hardening of 100-300 MPa). The T91 specimens in the non-irradiated state show modest cyclic softening, whereas irradiated specimens exhibit severe cyclic softening. Irradiation (2.5 dpa-573 K) reduces the fracture toughness of T91 steels, but significantly less compared to HT9 and MANET. Ranking of T91, HT9 and MANET, in terms of post-irradiation toughness, places T91 in first position, followed by HT9 and MANET in second and third position respectively. Particularly MANET steel has very low post-irradiation fracture resistance. First results on HFR irradiated F82H (not the mod. version) indicate significantly less irradiation hardening compared to MANET and T91.

It is concluded that the conventional 9Cr-steel T91 has excellent mechanical properties, in non-irradiated and in 2.5 dpa irradiated state. Further, the two 5000 kg heats of F82H-mod. fulfill the requirements on reproducibility, microstructure, homogeneity and mechanical properties. Preliminary post-irradiation results indicate improved irradiation behavior in terms of less hardening and less reduction of fracture toughness compared to MANET steel. The 2.5 dpa and 10 dpa irradiations of F82H-mod. plate material are on schedule, but the delayed delivery of welded materials will cause further delay of irradiation experiments.

Evaluation of ferritic/martensitic steels

N.Wanderka, E.Camus, and H.Wollenberger

Hahn-Meitner-Institut

Investigated ferritic/martensitic steels

- ◆ F82H-mod. steel
- ◆ MANET steel (DIN 1.4914)
- ◆ Steel DIN 1.4926

see nominal composition of the alloys in Table 1

Irradiation conditions

- ◆ Irradiation with 300 keV Fe ions; flux 10^{-2} dpa/s; fluence 50 dpa
- ◆ Implantation with 15 keV He ions; implantation rate 2 appm/s
- ◆ Temperature: 523 K to 773 K

Helium bubble density (Figure 1)

Results of the present study on the alloy F82H-mod. are presented together with results on selected ferritic/martensitic alloys. It is obvious from figure 1 that the helium bubble density depends both on the type of alloy and on the helium implantation rate. The latter result shows evidence for need of correlating the results obtained in facilities having different implantation rates.

Radiation-induced segregation of chromium (Figure 2)

The depth profiles obtained by atom probing show fine scale segregation of chromium. This is true for all investigated alloys, of mean chromium concentrations varying between 8 and 11.8 wt.%. Note that the segregation observed in the temperature range between 673 K

and 773K at the flux of 10^{-2} dpa/s is expected to occur at lower temperatures for a smaller displacement rate as being relevant for fusion reactors.

References:

- [1] B.N. Singh and H. Trinkaus, J. Nucl. Mater. 186 (1992), 153.
- [2] P. Dauben, R.P. Wahi, and H. Wollenberger, J. Nucl. Mater. 133-134 (1985) 707.
- [3] P. Dauben, Dissertation, TU Berlin (1986).
- [4] K. Farrell and E.H. Lee, in: Effects of Radiation on Materials, ASTM-STP 955 (1987), 498.
- [5] N. Wanderka, E. Camus, V. Naundorf, C. Keilonat, S. Welzel, and H. Wollenberger, J. Nucl. Mater. 228 (1996) 77.

wt.%	F82Hmod	Manet DIN 1.4914	Steel DIN 1.4926
Cr	8.0	10.3	11.8
C	0.1	0.1	0.21
Si	0.1	0.14	0.36
Mn	0.1	0.75	0.47
P	0.005	0.005	0.016
S	0.002	0.0045	0.003
Ni	0.03	0.65	0.63
Mo	0.01	0.57	0.90
V	0.2	0.19	0.29
Nb	0.0002	0.14	<0.005
⋮			
W	2.0	—	0.02
Ta	0.04	—	—
Fe	bal		

Table 1: Composition of different Fe-Cr martensitic/ferritic steels investigated in the study

Fe-12Cr	Manet DIN 1.4914	Ferritic Steel	F82Hmod	Implantation and Irradiation Conditions	
■	●			1 appm He/s	0.06 at.% He
■	●			1 appm He/s $8 \cdot 10^{-3}$ dpa/s	0.06 at.% He 30 dpa
		▲		0.06 appm He/s $6 \cdot 10^{-3}$ dpa/s	0.09 at.% He 100 dpa
			△	0.5 appm He/s $2.5 \cdot 10^{-3}$ dpa/s	1 at.% He 50 dpa
			□	2 appm He/s 10^{-2} dpa/s	1 at.% He 50 dpa
			●	5 appm He/s $2.5 \cdot 10^{-2}$ dpa/s	1 at.% He 50 dpa
			✱	5 appm He/s	10 at.% He

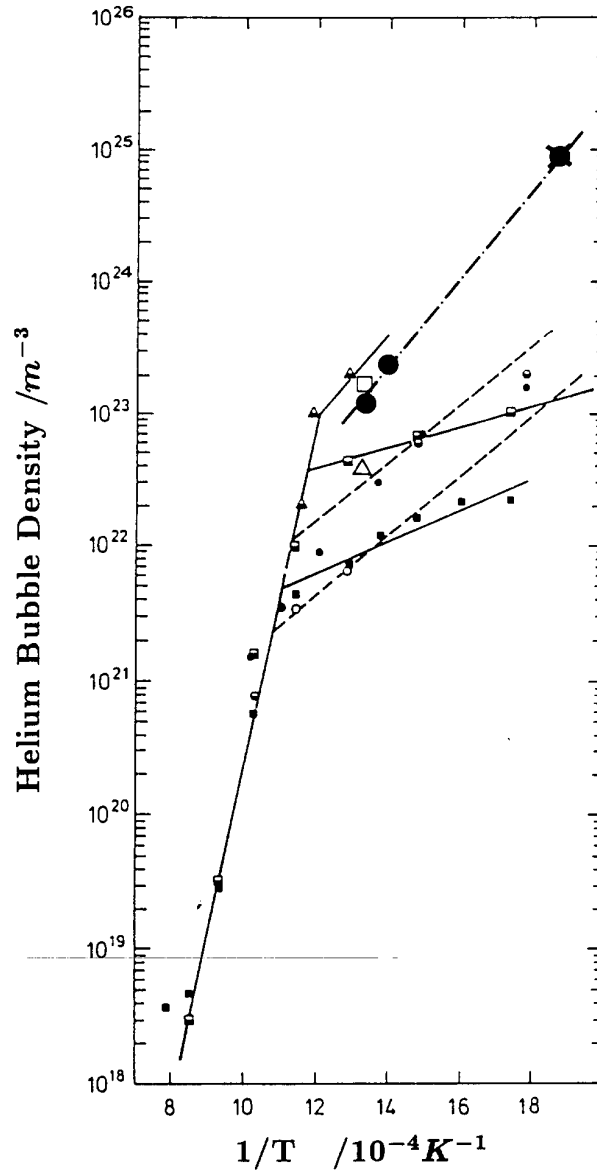


Figure 1: Helium bubble density as a function of reciprocal temperature for different ferritic steels implanted with helium. We show the data compilation by Singh and Trinkaus [1], Dauben et. al [2, 3] and Farrell and Lee [4] together with the present results on the F82H-mod. alloy. It turns out that the helium bubble density is significantly different from one alloy to the another one. (- - -present results)

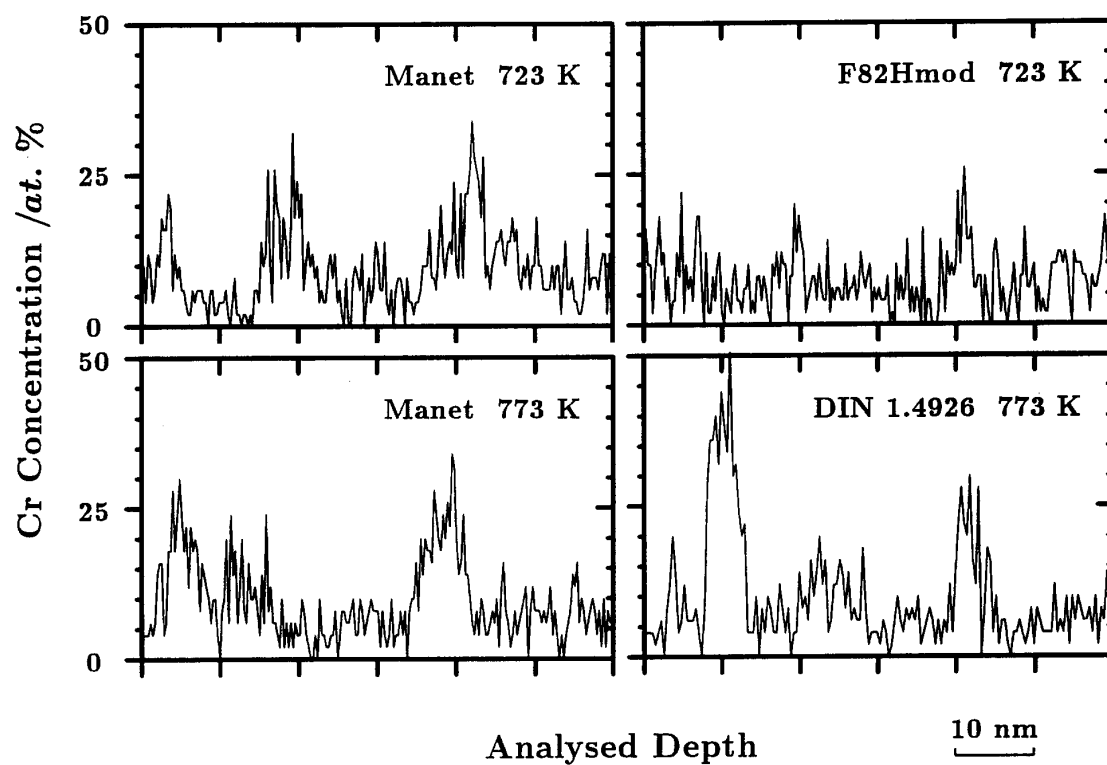


Figure 2: Chromium concentration depth profiles performed by means of atom probing after 300 keV Fe⁺ ion irradiation at a flux of 10⁻² dpa/s to a fluence of 50 dpa and simultaneous implantation of 15 keV He⁺ ions at a rate of 2 appm/s. The nominal chromium concentration varies between 8 and 12 wt.%. All profiles reveal clearly a segregation of chromium.

PRE- AND POST-IRRADIATION PROPERTIES OF PURE IRON AND LOW ACTIVATION STEELS

B.N. Singh and P. Toft

Risø National Laboratory

The present note provides a brief summary of preliminary tensile results on unirradiated and irradiated pure iron, F82H-mod. and MANET-2 low activation steels.

Materials and Experimental Procedure

Thin sheets (0.25 mm thick) of pure iron were purchased from Goodfellow (England) in cold-worked state. A series of annealing experiments were carried out to determine the appropriate annealing condition to give fully recrystallized material. The annealing at 650° for 2 h (in vacuum of $\sim 10^{-6}$ torr) was selected to be the reference annealing condition. This treatment gave an average grain size of ~ 30 μm . The F82H-mod. and MANET-II were obtained from Dr. M. Victoria and were used in the as-supplied condition (i.e. without any heat treatment).

Tensile specimens (see Fig. 1 for dimensions) of pure iron (0.25 mm thick), F82H-mod. (0.3 mm thick) and MANET-2 (0.3 mm thick) were fabricated from the as-supplied materials. The tensile specimens of pure iron were annealed at 650° for 2 h (in vacuum of $\sim 10^{-6}$ torr) before irradiation and tensile testing in the unirradiated condition. Tensile specimens of the F82H-mod. and MANET-II were irradiated and tensile tested (in the unirradiated condition) in the as-supplied condition.

Tensile specimens of pure iron were irradiated with fission neutrons in the DR-3 reactor at Risø (a) at 50°C to dose levels of ~ 0.01 , 0.1 and 0.5 dpa and (b) at 250°C to dose levels of 0.1 and 0.3 dpa. Tensile specimens of F82H-mod. and MANET-II steels were irradiated at 250°C to dose levels of 0.1 and 0.3 dpa. All irradiation experiments were carried out with a damage rate of $\sim 5 \times 10^{-8}$ dpa/s.

Both unirradiated and irradiated specimens of pure iron, F82H-mod. and MANET-2 were tested in an INSTRON machine at a strain rate of $1.3 \times 10^{-3} \text{ s}^{-1}$. In all cases, irradiated and unirradiated specimens were tested at the irradiation temperature. In addition, tensile specimens of unirradiated F82H-mod. and MANET-II were tested at 22, 250 and 350 °C. All tests were carried out in vacuum (10^{-5} torr).

Tensile Results

The average (of minimum two and maximum six) values of the upper yield stress (σ_y^u) or flow stress ($\sigma_{0.2}$), ultimate tensile stress (σ_{max}), uniform plastic elongation (ϵ_u^p) and total elongation (ϵ_t) extracted from stress-strain curves are presented in Table 1 for unirradiated as well as irradiated specimens.

The deformation behavior of pure iron in unirradiated as well as irradiated conditions is shown in Figs. 2 and 3 for 50 and 250 °C, respectively. These results illustrate effects of test temperature, irradiation temperature and displacement dose level (see Figs. 2 and 3). It is interesting to note, for instance, that the specimens irradiated and tested at 250 °C show absence of upper yield stress and yield drop, lower yield stress but significantly higher workhardening rate and lower uniform and total elongations than that in specimens irradiated and tested at ~50 °C.

At the irradiation and test temperature of ~50 °C (Fig. 2), the effects of irradiation on the deformation behavior of pure iron became clearly visible already at the dose level of 0.01 dpa. The most striking feature of these results is the absence of workhardening in the irradiated specimens. It should be noted, however, that at the dose level of 0.5 dpa, there is an indication of some workhardening. It is also of interest to note that the magnitude of yield drop increases with increasing dose level (Fig. 2).

The specimens of pure iron irradiated and tested at 250 °C show a somewhat unusual behavior in that the ultimate tensile strength, σ_{max} , of the irradiated specimens are found to be lower than that of the unirradiated ones (Fig. 3). As can be seen in Fig. 3, this is the result of a reduction in workhardening rate due to irradiation. The observed increase in the yield stress due to irradiation is consistent with the commonly expected effect of irradiation on hardening. It may be significant that at the dose level of 0.3 dpa, there is a clear indication of an upper yield point and a small but finite Lüders strain.

The effect of irradiation on deformation behavior of MANET-II irradiated and tested at 250 °C to dose levels of 0.1 and 0.3 dpa is shown in Fig. 4. It can be seen that both $\sigma_{0.2}$ and σ_{max} increase with irradiation dose level. It is important to note that the uniform elongation is not affected by irradiation.

The specimens of F82H-mod. irradiated and tested at 250 °C showed no clear effect of irradiation on hardening or elongation (see Table 1).

Fig. 5 shows the temperature dependence of $\sigma_{0.2}$ and σ_{max} for the unirradiated F82H and MANET-II steels. In this temperature range (22 - 350 °C) the decrease in strength with increasing temperature is rather small.

Tensile Test Specimen (0.3 mm thick)

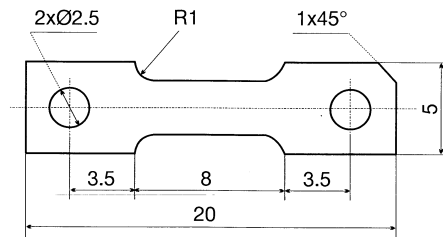


Figure 1:

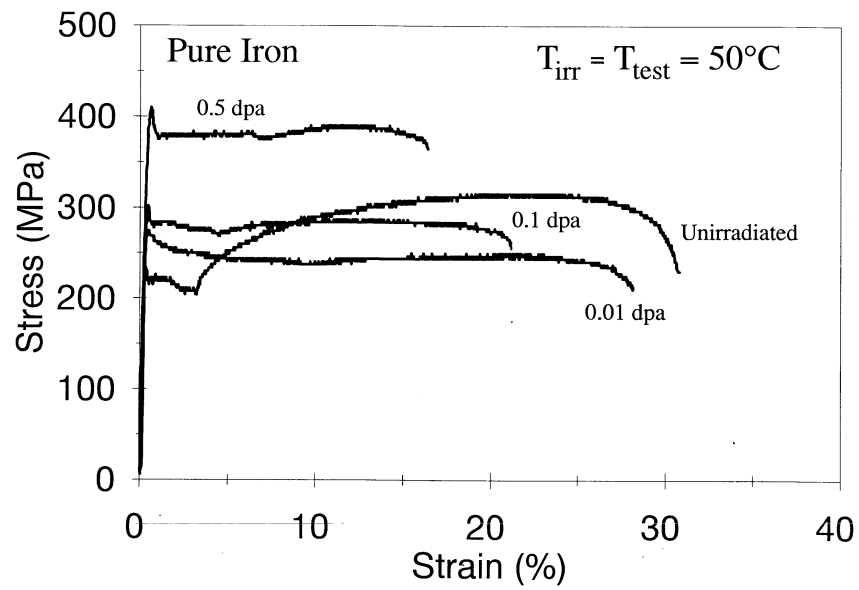


Figure 2:

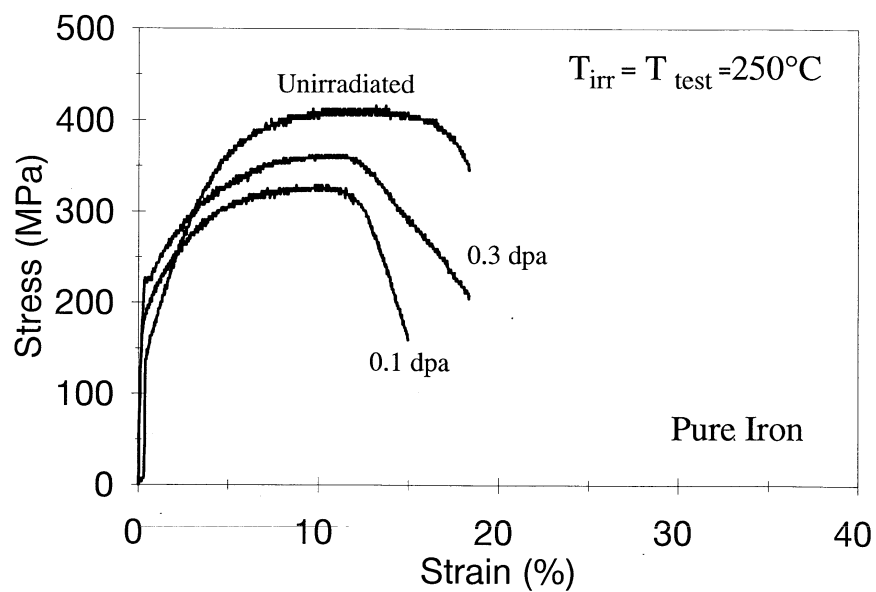


Figure 3:

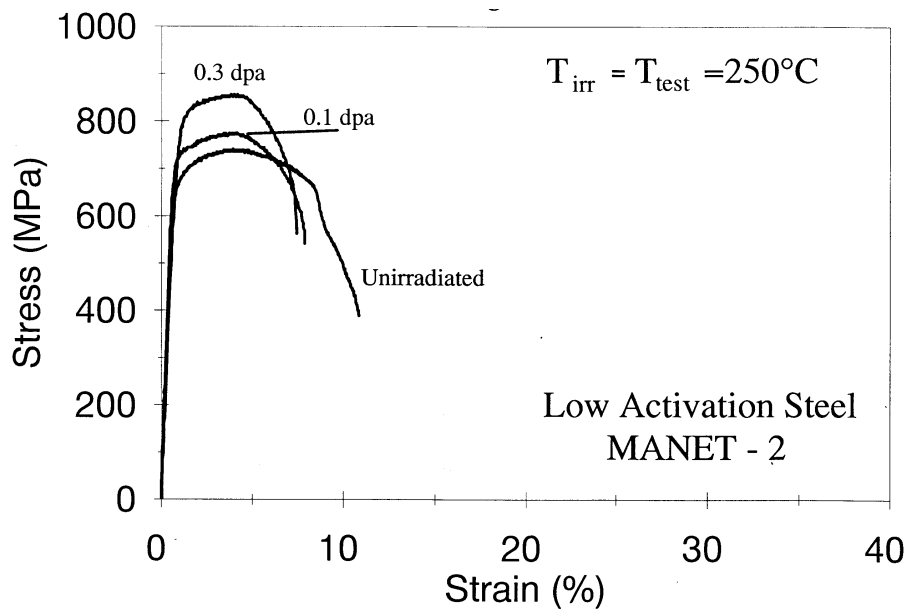


Figure 4:

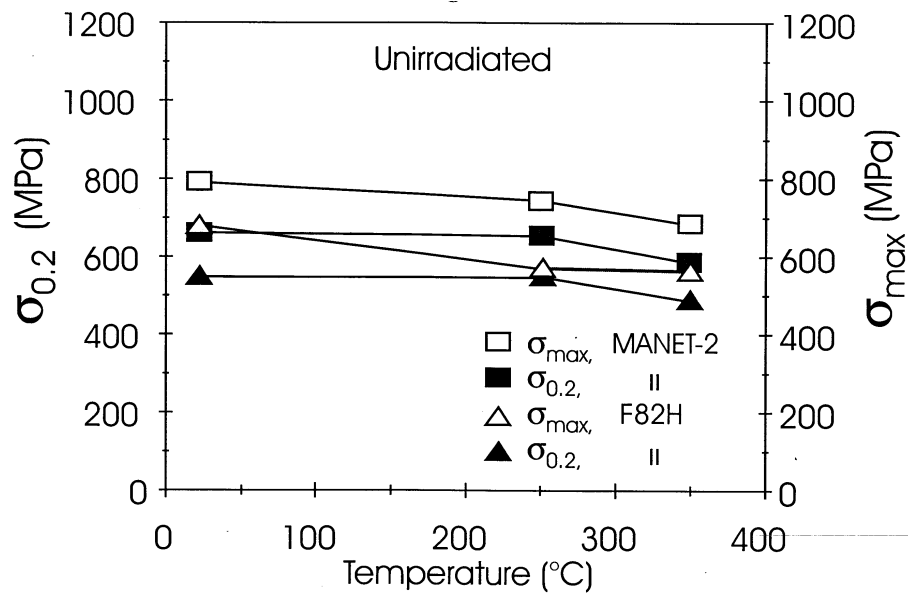


Figure 5:

TABLE 1. Tensile Properties of Unirradiated and Irradiated Pure iron, Modified F82H and MANET-2 Steels

Material	Dose (dpa)	Irradiation Temperature (°C)	Test Temperature (°C)	σ_y^u (MPa)	σ_y (MPa)	σ_{max} (MPa)	ϵ_u^p (%)	ϵ_t (%)
Pure Iron	0	-	50	218	-	311	24.5	27.0
	0.01	50	50	261	-	246	25.7	28.5
	0.1	50	50	315	-	307	16.2	19.2
	0.5	50	50	414	-	398	15.1	16.8
	0	-	250	-	156	409	13.1	16.4
	0.1	250	250	-	225	340	10.3	12.5
	0.3	250	250	190	210	343	12.1	20.0
Modified F82H	0	-	22	-	560	688	6.5	7.0
	0	-	250	-	525	595	3.5	10.5
	0	-	350	-	490	565	2.5	8.5
	0.1	250	250	-	535	578	3.0	10.5
	0.3	250	250	-	568	595	2.5	9.5
MANET-II	0	-	22	-	667	800	6.2	13.2
	0	-	250	-	675	760	3.8	8.4
	0	-	350	-	585	662	2.8	7.1
	0.1	250	250	-	713	772	3.5	8.0
	0.3	250	250	-	785	845	3.7	7.9

Tensile properties of MANET and F82H-mod. after helium implantation

R. Lindau and A. Möslang

Forschungszentrum Karlsruhe

Introduction

In plasmanear structural materials hydrogen isotopes and helium will be generated by inelastically scattered fusion neutrons. For the next generation of fusion reactors helium production rates of about 100 appm/y and hydrogen production rates of about 500 appm/y are expected in typical structural alloys. As ongoing controversial discussions in the present international literature indicate, is the behavior of helium in some reduced activation materials a serious matter of concern. HFIR irradiations on f/m steels often show a significant ductility reduction and a pronounced DBTT increase if the steels are doped with B or Ni additions to increase the helium content by non-elastically produced transmutations. However, due to the nature of these experiments it is hardly possible to distinguish between B/Ni segregation induced and helium bubble generated embrittlement. This note describes briefly initial tensile results on unirradiated and helium implanted MANET I and F82H-mod. steels.

Experimental

Helium implantations at the FZK Dual Beam Facility are a suitable tool to get a very homogeneous helium distribution in sufficiently thick specimens without the need to change the materials composition. The chemical compositions of the 10.5% CrMoVNb-steel MANET I and the 9% CrWVTa steel F82H-mod. are given elsewhere in this report. Sheet tensile specimens with a reduced gauge volume of $7.0 \times 2.0 \times 0.20 \text{ mm}^3$ were produced by spark erosion from foils following the reference heat treatment. The irradiations were performed between 50 and 420 °C in helium gas using a degraded 104 MeV alpha-particle of the high energy dual beam facility at FZK. Although a fusion similar ratio of He/dpa was not used, these experiments provide suitable information of the impact of helium on strength and ductility parameters within a wide temperature range. The irradiation conditions are listed in table 1. Special emphasize was put on fairly low helium and damage production rates. After irradiation the specimens were tensile tested together with unirradiated control specimens at test temperatures equal to the irradiation temperature in a vacuum furnace (10^{-4} Pa) at a constant nominal strain rate of $1.2 \times 10^{-4} \text{ s}^{-1}$.

Table 1: Irradiation parameters at the Dual Beam Facility

Temperature range	50-420 °C
Helium production rate	$(2.5-3) \times 10^{-3}$ appm/s
Displacement damage rate	$(1.4-1.8) \times 10^{-6}$ dpa/s
Irradiation time	~ 50 h
Implanted concentration	500 appm He
Displacement damage dose	0.3 dpa
Specimen environment	purified He-gas

Tensile results

In figs 1-4 the tensile properties of α -particle irradiated F82H-mod. tensile specimens are shown together with unirradiated control specimens. The irradiation induced yield strength change (80 MPa at 250 °C decreases moderately with increasing temperature up to 350 °C and diminishes rapidly above about 400 °C.

Irradiation induced hardening predominant at temperatures below 400 °C and small softening prevailing above about 450 °C is a common feature of martensitic/ferritic Cr-steels. By analyzing various strengthening contributions the authors have shown in the past that the dominant hardening contribution can be explained by dislocation loop formation or irradiation enhanced precipitation. Helium only tends to stabilize these effects. However, if figs. 1 and 2 are compared with earlier α -particle irradiations on MANET tensile specimens under the same conditions (figs. 5 and 6), it turns out that the irradiation induced hardening is much smaller in the F82H-mod. specimens. For helium implanted specimens the hardening ratio between F82H and MANET I is about 0.55 ± 0.09 within a wide temperature region. Microstructural examinations of the defect and helium bubble morphology are planned to investigate the different hardening efficiencies of both steels.

While a significant ductility reduction has been observed at the lowest irradiation temperature (fig. 3) in F82H-mod. specimens, the uniform and total elongation are nearly unaffected by the helium implantations at 250°C and above. It is important to note that in contrast to MANET I specimens that showed a pronounced, dynamic strain aging related ductility drop from 3 to 0.3% after helium implantation between 280 and 350 °C (figs. 7 and 8), no DSA was observed in unirradiated and helium implanted F82H-mod. specimens. At all temperatures investigated, the rupture mode always remains ductile and transcrystalline for all implanted specimens and unirradiated controls.

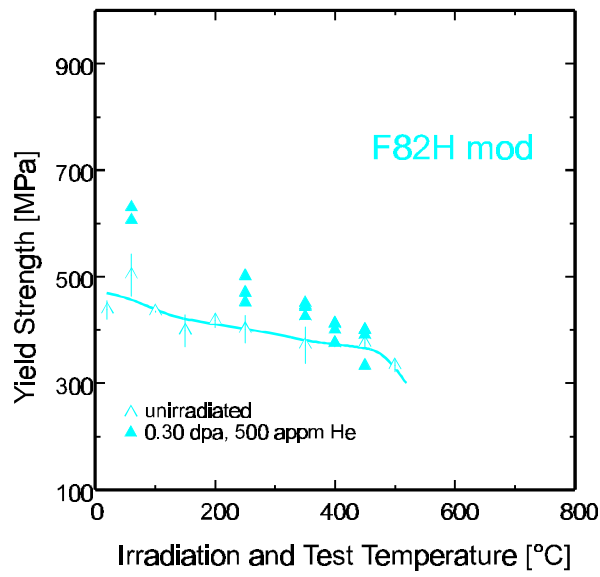


Fig. 1: Yield strength of F82H-mod. specimens after He-implantation

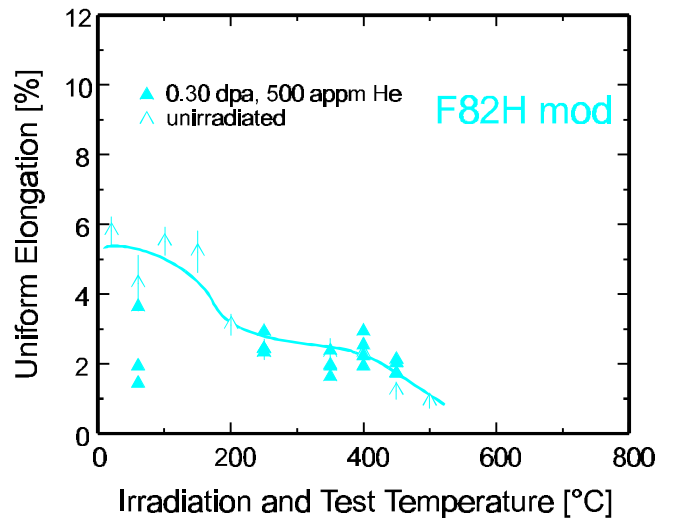


Fig. 3: Uniform elongation of F82H-mod. specimens after He-implantation

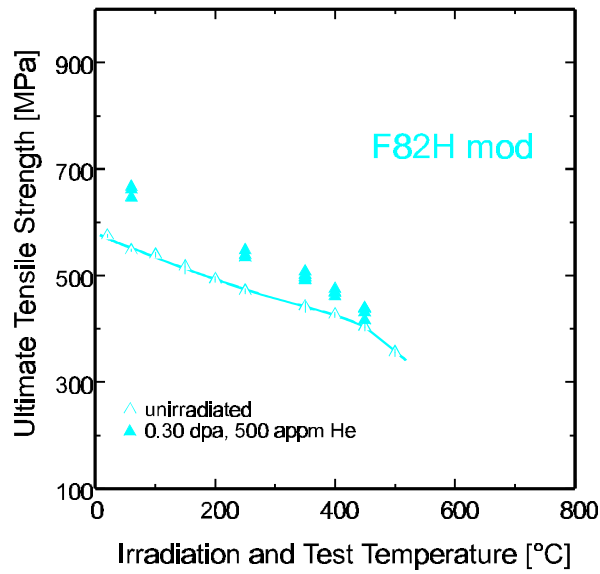


Fig. 2: Ultimate tensile strength of F82H-mod. specimens after He-implantation

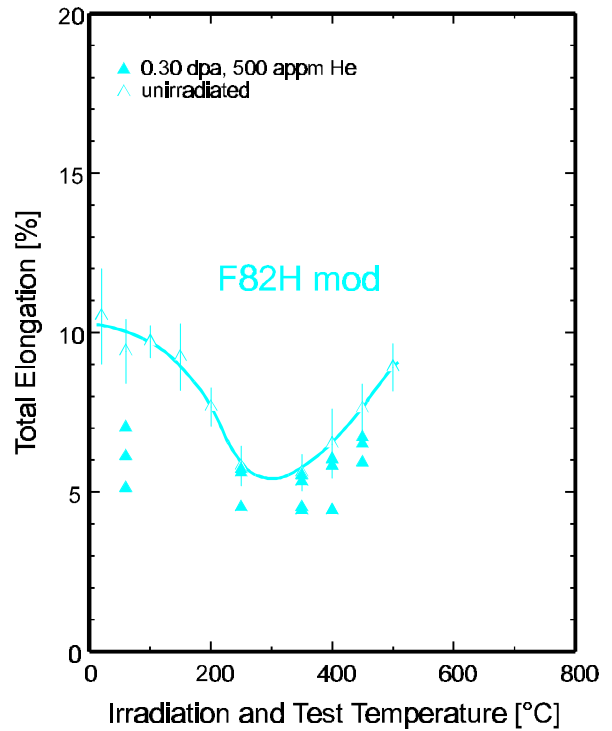


Fig. 4: Total elongation of F82H-mod. specimens after implantation

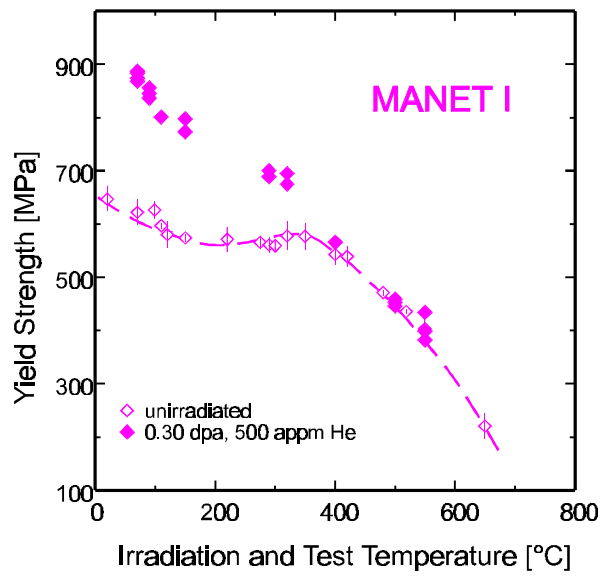


Fig 5: Yield strength of MANET I specimens after He-implantation

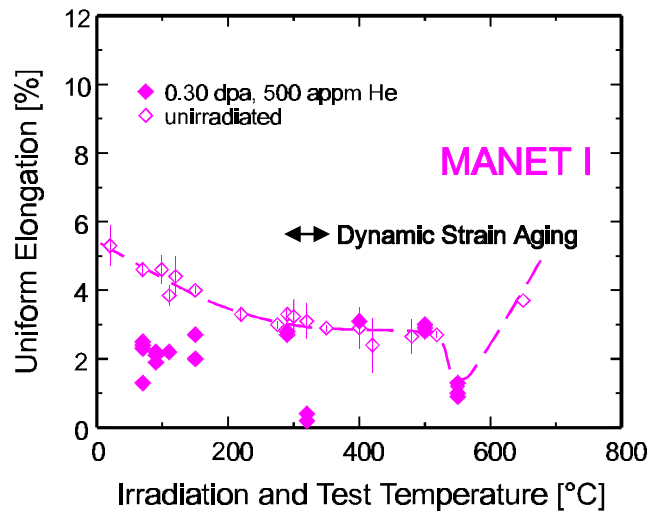


Fig. 7: Uniform elongation of MANET I specimens after He-implantation

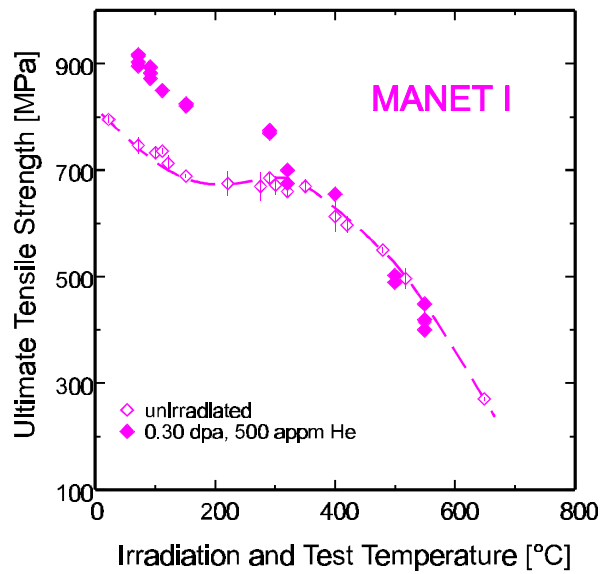


Fig. 6: Ultimate tensile strength of MANET I specimens after He-implantation

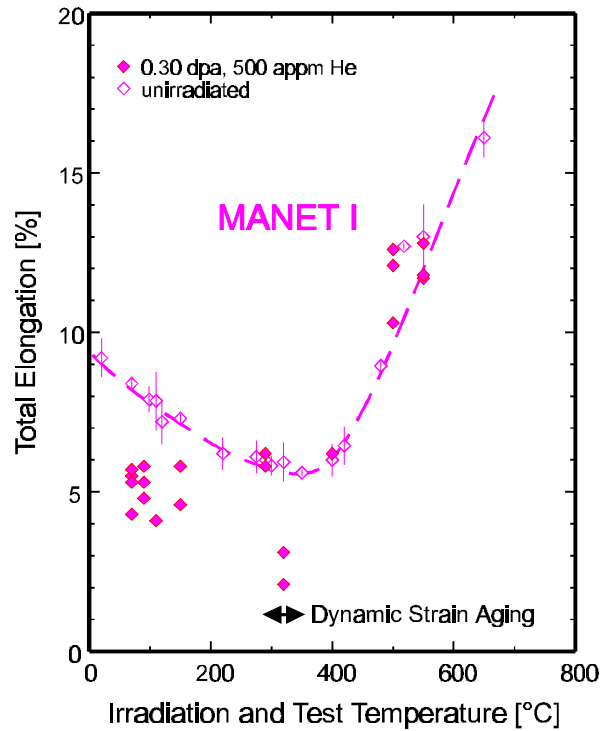


Fig. 8: Total elongation of MANET I specimens after implantation

MANITU IRRADIATION PROGRAM

M. Rieth

Forschungszentrum Karlsruhe

1. Introduction

The problem of radiation-induced deterioration of fracture toughness remains to be a key issue for the application of ferritic/martensitic steels as structural materials for fusion reactors. In the previous investigation (SIENA program) it has been demonstrated that, after irradiation in a materials testing reactor to a dose of 10 dpa or even less, at temperatures around 300 °C, the shift in Charpy impact properties of 10-12 % Cr steels, as characterized by an increase of the ductile-to-brittle transition temperature (DBTT) and a decrease of the upper shelf energy (USE), can be unacceptably high. In the context of these results there was, at that time, a vital interest to learn more about the evolution of this degradation with fluence and about the possibility of even more damage (or lack of annealing effects) at lower irradiation temperatures.

With these objectives the MANITU irradiation project was started with staged doses of 0.2, 0.8, and 2.4 dpa and temperatures between 250 and 450 °C as target values. During the planning of the experiment several new aspects came at right time, which enabled us to fill the available space in the rigs in addition to the MANET steels with specimens of different promising low-activation alloys and thus redirect the goals of the experimental program.

Up to now all of the results from the 300 °C irradiation are available and allow us to draw interesting conclusions with respect to the dose effect on impact properties and the improvement attained by the introduction of new alloys with reduced long-term activation.

2. Experiments

The heat treatments of the alloys have not in all cases been optimized to the utmost and may thus leave some room for further improvement. Table 1 gives the chemical composition of the steels with a ranking order of the alloying elements that facilitates the distinction of

characteristic deviations and allows for numerous speculations about the influence of composition on the different impact properties before and after irradiation.

Charpy specimens have been produced from the available materials according to the European standard for subsize specimens. All tests have been carried out with the same, instrumented facility which is installed in the Hot Cells.

The irradiations of the MANITU program are all carried out in the HFR, Petten. The target values of the neutron doses was reached within about -2 % and +15 % depending on the core position of the specimens. The irradiation temperature of 300 °C was maintained within about ± 5 % by a proper balance between n, γ -heating and compartment cooling with different He-Ne mixtures. A total number of 180 specimens for each dose level (or at least 5 for each material and temperature) ensured a sufficient number of measurement points in order to connect and group them to curves with the irradiation temperature as abscissa and the materials as parameter.

3. Results

Fig. 1 shows the USE as a function of irradiation dose. The number of curves can be divided into two groups where the low activation alloys (LAA) generally maintain a high impact energy in the whole dose range, whereas the MANET steels behave much poorer.

If we now look at the DBTT curves (Fig. 2) we find again that the MANET steels behave quite bad, whereas the LAA are significantly better. At an irradiation dose of 2.4 dpa the difference in DBTT between MANET-I and the ORNL steel is 220 °C and it seems, if we extrapolate the DBTT curves to higher dose levels, that the further embrittlement of the LAA is much smaller compared to the MANET steels.

The dynamic yield stress measured at 100 °C is shown in Fig. 3. Up to the dose level of 0.8 dpa all LAA are suffering less of irradiation hardening compared to the MANET-II steel. But above 0.8 dpa the ORNL and OPTIFER-II steels show a bigger increase in dynamic yield strength compared to the other alloys. At 2.4 dpa the dynamic yield strength of the ORNL steel is even comparable to the MANET-II steel.

4. Conclusions

- All LAA show a better embrittlement behavior after neutron irradiation compared to the MANET steels. Especially in the higher dose range (>0.8 dpa) the difference becomes more and more significant.
- Among all examined materials the ORNL steel shows the very best embrittlement behavior. Prior investigations have shown, that below irradiation temperatures of $400\text{ }^{\circ}\text{C}$ the already minor deterioration in DBTT remains practically constant.
- All materials show irradiation hardening which increases with higher neutron doses. The ORNL and OPTIFER-II steels show the biggest increase in dynamic yield stress compared to the other alloys.
- Though the low neutron fluence of this irradiation experiment does not yet allow to draw general conclusions, it can be stated that all examined low activation materials provide clearly better impact properties than the corresponding MANET alloys.
- Further irradiation experiments have to verify these encouraging results with the low activation alloys at higher and especially more fusion relevant dose levels.

Literature:

- [1] M. Rieth, B. Dafferner, H.D. Röhrig, C. Wassilew, Fusion Engineering and Design 29 (1995) 365-370.
- [2] M. Rieth, B. Dafferner, H.D. Röhrig, Charpy Impact Properties of Low Activation Alloys for Fusion Applications after Neutron Irradiation, Seventh International Conference on Fusion Reactor Materials, Obninsk, Russia, 25-29 September, 1995.

Table 1: Chemical composition of the different alloys in wt.%

	10-11 % Cr- NiMoVNb steels		low activation alloys			
	MANET I	MANET II	OPTIFER Ia	OPTIFER II	F82H std.	ORNL
Cr	10.8	9.94	9.3	9.43	7.73	8.9
W			0.965	0.005	2.06	2.01
Ge				1.1		
N	0.02	0.023	0.015	0.016	0.0027	0.0215
C	0.14	0.1	0.1	0.125	0.092	0.11
Mn	0.76	0.79	0.5	0.5	0.083	0.44
Ta			0.066	ca. 0.02	0.018	0.06
P	0.005	<0.006	0.0047	0.004	0.003	0.015
S	0.004	<0.007	0.005	0.002	0.003	0.008
V	0.2	0.22	0.26	0.28	0.189	0.23
B	0.0085	0.007	0.006	0.006	0.003	<0.001
Si	0.37	0.14	0.06	0.038	0.09	0.21
Ni	0.92	0.66	0.005	0.005	0.032	<0.01
Mo	0.77	0.59	0.005	0.005	0.0053	0.01
Al	0.054	<0.02	0.008	0.008	0.01	0.017
Co	0.01	<0.02			0.0024	0.012
Cu	0.015	<0.01	0.035	0.007	0.0059	0.03
Nb	0.16	0.14	0.009	0.009	0.0057	
Zr	0.059	0.034				<0.001
Ce			<0.001	<0.001		
Ti			0.007	0.007	0.0104	<0.01
Fe	balance	balance	balance	balance	balance	balance

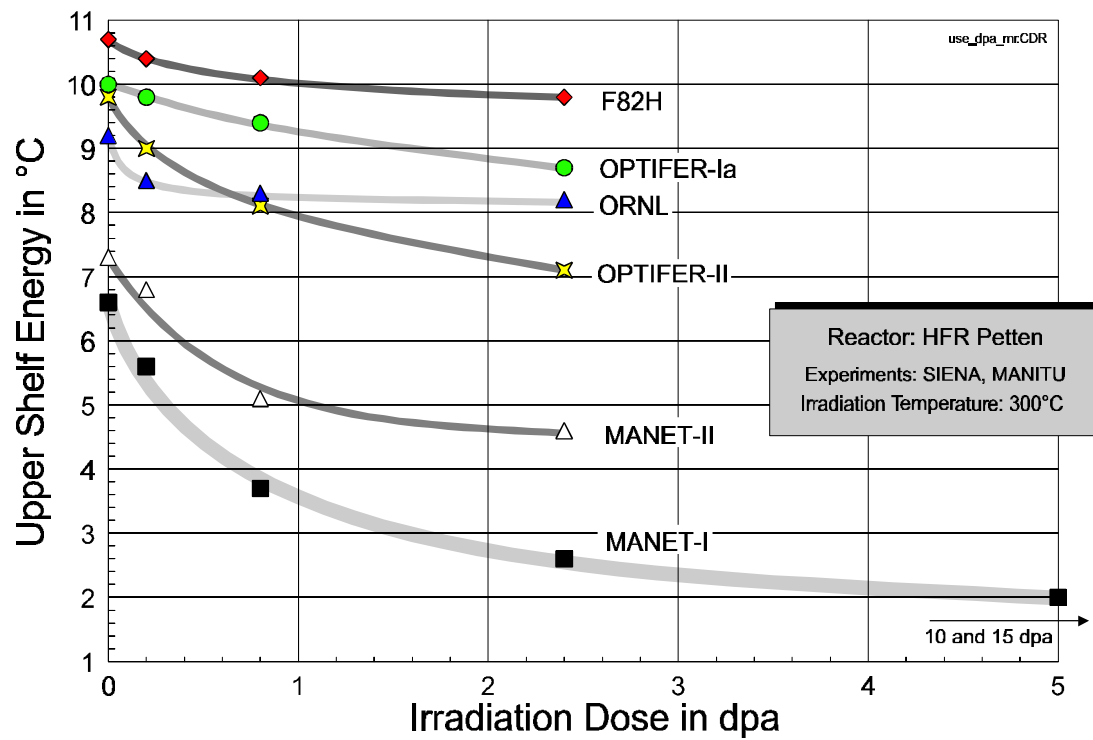


Fig. 1

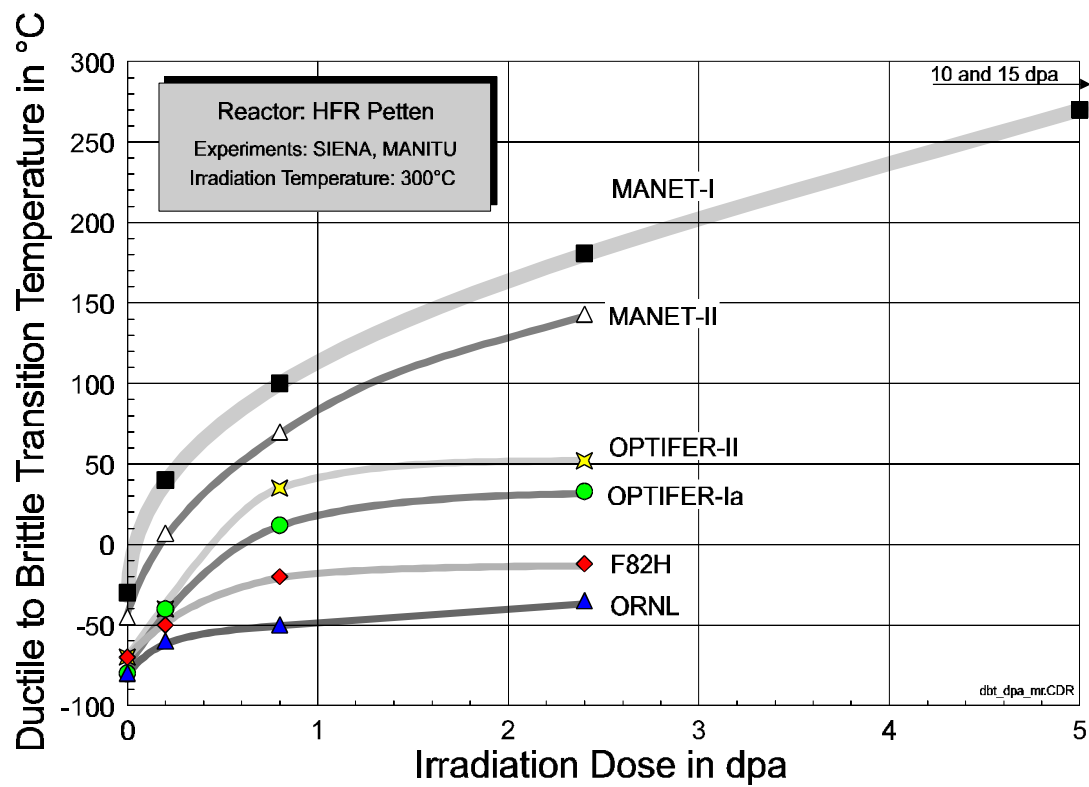


Fig. 2

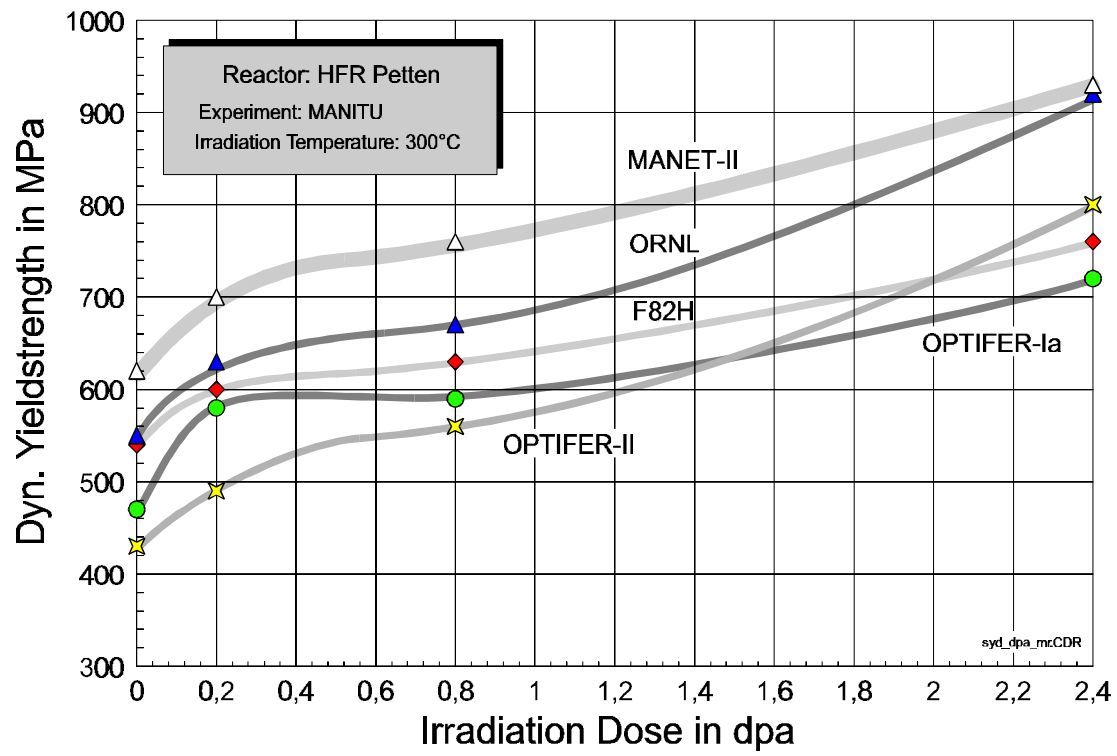


Fig. 3

Chapter 3

Property Comparison and Evaluation

Based on data presented at this meeting a comparison of conventional 9-12% CrMoVNb steels with experimental LA (low-activation) 7-10% CrWV(Ta, Ti) alloys has been made. Additional data input for the conventional steels MANET II and T 91 were taken from references [1-6] and further informations on the experimental LA-alloys were extracted from [7-13].

3.1 Physical metallurgy

For practical applications the transformation characteristics, hardenability and tempering behavior of ferritic/martensitic steels are of great importance. Specifically two criteria have to be taken into account: the transformation temperatures and the critical cooling rates below which pearlite formation can be expected. Such informations can be deduced from transformation diagrams under isothermal annealing or continuous cooling treatments. In Figs. 1 and 2 a comparison of the continuous TTT- transformation diagrams for the steels MANET II and F82H-mod. as typical examples of conventional and LA -alloys is given. According to these plots there is no qualitative difference for both materials, but in detail the transformation temperatures and the critical cooling rates vary somewhat, i. e. the formation of pearlite occurs earlier for F82H-mod. Such characteristic data are summarized for nearly all LA-alloys in Tab. 1.

Material (steel name)	Transformation Temperatures				Critical cooling- rate for pearlite	Reference
	Ac _{1b} °C	Ac _{1e} °C	M _s °C	M _f °C		
MANET-II 6 heats	775-780	890-900	340-357	155-161	< 0,2°/min	FZKA 5607, 9/95, Schirra
Steel 91 3 heats	810-820	870-885	385-400	100-120	3-4°/min	„
F82H-mod. heat 9741	835	915	425	220	1°/min	„
OPTIFER-Ia heat 664	820	900	418	222	< 4°/min	„
OPTIFER-II heat 668	825	920	395	172	2,5°/min	„
BATMAN heat 1953	837	911	440	230	0,7°/min	G. Filacchioni Notice 1.8.96
BATMAN heat 1955	843	913	430	215	0,7°/min	„
LA 13 Ta	821	925	325	n.d.	1,25°/min	NT-SRMA 96-2173 Alamo et al.
LA 12 TaLC	820	940	405	n.d.	1,5°/min	„

Table 1: Compilation of transformation data and critical cooling rates for pearlite formation in conventional and LA-ferritic/martensitic steels

Material: MANET-II Heat-Nº: 50806
 Austenitizing: 1075°C 15 min. Grain-size(ASTM): 9-10

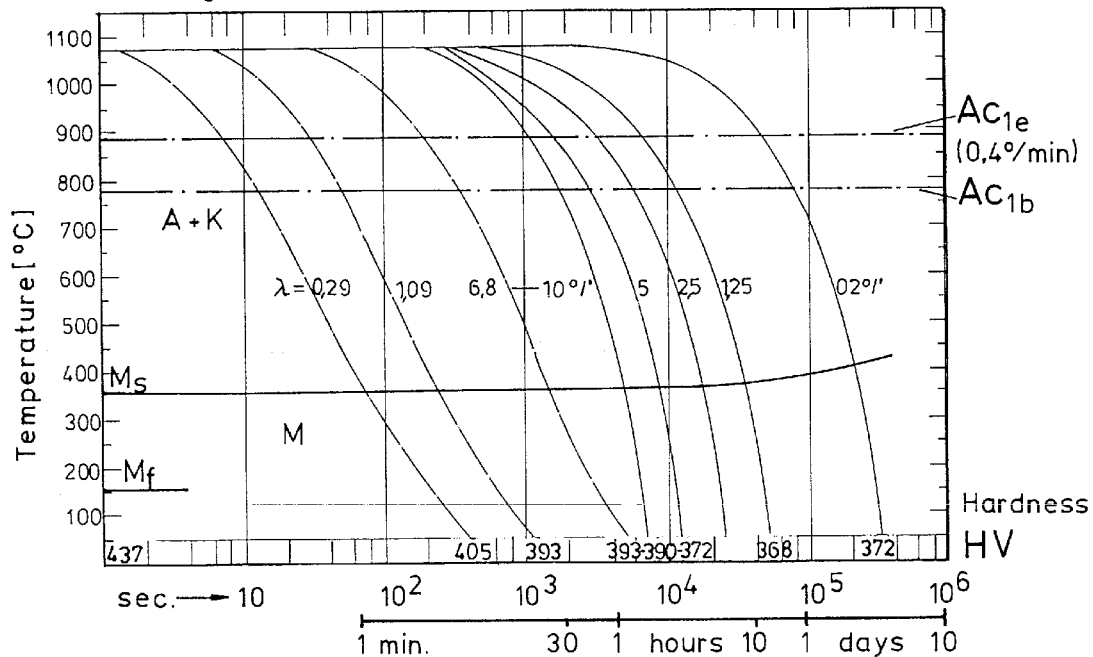


Figure 1: CCT-Diagram of MANET II

Material: F82H - mod Heat-Nº: 9741
 Austenitizing: 1040°C 15min. Grain-size(ASTM): 7-8, +6

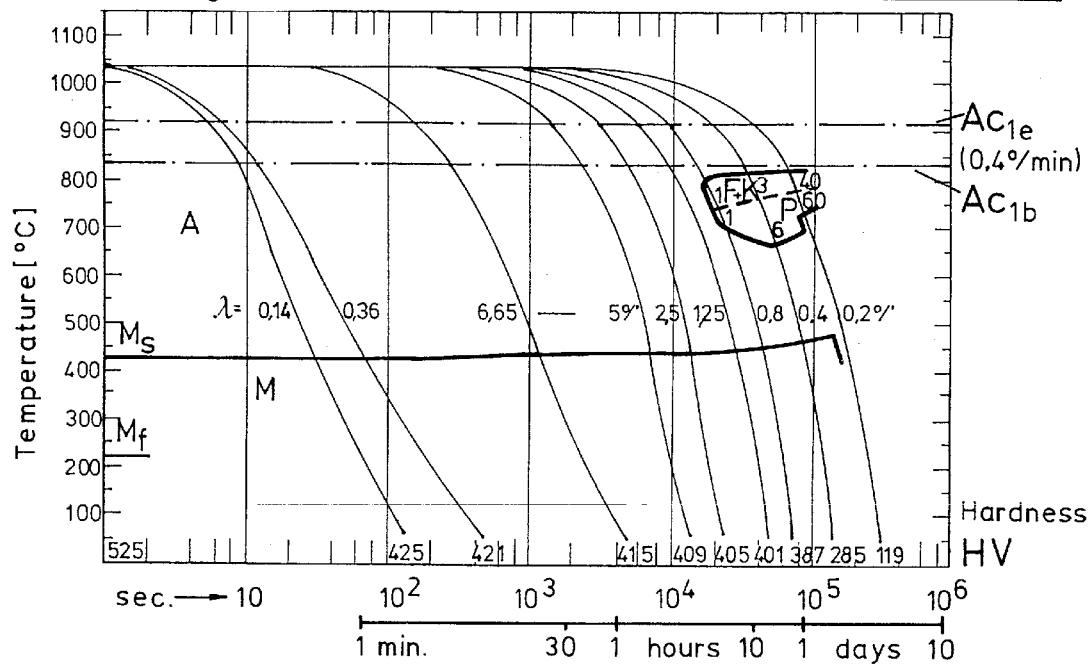


Figure 2: CCT-Diagram of F82H-mod.

As can be deduced, the martensite start- and finish-temperatures M_s and M_f increase slightly for all LA-alloys and a complete transformation into martensite is guaranteed for all of them at RT. This is a necessary prerequisite for reasonable toughness properties. An increase is also observed for the austenitization temperatures A_{1b} and A_{1e} and it is assumed that the elimination of Ni in the LA-alloys is responsible for this behavior. As will be discussed later this will allow a greater temperature range for tempering treatments and hence a better potential for optimizing the strength/ toughness properties.

Regarding the critical cooling rates, below which the formation of pearlite is expected, the values for the LA-alloys are in the same range as for the conventional steels with only small variations. In other words the new LA-alloys are also air hardeners. This is a very important property for the fabrication of thick-walled components with nearly homogeneous mechanical and structural properties.

Hardenability

Hardenability can be influenced by the selection of appropriate alloying elements and to a certain extent by the choice of the austenitization temperature. A comparison of the LA-alloys with MANET II shows in Figs. 3 and 4 that these alloys generally have a slightly higher hardenability. As expected, the alloys with higher carbon- or nitrogen content like OPTIFER IV and BATMAN lie at the upper range of data. An optimum in hardenability can be achieved for an austenitization temperature above 950°C, i. e. beyond the A_{1e} -temperature. A further increase in austenitization temperature does not lead to an improved hardenability in these alloys which can eventually be understood by their relatively low carbon content and a small amount of such precipitates which would need a higher temperature for resolution.

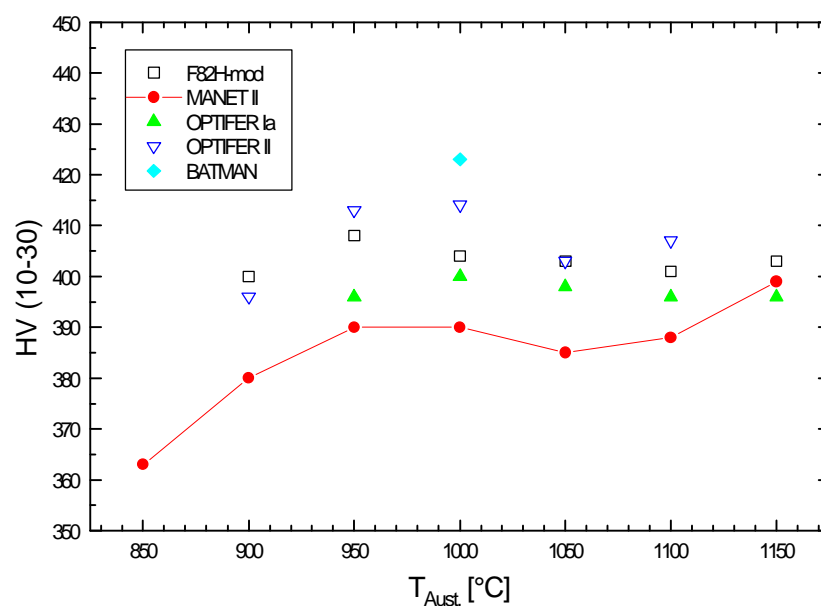


Figure 3: Comparison of the hardening behavior

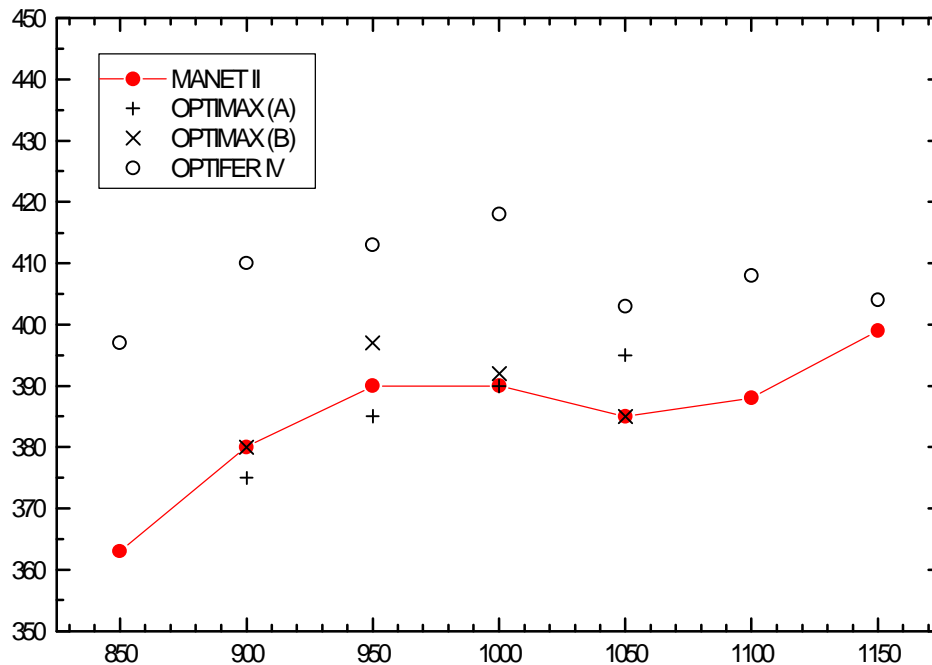


Figure 4: Comparison of the hardening behavior

Grain Size

An open question at the beginning of the development of the new LA-alloys was, whether or not Ta is as effective as Nb in stabilizing the grain size during the austenitization treatment. Figs. 5 and 6 which show the development of the grain size as function of the austenitization temperature for the different alloys indicate that additions of about 0,08- 0,1 wt-% Ta are generally sufficient to stabilize the grain size to values comparable to conventional Nb-stabilized steels. Like for the conventional alloys a temperature range from 950 to 1050°C is most appropriate for the austenitization treatment with the additional recommendation to prefer- if possible- the lower end of this temperature range in order to achieve a small grain size and hence an optimum in fracture toughness properties. For the alloy F82H-mod. which has only 0,02 % Ta, grain growth is especially pronounced with increasing austenitization temperature. This material has in the present reference heat treatment at 1040°C a relatively large mean grain size and a broad size distribution, which demonstrates that this low level of Ta is not sufficient for a grain boundary stabilization. Not understood why the OPTIMAX-alloys also suffer from grain growth with increasing austenitization temperature, though a sufficiently high Ta-content has been added. The

BATMAN alloys show also a good grain stability, though they do not possess Ta and only a very small amount of Ti.

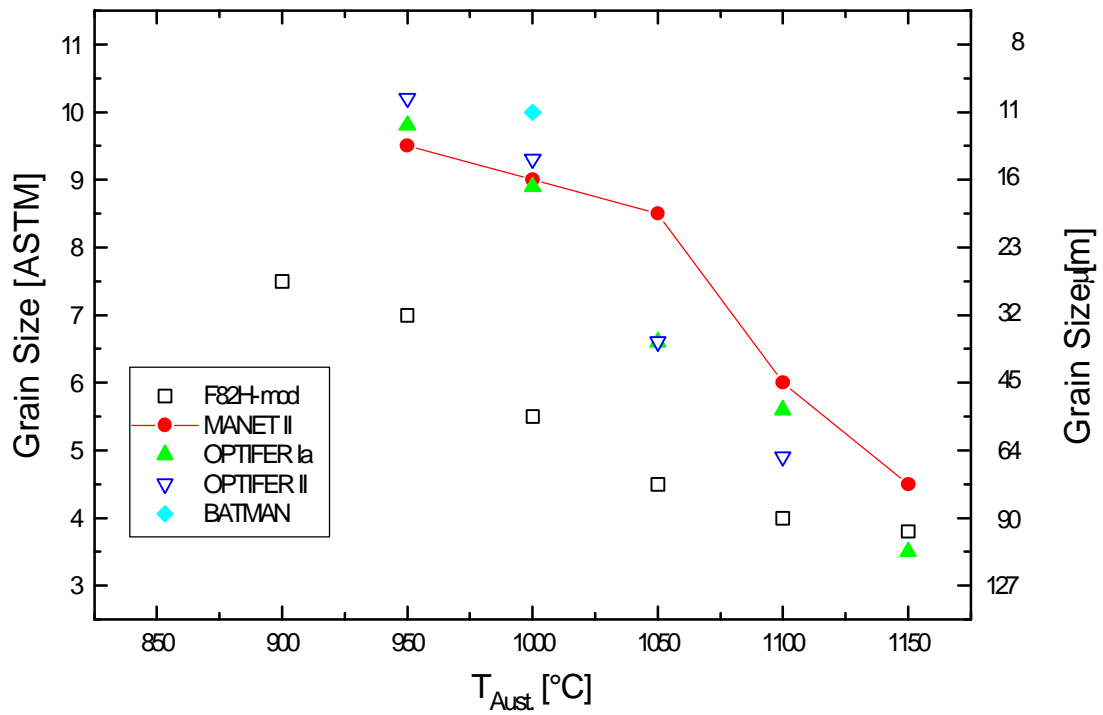


Figure 5: Comparison of grain size vs. hardening temperature

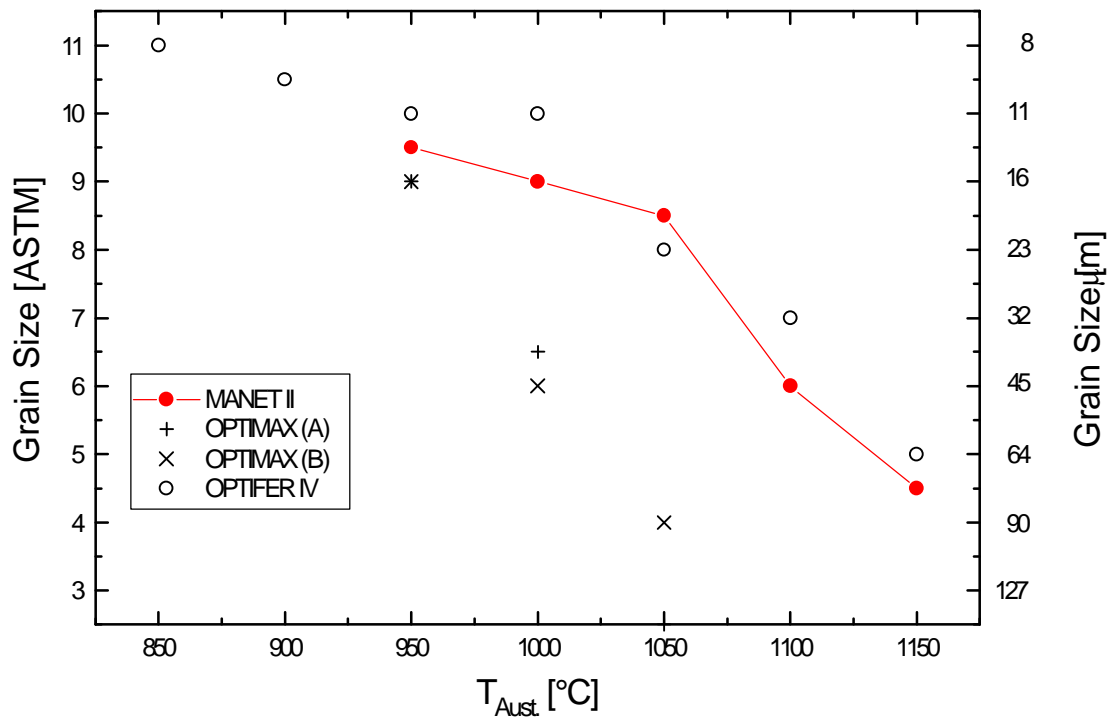


Figure 6: Comparison of grain size vs. hardening temperature

Tempering treatment

The appropriate tempering treatment determines the balance between achievable strength- and fracture toughness properties. In general the upper tempering temperature is limited to about 30 - 50°C below the austenitization start temperature A_{1b} in order to safely avoid any new formation of martensite after this heat treatment and the cooling down to RT. Since all new LA-alloys have a higher A_{1b} temperature than the conventional ones the upper tempering treatment could well be conducted at 780°C which could be advantageous for achieving high fracture toughness data. On the other hand such a treatment would cause a reduction in RT strength and hardness as seen in Fig 7.

The general annealing behavior is similar for both types of alloys. Conventional as well as LA- steels show with increasing annealing treatment a stable structure up to 550°C and a typical strong softening characteristics which can be attributed to dislocation annealing, partial resolution of martensite laths and an intense formation of carbide precipitates at internal lath boundaries. A systematic deviation can, however, be observed above 650°C until the restart of austenite formation. From a reason not yet understood the softening is stronger in the LA-alloys, so that for an often used tempering temperature of 750°C the new LA- materials are weaker than the conventional ones, though their RT-hardenability is higher.

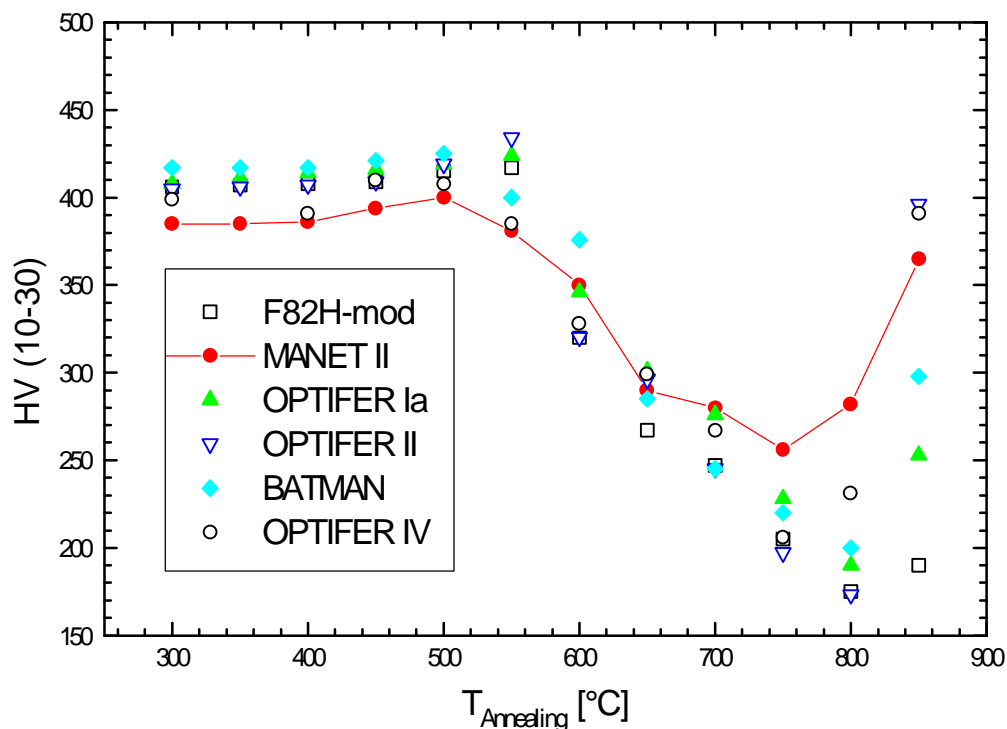


Figure 7: Comparison of the annealing behavior

3.2 Mechanical properties

From the above mentioned influence of austenitization - and tempering treatment on hardness it is clear that a reasonable data comparison can only be made if at least the tempering treatment is identical for all materials. Therefore for the following plots data were selected for a tempering treatment at 750°C/ 1-2 hours followed by air cooling to RT. Deviations from this “reference treatment” can be found in Tab. 2 where the complete treatments are compiled.

Table 2: Compilation of complete treatments

MANET-II	1075°C hardened	+ 750°C tempered	
Steel 91	1040°C hardened	+ 730°C + 705°C tempered	(US-specification)
	1040°C hardened	+ 750°C tempered	(Wareing/Tavassoli)
F82H-mod.	1040°C hardened	+ 759°C tempered	
OPTIFER-Ia	1075°C hardened	+ 750°C tempered	
OPTIFER-II	1075°C hardened	+ 750°C tempered	
BATMAN	1020°C+1020°C hardened	+ 730°C tempered	
LA12LC	1100°C hardened	+750°C tempered	
LA12TaLC		+ 10% cold working	
JLF-1	1050°C hardened	+ 780°C tempered	

Ultimate Tensile Strength and 0,2% Yield Strength

As expected from the above mentioned stronger softening of LA-alloys for temper treatments above 650°C ultimate tensile strength and yield strength data are generally lower for the LA-alloys up to 500°C (Figs. 8-10 and 11-13). At the lower end of the scatter band lie the W-free alloy OPTIFER II , the alloy F82H-mod. and surprisingly the two OPTIMAX-alloys. The low strength data for JFL1 are possibly due to the higher tempering temperature (780°C). Above 550°C there is practically no difference detectable so that in this respect the variation of Cr, W, Ta, Ti and V contents in the range covered by these alloys is not critical.

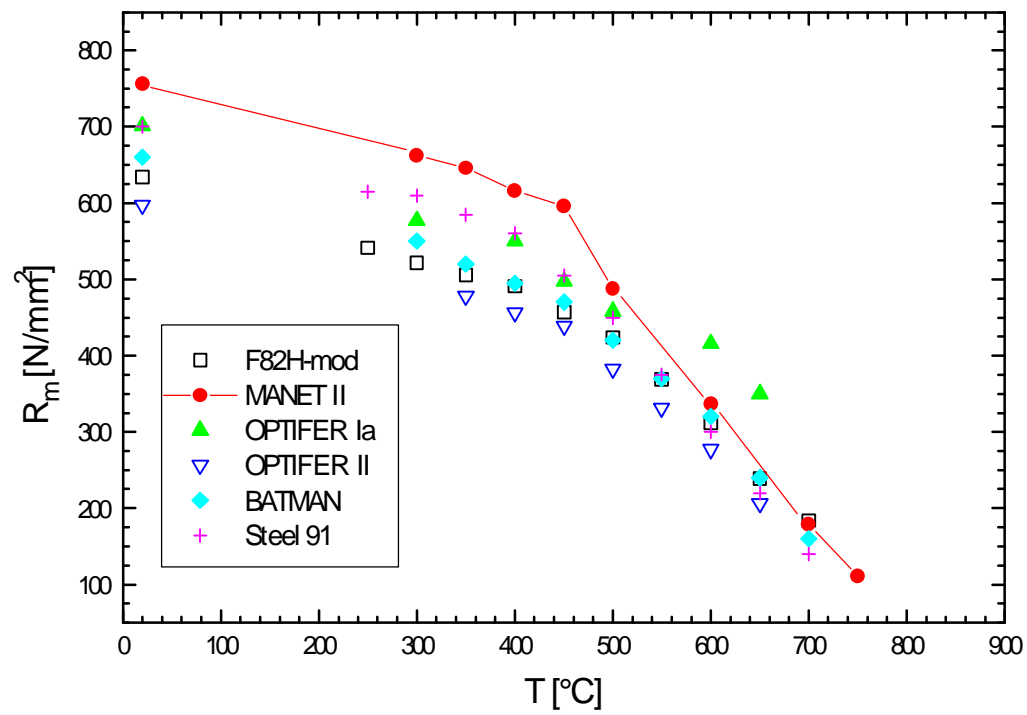


Figure 8: Comparison of the ultimate tensile strength

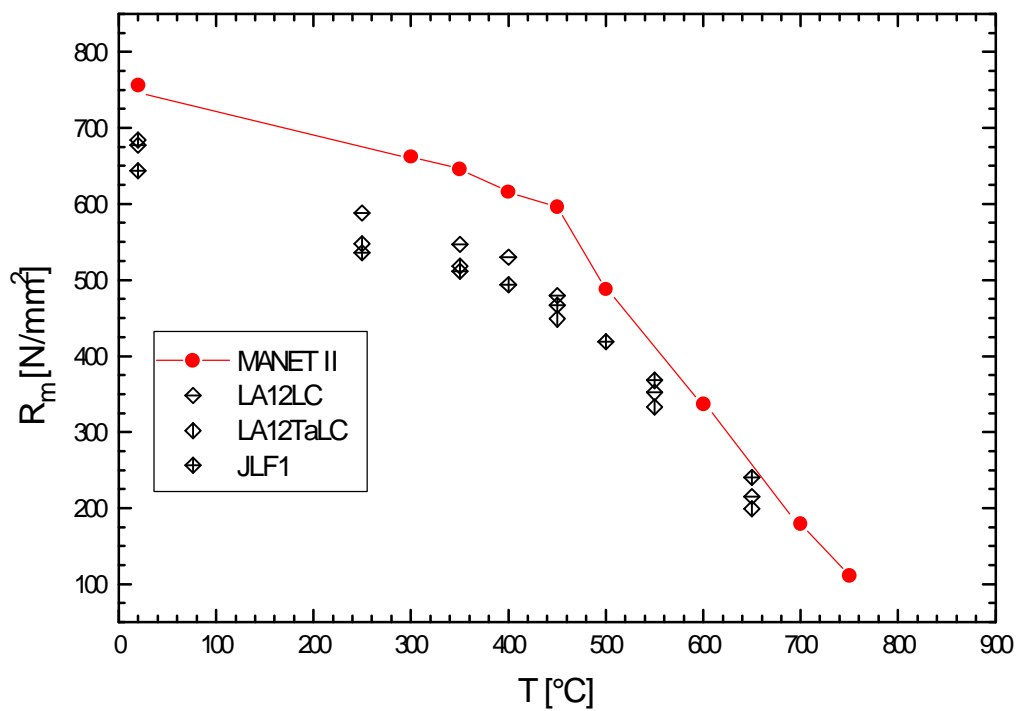


Figure 9: Comparison of the ultimate tensile strength

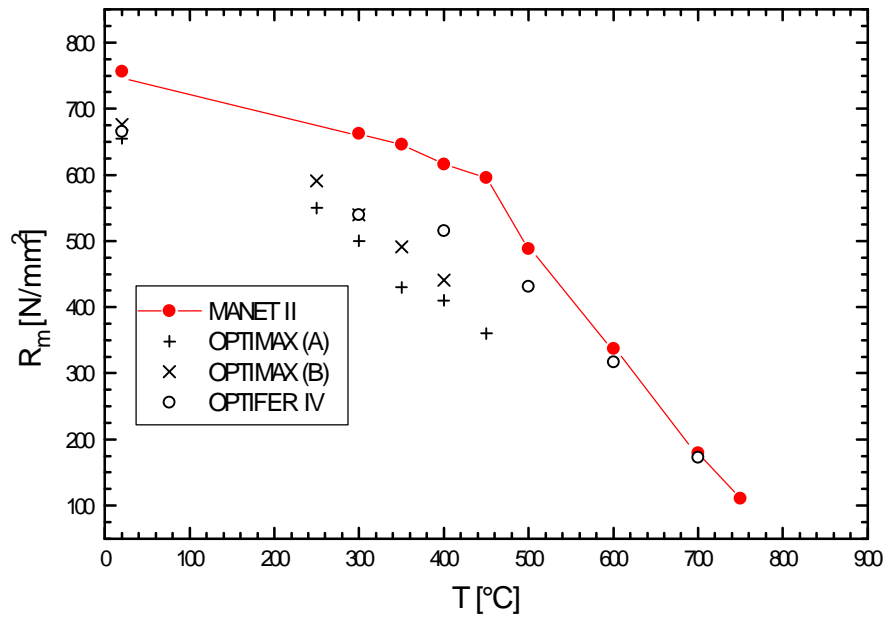


Figure 10: Comparison of the ultimate tensile strength

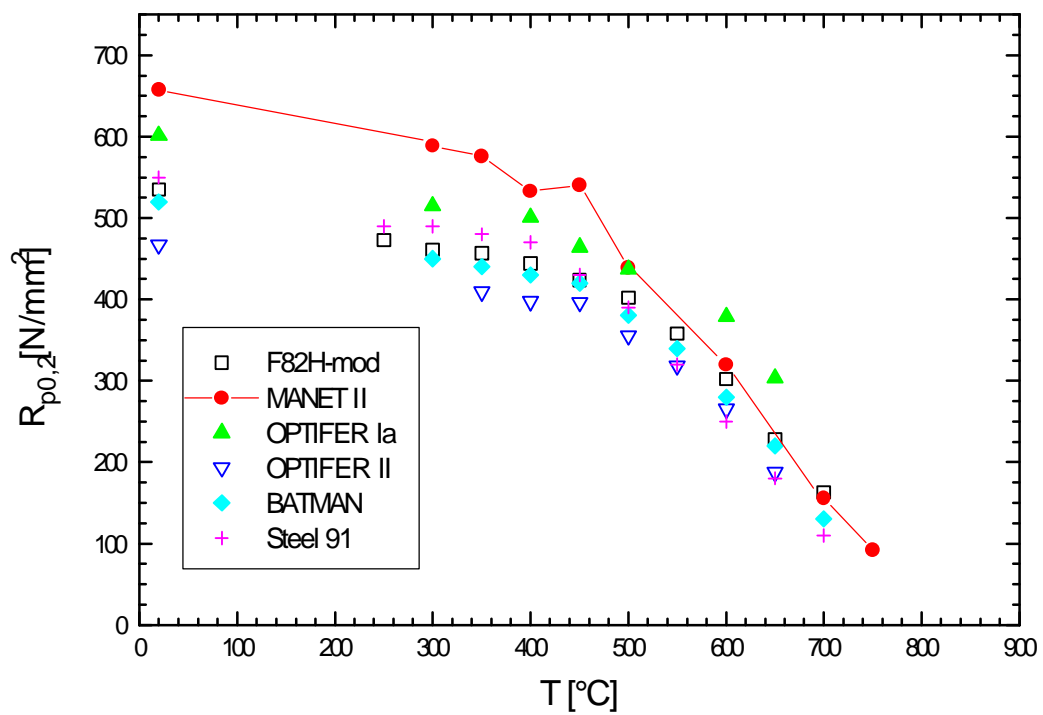


Figure 11: Comparison of the 0.2 % yield strength

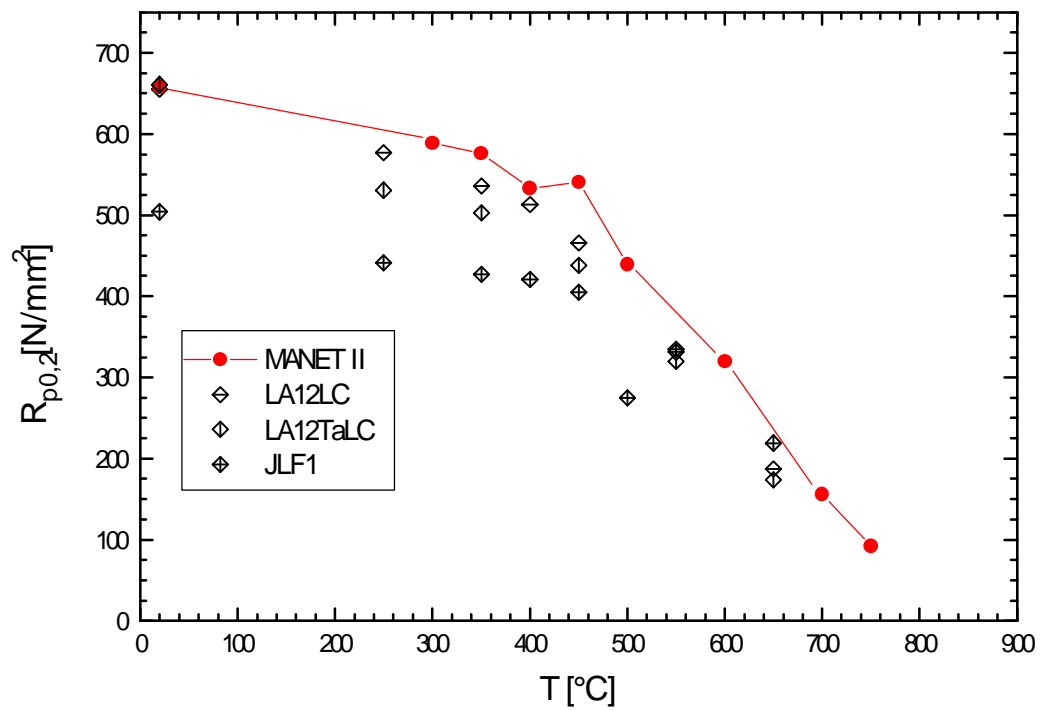


Figure 12: Comparison of the 0.2 % yield strength

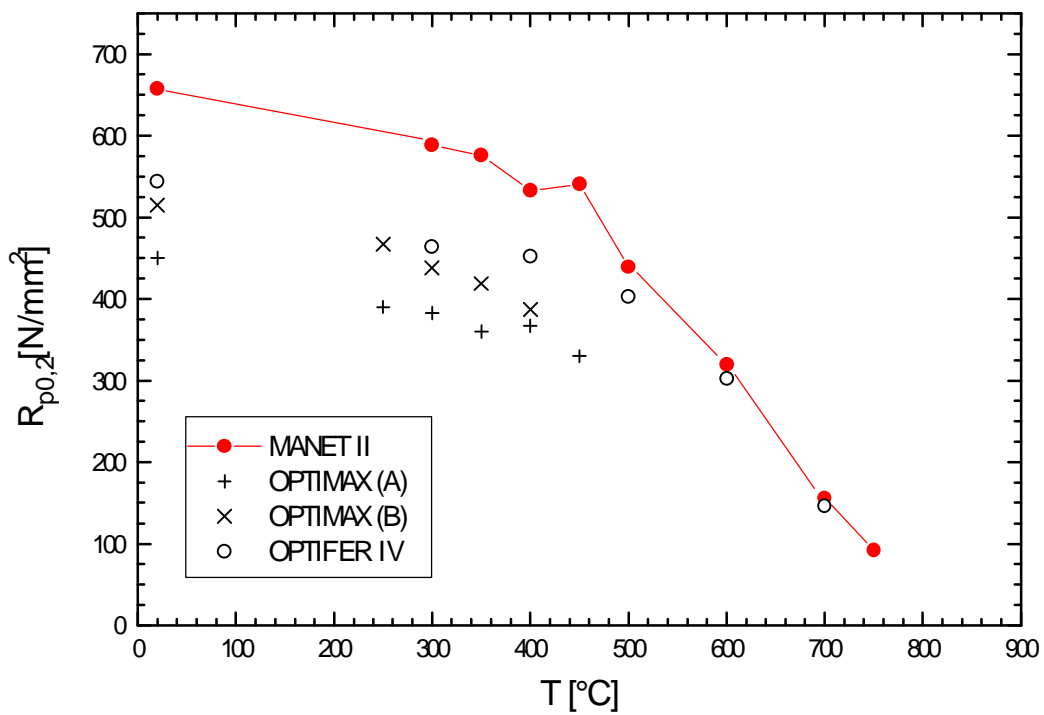


Figure 13: Comparison of the 0.2 % yield strength

Total and Uniform Elongation

Total elongation data from tensile tests are compiled in Figs. 14 to 16. The general temperature dependence follows a very similar trend for all materials. Total elongation A decreases from RT with increasing temperature, shows a minimum around 250-350°C and increases above that temperature. In the temperature range of minimum ductility a dynamic strain ageing effect can be observed which is caused by the direct interaction of the interstitial elements C and N with dislocations during the deformation process. The highest ductility values are observed for the conventional alloy T91 followed by the BATMAN alloy and at the lower end of the scatter band the 9% CrWV Ta alloys LA 12LC and LA 12Ta LC can be found. These latter alloys have, however, received a cold-working in the range of 5-10% after tempering treatment, which explains the low values in ductility. From these data the influence of an eventually necessary final cold-working on the mechanical properties can be deduced.

Regarding the uniform elongation A_g the general temperature dependence is different when compared with the total elongation. With increasing temperature continuously decreasing ductility values are observed. One exception from this general trend are again the 9% CrWVTa alloys LA12LC and LA12TaLC which show a low uniform elongation of about 1% over the whole temperature range. Again this behavior can be attributed to the additional cold working. On the other hand the OPTIMAX-alloys show a steeper temperature dependence. All other data lie in a small scatter band. The data are plotted in Figs. 17-19.

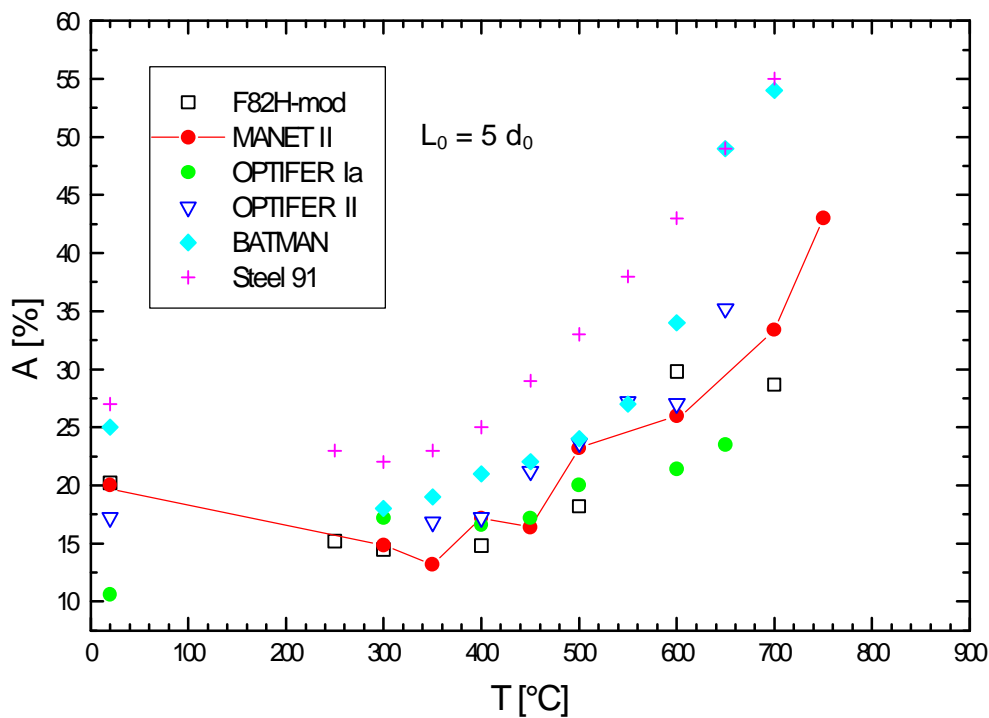


Figure 14: Comparison of the total elongation

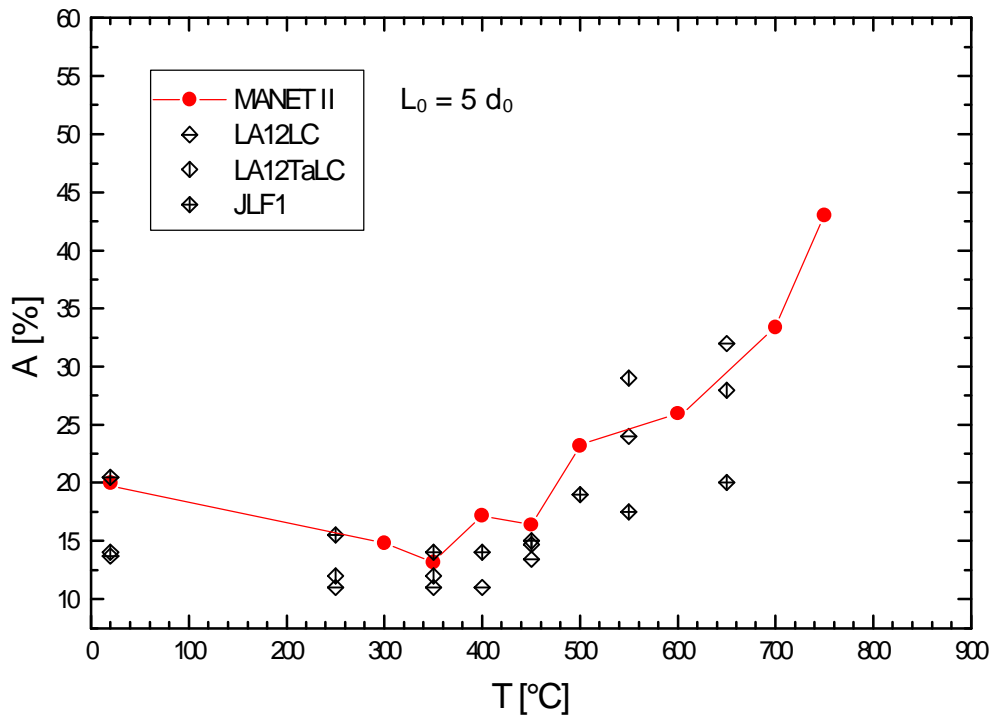


Figure 15: Comparison of the total elongation

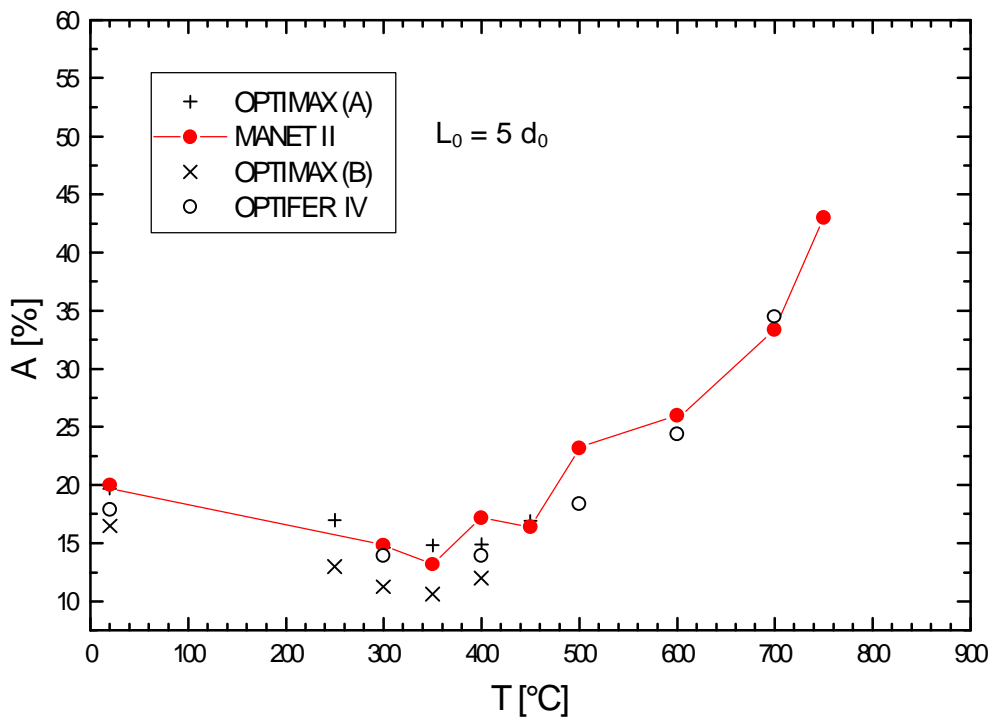


Figure 16: Comparison of the total elongation

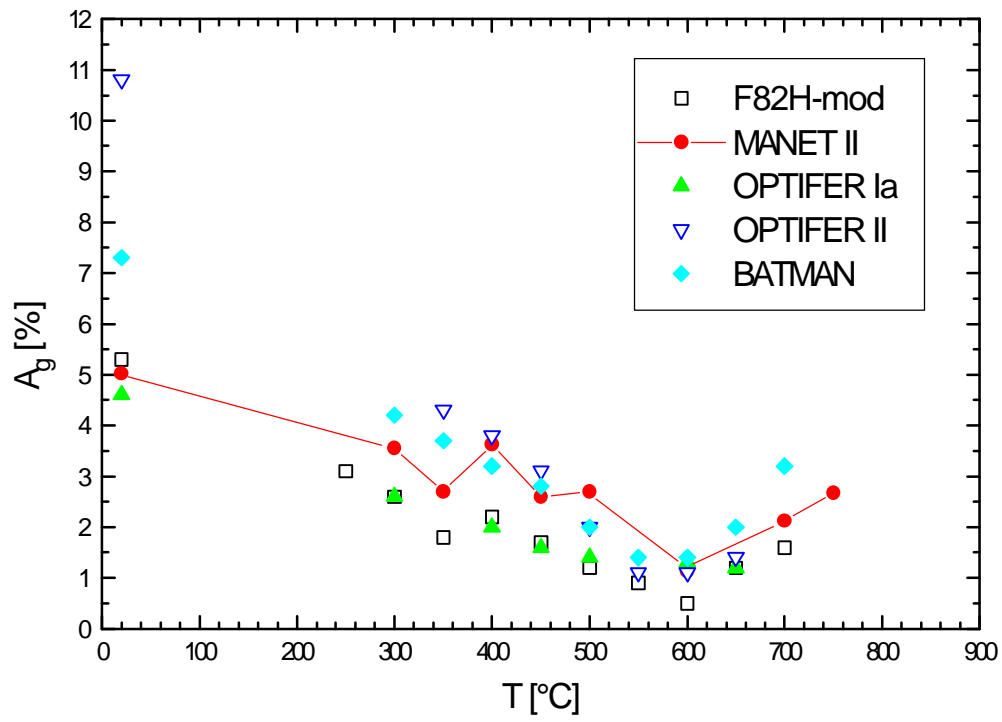


Figure 17: Comparison of the uniform elongation

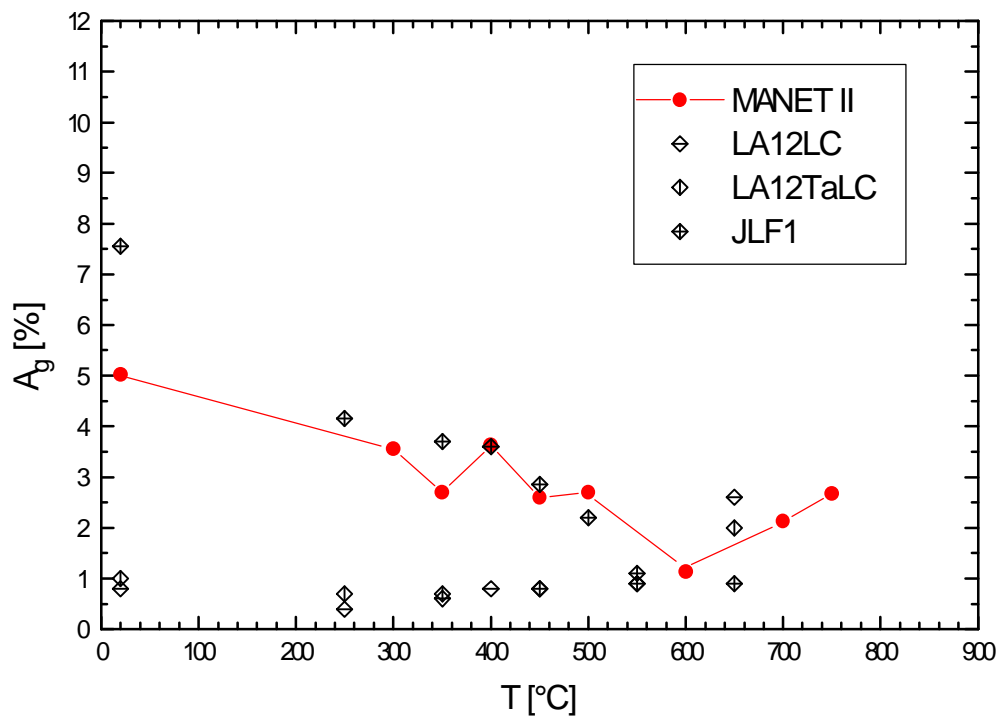


Figure 18: Comparison of the uniform elongation

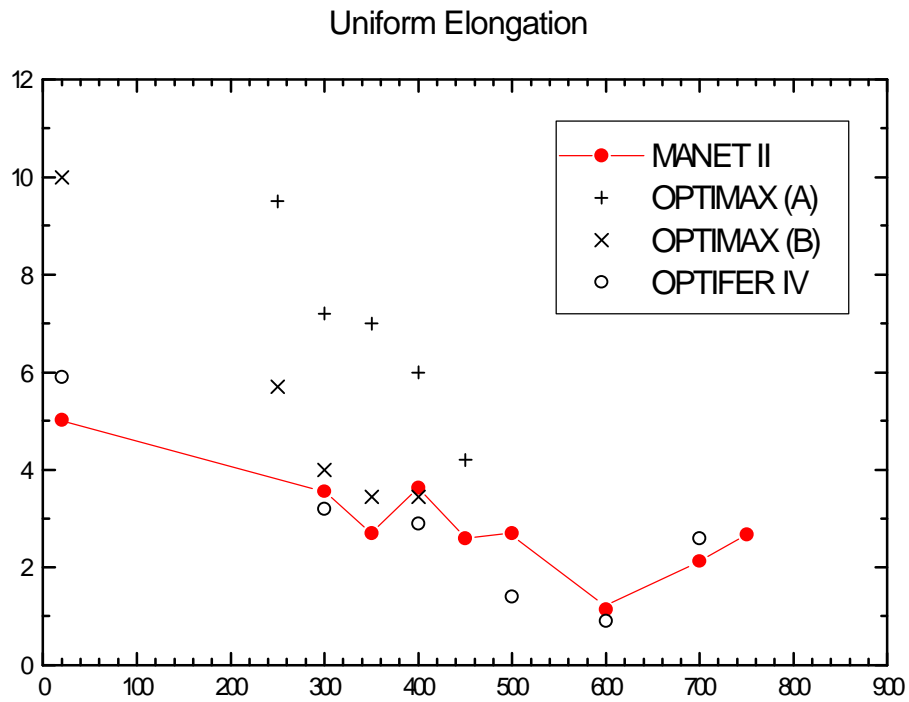


Figure 19: Comparison of the uniform elongation

Area Reduction

The area reduction values Z are very high under tensile testing over the whole range of test temperature. The data are plotted in Figs. 20-22. The conventional alloy MANET II is the lower envelope of all data and shows between 300 and 420°C a small minimum which again should reflect the appearance of dynamic strain ageing.

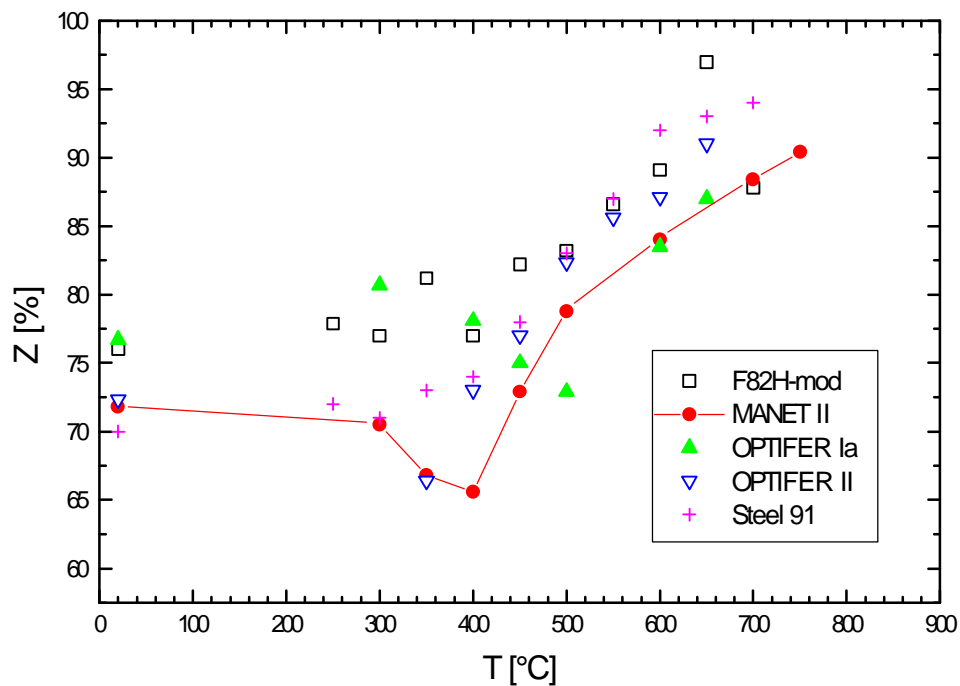


Figure 20: Comparison of the area reduction

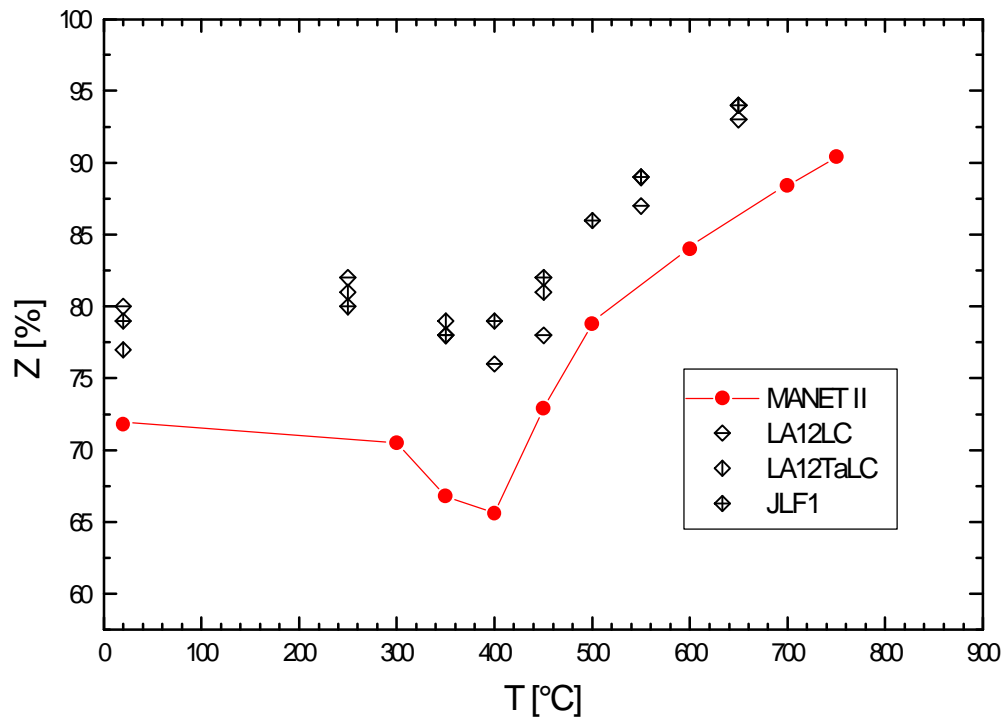


Figure 21: Comparison of the area reduction

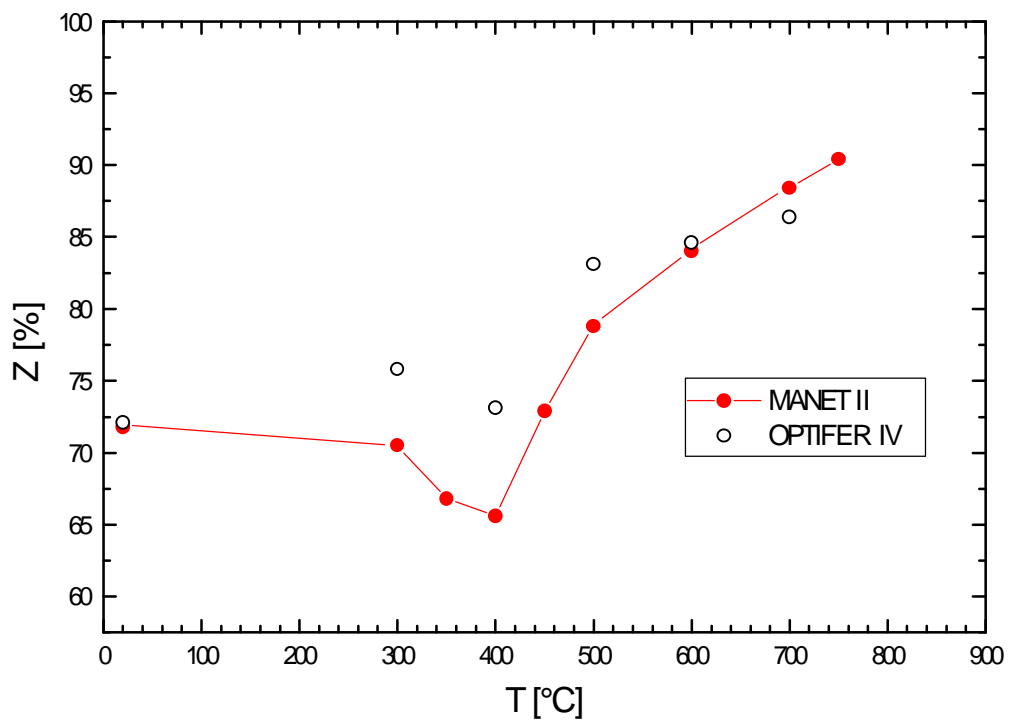


Figure 22: Comparison of the area reduction

Creep- and creep-rupture properties

The creep-rupture strength- and 1% -time yield limit properties are plotted in Figs 23 and 24 in the Larson-Miller presentation for the conventional MANET II and T 91 steels. In comparison with this data set the new LA-alloys OPTIFER and F82H-mod. are weaker at the lower temperature end and for shorter exposure time. It is, however, interesting to see that the alloy with 2% W (F82H-mod.) approaches at the high temperature end the alloy (600°C for 1000 hours) without W (OPTIFER II), whereas OPTIFER I with 1% W approaches to values in the range of the conventional alloys. This finding could eventually help to optimize the W-content to get balanced mechanical and radiological properties.

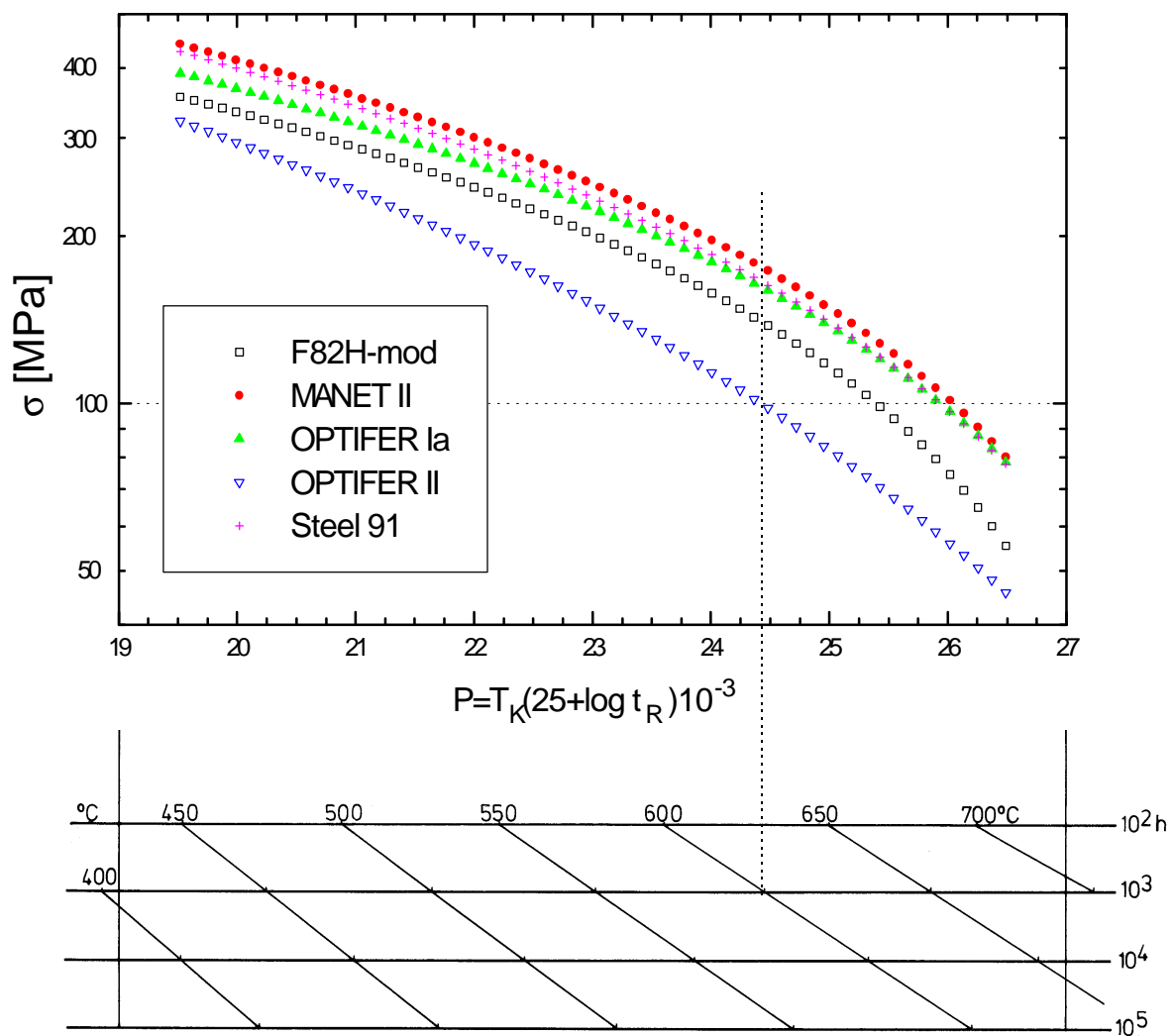


Figure 23: Comparison of Larson-Miller plots for rupture time

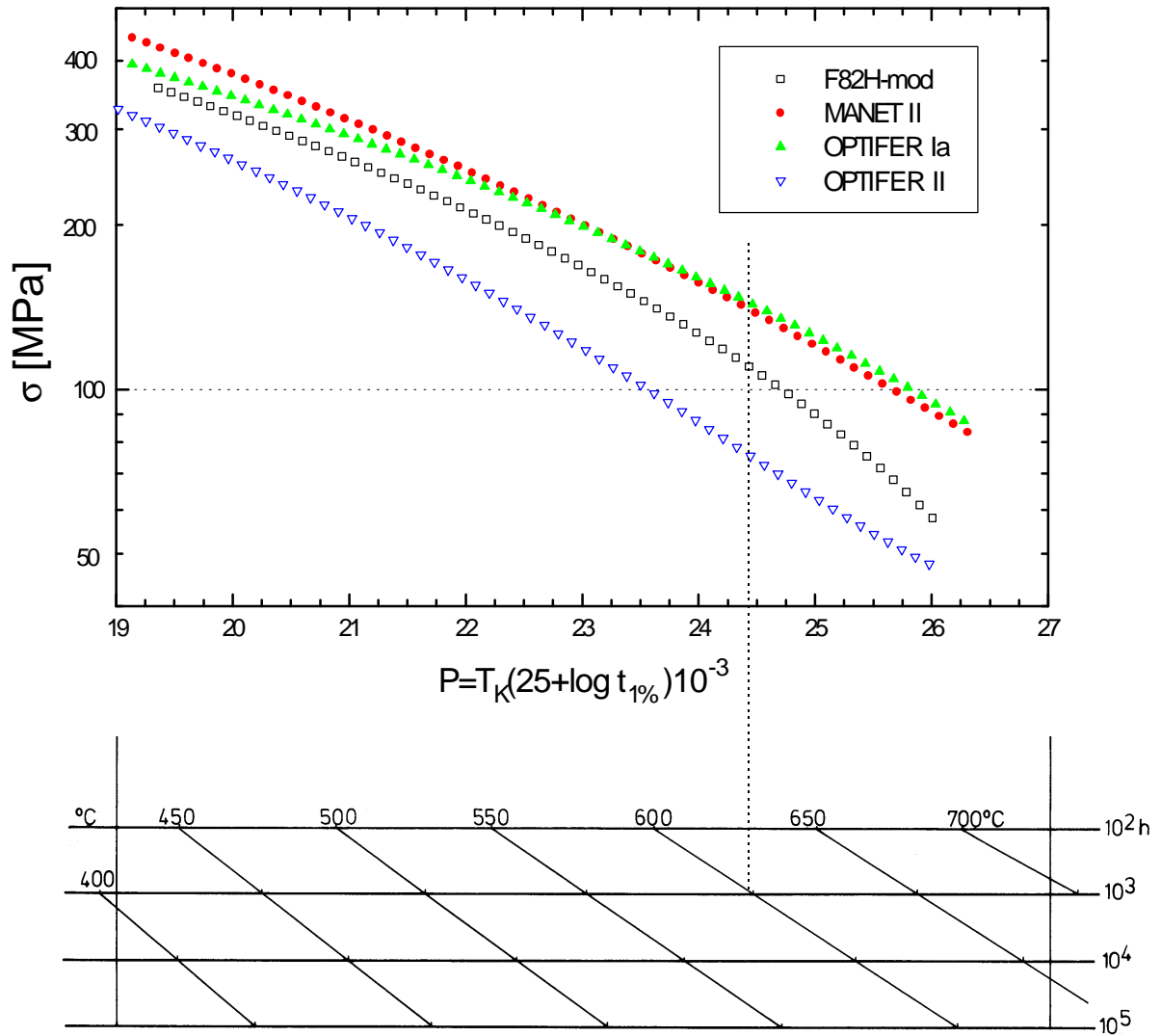


Figure 24: Comparison of Larson-Miller plots for 1 % creep strain

Impact properties

Charpy -V tests with Iso-V specimen reveal a very interesting general features. According to Fig. 25 the conventional alloys MANET II and T91 show the characteristic transition from the brittle to the ductile regime around RT and have an upper shelf energy USE in the range of 150 -200 Joule. All investigated LA-alloys show a much lower ductile-to-brittle transition temperature DBTT and a larger USE. This is a very important improvement especially when an additional shift in DBTT towards higher temperature is expected under low-temperature irradiation. There are, however, peculiarities to be found in the LA-alloys. In alloys like OPTIFER I and II the transition range is broad and is eventually divided in two steps, or the onset of the transition regime varies over a larger temperature range (-80 to -45°C) as shown in Fig. 26 for F82H-mod. Another characteristic feature of this material is the extremely steep transition from the brittle to the ductile temperature regime. The reason for

this behavior is unclear. In general, however, the results of the impact properties of the LA-alloys are very promising.

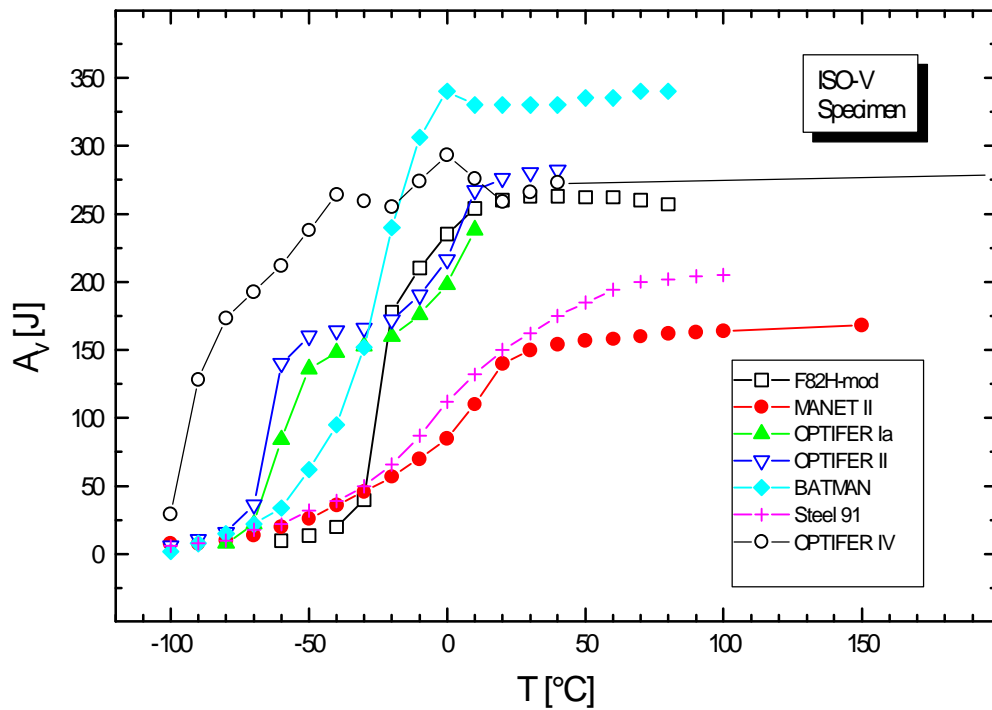


Figure 25: Comparison of test temperature vs. absorbed energy

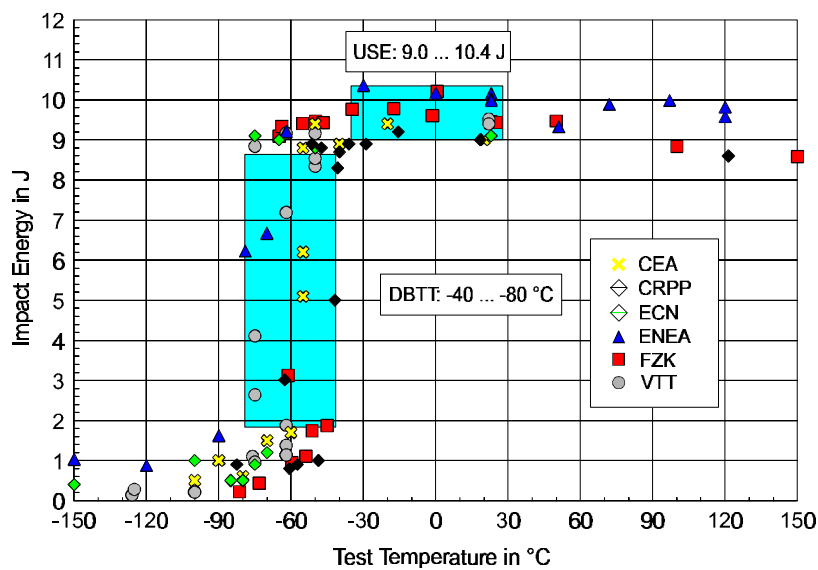


Figure 26: Charpy-V properties of F82H-mod. tested in different European laboratories

References

1. M. Schirra, P. Graf, S. Heger, H. Meinzer, W. Schweiger, H. Zimmermann; „MANET-II, Untersuchungsergebnisse zum Umwandlungs- und Vergütungsverhalten und Prüfung mechanischer Eigenschaften“. KfK 5177, Mai 1993
2. M. Schirra, S. Heger, A. Falkenstein; „Das Zeitstandfestigkeits- und Kriechverhalten des martensitischen Stahles MANET-II“. FZKA 5722, Oktober 1996
3. F. Brühl; „Verhalten des 9% Cr-Stahles X 10 CrMoVNb 91 und seiner Schweißverbindungen im Kurz- und Langzeitversuch“. Dissertation TU Graz, Mai 1989
4. Farhad, Tavassoli, Wareing, CEA; Priv. Com. 1996
5. CEA-ENEA-DEBENE-PNC-Exchange Meeting, Saclay, June 1988, Proceedings
6. NRI-M-Creep-Data Sheet No. 43, 1996; 9Cr1MoVNb-steel (Grade 91). National Research Institute for Metals, Japan
7. M. Schirra, K. Ehrlich, S. Heger, M.T. Hernandez, J. Lapena; „Optifer, ein weiterer Schritt zur Entwicklung niedrigaktivierender martensitischer Stähle“. FZKA 5624, Nov. 1995
8. M. Schirra, K. Ehrlich; „Mechanische Eigenschaften von niedrigaktivierenden martensitischen Stählen (Typ OPTIFER)“. 19. Vortragsveranstaltung VDEh, 29. Nov. 1996, Düsseldorf, Tagungsband S. 64-76
9. M. Schirra, Ch. Adelhelm, A. Falkenstein, M.P. Fernandez, P. Graf, S. Heger, L. Schäfer, W. Schweiger, H. Zimmermann; „Ergebnisse der Charakterisierung des Stahles F82H-mod., Chg. 9741“. Internal Report 1995
10. M. Schäfer, M. Schirra, R. Lindau; „Mechanical Properties of the Low Activation Martensitic Chromium Steel F82H-mod.“. 19th Symposium on Fusion Technology, 16.-20.9.1996, Lisboa, Portugal
11. R. Lindau (Ed.); „Homogeneity Tests of European Laboratories on Alloy F82H-mod.“, FZKA-Report 5814, in press
12. M. Schirra, H. Finkler; „Das Umwandlungsverhalten der hochwarmfesten martensitischen Stähle mit 8-14% Cr“. FZKA 5607, Sept. 1995
13. G. Filacchioni; BATMAN-results, Priv. Com., Aug. 1996

4. Summary and Conclusions

The conventional 9-12% CrMoVNb steels which possess a number of attractive properties for fusion application can be improved in their radiological decay data by substituting elements like Mo, Nb and Ni through W, Ge Ta and Ti. In the European Fusion Materials Program a series of 8 experimental LA-alloys (OPTIFER-, OPTIMAX-, BATMAN- and LA12-alloys), in which a broad compositional range has been covered, was developed in different European laboratories. In addition under the Implementing Agreement for Research and Development of Fusion Materials organized by the International Energy Agency IEA, a 5 ton industrial batch of an LA-alloy, denominated as F82H-mod. and provided by JAERI, has been investigated and characterized in a common effort by the partners in Europe, USA and Japan as a reference material. Additional informations for a first evaluation of data are also available from US and Japanese developmental alloys.

The new LA-alloys which lie in their majority in a compositional range of 7-10%Cr, 0-2%W, 0,1-0,3% V, 0-0,15%Ta, 0,09-0,13% C and 0,005-0,04%N have similar transformation-, hardenability- and tempering behavior like the conventional alloys and also possess a fully martensitic structure. Of practical importance for the use of the new LA-alloys is their greater variability for temper treatment, because they have a higher α - γ transformation start temperature.

Grain boundary stabilization can be achieved in these alloys by a Ta addition of more than 0,05 wt-%, otherwise enforced grain growth during the austenitization treatment has to be expected. Grain refinement is also possible by application of a normalization treatment in two consecutive steps as has been shown for the BATMAN alloys. A possible beneficial effect of low Ti-concentrations on the development of the prior austenitic grain size during an austenitization treatment has also been postulated.

First measurements of thermophysical properties provide data very similar to those found in the conventional alloys.

Regarding the tensile properties, the majority of LA-alloys has slightly reduced strength and improved ductility values. Similarly, creep strength and isothermal as well as thermal fatigue data for the F82H-mod. alloy are lower than those for the conventional MANET II steel. The beneficial role of W as effective solid solution hardener is evident in the investigated alloys. However, a comparison of the creep data of several alloys with different W-contents let us assume that there exists an optimum of creep strength within the covered W-range.

The new LA-alloys have altogether a lower ductile- to- brittle transition temperature DBTT and a strongly increased upper shelf energy USE in comparison to the conventional ones. First results of low dose neutron- and Dual Beam irradiations also indicate a lower radiation

hardening and a smaller irradiation-induced shift in DBT-temperature at the interesting temperature regime of 250-400°C.

A positive experience can also be reported for the overall performance of the material F82H-mod. alloy which had been fabricated as a 5 ton batch on an industrial scale. The homogeneity tests have shown that it is possible to produce such an LA-alloy with a high degree of homogeneity in structural and mechanical properties. By a proper selection of the ingot elements it was also possible to achieve a relatively low concentration of unwanted elements like Nb (about 1wt.-ppm) by the present steelmaking techniques. This gives the confidence that the more stringent conditions regarding very low allowable concentrations of unwanted elements can in future be achieved by advanced steelmaking technologies, thus allowing the final step from present alloys with reduced activation to those with very low long-term activity.

In summarizing, the results of the exploratory work for the development of a low activation ferritic/martensitic steel of Type 7-10% CrMoVTa are very promising, especially what the improvements in fracture toughness and impact properties and the elimination of detrimental elements for the long-term activation are concerned. Assuming that the forthcoming data on the irradiation behavior confirm this positive trend, it should be possible to specify, as planned, a primary candidate ferritic/martensitic alloy in 1998 at the end of the present screening phase.